# Heterogeneous chemistry of HONO and surface exchange

A dissertation submitted to the
Faculty of Biology, Chemistry and Geoscience
at the University of Bayreuth
for the degree of
Dr. rer. nat.

presented by
Matthias Sörgel
born in Nürnberg

Bayreuth, January 2012

Die vorliegende Arbeit wurde in der Zeit von April 2007 bis Januar 2012 an der Forschungsstelle für Atmosphärische Chemie der Universität Bayreuth unter der Betreuung von Herrn Prof. Dr. Cornelius Zetzsch angefertigt.

Vollständiger Abdruck der von der Fakultät für Biologie, Chemie und Geowissenschaften der Universität Bayreuth genehmigten Dissertation zur Erlangung des akademischen Grades Doktor der Naturwissenschaften (Dr. rer. nat.)

Amtierende Dekanin:                          Prof. Dr. Beate Lohnert

Tag des Einreichens der Dissertation:       11. Januar 2012

Tag des wissenschaftlichen Kolloquiums:   06. August 2012

Prüfungsausschuss:

Prof. Dr. Cornelius Zetzsch (Erstgutachter)

Prof. Dr. Thomas Foken (Zweitgutachter)

Prof. Dr. Andreas Held (Vorsitzender)

Prof. Dr. Britta Planer-Friedrich

Prof. Dr. Jürgen Senker

Drittgutachter: Priv. Doz. Dr. Jörg Kleffmann

# Summary

Nitrous acid (HONO) is an important precursor of OH radicals, which are the key oxidizing species in the atmosphere and are therefore called the detergent of the atmosphere. Despite the importance of HONO for atmospheric chemistry and about 30 years of detailed research the exact formation mechanisms of both day-and night-time formation remain unclear. The main formation pathways discussed to date are heterogeneous reactions with $NO_2$ as the HONO precursor or microbiological activity in soil. As the ground surface is a major source of HONO, the vertical distribution of HONO is very sensitive to the extent of vertical mixing. Additionally, some uncertainty in comparing laboratory and field measurements might be caused by the not yet clarified role of relative humidity and surface wetness on HONO formation and deposition, respectively.

This study presents field measurements of HONO by fast (~ 5 min time resolution) and sensitive (~ 2 ppt detection limit) long path absorption photometers (LOPAPs). The analysis of the data addresses three major questions: a) Can the HONO daytime source be explained by light-induced $NO_2$ conversion? b) What is the influence of vertical mixing on HONO mixing ratios, measured simultaneously in and above a forest canopy? c) Can the influence of relative humidity (RH) on HONO mixing ratios be inferred from the field measurements using time series analysis?

During the Diel Oxidant Mechanism In relation to Nitrogen Oxides (DOMINO) campaign, HONO and other reactive trace gases were measured above a pine forest in south west Spain. In line with all recently published work, this study also found a substantial daytime formation of HONO. This so called additional daytime source or unknown source was found to be slightly correlated ($r^2$ = 0.16) with actinic flux. Normalizing this unknown source to $NO_2$ mixing ratios improved the correlation ($r^2$ = 0.38), which indicates an influence of $NO_2$ availability. The coefficient of determination improved further to 0.47 by restricting the data to clear days and rejecting data from advection events. Thus, a fraction of the unknown source might be explained by light-induced $NO_2$ conversion but other factors have to be taken into account. Two processes of light-induced $NO_2$ conversion, proposed by recent laboratory studies, were shown to be negligible for the semirural conditions during our study. HONO photolysis was found to be the most important primary OH-radical source during DOMINO, contributing 20 % more OH than ozone photolysis integrated over the day.

Vertical exchange of HONO was studied at the "Waldstein-Weidenbrunnen" field site of the University of Bayreuth in the Fichtelgebirge Mountains in south east Germany. The simultaneous HONO measurements in and above a forest canopy highlighted the importance of turbulent exchange for the vertical distribution of HONO mixing ratios. The so-called coupling regimes of the forest (with the air layers above) were found to be a very useful micrometeorological concept to study vertical differences of mixing ratios in a forest. They denote which parts of the forest are coupled to the air layer above the canopy and thus take part in turbulent exchange of energy and matter. With this coupling tool it was possible to explain vertical mixing ratio differences by different sources and sinks and the magnitude of the difference by the intensity of vertical exchange. In order to evaluate the reliability of the vertical differences in HONO mixing ratios measured by two LOPAPs, these instruments have been compared side-by-side under field conditions. The comparison revealed that the LOPAPs agreed within 12 % relative error during dry conditions, but mixing ratios measured under rainy and foggy conditions were ambiguous. Studying the vertical mixing ratio differences of HONO, an unexpected result was that during late morning and around noon they were close to zero. As the lifetime of HONO below canopy of about 250 to 300 min was a factor of 25 to 30 longer than that above canopy of about 10 min, large mixing ratio differences would have been expected. The lack of these differences could be explained by efficient vertical mixing, which was indicated by a full coupling of the forest or a coupling by sweeps and only intermittent decoupling of the subcanopy during these periods. Around sunset, the whole forest became decoupled from the air layers above. This caused a steep increase in mixing ratio differences up to about 170 ppt due to a faster increase below canopy, indicating local formation below the canopy.

HONO and RH are correlated due to their diurnal cycles which are mainly caused by radiation. This diurnal contribution has to be removed from the respective signals in order to extract correlations on other timescales. Singular System Analysis, a tool for time series analysis, has been applied successfully to remove diurnal variations and long-term trends from the HONO and RH time series of three different measurement campaigns. Correlations of the higher frequency contributions of the remaining signals were poor but slightly positive. The HONO mixing ratios increase exponentially with RH from about 25 % RH to about 70 % RH. This was not the case for measurements in marine air masses which were possibly influenced by an equilibrium with the sea surface. No clear correlation was found between around 70 and 95 % RH. Above 95 % RH, HONO mixing ratios decreased due to HONO

uptake in droplets and liquid films. These features are in line with previously proposed mechanisms for interactions of water and HONO on surfaces.

The study highlighted the need to assess turbulent transport and surface properties in addition to chemistry for understanding the heterogeneous reactions and processes forming HONO.

# Zusammenfassung

Salpetrige Säure (HONO) ist ein bedeutendes Vorläufermolekül für OH-Radikale. Diese wirken als bedeutendstes Oxidationsmittel in der Atmosphäre und werden deshalb auch Waschmittel der Atmosphäre genannt. Trotz ihrer Bedeutung für die atmosphärische Chemie und nach 30 Jahren intensiver Forschung sind die Bildungsmechanismen der salpetrigen Säure nach wie vor nicht vollständig bekannt. Aktuell werden überwiegend heterogene Reaktionen von $NO_2$ als HONO-Vorläufersubstanz diskutiert, und zwar sowohl für die Dunkelreaktion als auch für die lichtinduzierten Reaktionen. Als weitere mögliche Quelle wird die HONO-Freisetzung durch Mikroorganismen im Boden diskutiert. Da sich demnach die wichtigsten HONO-Quellen in Bodennähe befinden, ist die vertikale Verteilung von HONO stark von der Effizienz des Vertikaltransports abhängig. Beim Vergleich der in Labormessungen bestimmten HONO-Bildungsraten mit Feldmessungen besteht zudem Unsicherheit durch den möglichen Einfluss der Oberflächenfeuchte, die von der relativen Feuchte abhängt.

Die Messungen der salpetrigen Säure wurden mit sogenannten Lang-Pfad-Absorptions-Photometern (LOPAP) durchgeführt. Diese Instrumente erlauben verhältnismäßig schnelle Messungen mit ca. 5 min Zeitauflösung und sind gleichzeitig sehr sensitiv (~ 2 ppt Nachweisgrenze). Die Analyse der gewonnenen Daten gliedert sich in drei Hauptbereiche: a) Kann die unbekannte Tagesquelle von HONO mit der lichtinduzierten Reduktion von $NO_2$ erklärt werden? b) Wie und wie stark beeinflusst die vertikale Durchmischung HONO Messreihen, die gleichzeitig im Wald und über dem Bestand gemessen wurden? c) Kann, unter Verwendung von Methoden der Zeitreihenanalyse, ein Einfluss der relativen Feuchte auf die HONO-Messwerte abgeleitet werden?

Bei der Messkampagne „Diel Oxidant Mechanism In relation to Nitrogen Oxides (DOMINO)" wurden HONO und andere Spurengase über einem Pinienwald in Südwest-Spanien gemessen. In Übereinstimmung mit anderen kürzlich veröffentlichten Studien wurde auch hier eine bedeutende HONO-Tagesquelle gefunden. Es konnte eine schwache Korrelation dieser so genannten zusätzlichen oder unbekannten Quelle mit dem aktinischen Fluss festgestellt werden ($r^2$ = 0.16). Normiert man diese unbekannte Quelle auf die gleichzeitig gemessenen $NO_2$-Werte, so verbessert sich die Korrelation zum aktinischen Fluss ($r^2$ = 0.38), was auf einen Einfluss der $NO_2$-Verfügbarkeit hindeutet. Berücksichtigt man nur Sonnentage und schließt gleichzeitig Advektionsereignisse von der Analyse aus so erhält man

einen Korrelationskoeffizienten ($r^2$) von 0.47. Daraus lässt sich schließen, dass zumindest ein Teil der HONO-Tagesquelle durch die lichtinduzierte $NO_2$-Reduktion erklärbar ist. Jedoch scheinen auch andere Faktoren eine wichtige Rolle zu spielen. Für zwei kürzlich publizierte, aus Labormessungen abgeleitete Mechanismen der lichtinduzierten $NO_2$-Umwandlung wurde allerdings kein nennenswerter Beitrag zur HONO-Tagesquelle festgestellt. Dies gilt zumindest für die Bedingungen während dieser Messkampagne, die jedoch auf andere ländliche Gegenden übertragbar sind. Über den Tag integriert war der Beitrag der HONO-Photolyse zur OH-Radikal-Produktion um 20 % größer als derjenige der Ozonphotolyse, und somit verantwortlich für den größten Teil der Primärproduktion an OH-Radikalen.

Die Messungen zum Vertikalaustausch von HONO in einem Waldökosystem wurden auf den Messflächen der Universität Bayreuth im Fichtelgebirge („Waldstein-Weidenbrunnen") durchgeführt. Dieser Teil der Untersuchung unterstreicht die Bedeutung des turbulenten Austauschs für die vertikale Verteilung von HONO. Als äußerst wichtig für die Interpretation der vertikalen Differenzen der HONO-Mischungsverhältnisse erwiesen sich die sogenannten „Kopplungszustände" des Waldes mit den Luftschichten darüber. Die Bestimmung der Kopplungszustände basiert auf der Detektion von organisierten Strukturen in der Turbulenz, so genannten kohärenten Strukturen. Durch die Betrachtung der Kopplungszustände war es möglich, die vertikalen Differenzen in den HONO-Mischungsverhältnissen, die jeweils über und im Bestand gemessen wurden, durch die Kombination verschiedener Quellen und Senken zu erklären und die Größe der Differenz auf den Vertikaltransport zurückzuführen. Um die Messunsicherheit für die vertikalen Differenzen zu bestimmen, wurden Vergleichsmessungen (side-by-side) mit den beiden LOPAPs im Feld durchgeführt. Unter trockenen Bedingungen waren keine systematischen Abweichungen festzustellen, und die Geräte stimmten innerhalb eines relativen Fehlers von 12 % überein. Bei Nebel und Regen hingegen waren die Abweichungen so groß, dass den Messergebnissen nicht vertraut werden kann. Die Differenzen der HONO-Mischungsverhältnisse vom späten Vormittag bis zum frühen Nachmittag lagen nahe bei null. Auf Grund der immensen Unterschiede der Lebensdauern der HONO Moleküle (~ 10 min über dem Bestand und 250-300 min darunter, durch die Beschattung durch das Kronendach) waren hohe vertikale Differenzen erwartet worden.

Die kaum messbaren Unterschiede in den Mischungsverhältnissen konnten mit dem effizienten Vertikalaustausch erklärt werden. Dieser wurde durch die überwiegend vollkomme Kopplung des Waldes mit den darüber liegenden Luftschichten und nur zwischenzeitlicher Entkopplung des Stammraumes angezeigt. Mit der Entkopplung des

gesamten Bestandes bei Sonnenuntergang wurde die lokale Bildung von HONO in den sehr schnell ansteigenden HONO-Werten unterhalb der Krone sichtbar.

Da HONO und relative Feuchte (RF) schon allein durch den Tagesgang der Strahlung korreliert sind, muss dieser Anteil der Signale vor einer Analyse, die nach Korrelation auf kürzeren Zeitskalen sucht, herausgefiltert werden. Mit diesem Ziel wurde „Singular System Analysis", ein mathematisches Werkzeug der Zeitreihenanalyse, erfolgreich auf die Zeitreihen von HONO und RF aus den drei verschiedenen Messkampagnen angewandt. Der Tagesgang und Trends wurden erfolgreich separiert, die Korrelation der verbleibenden (höherfrequenten) Signale war jedoch nur sehr schwach, wenn auch für alle Messreihen leicht positiv. Die HONO-Mischungsverhältnisse stiegen von ca. 25 % bis ca. 70 % RF exponentiell mit der Feuchte an. Dies galt nicht für die Messwerte in marinen Luftmassen, die eventuell von einem Gleichgewicht mit der Meeresoberfläche beeinflusst waren. Zwischen 70 % und etwa 95 % RF gab es keine eindeutige Korrelation. Über 95 % waren die HONO-Werte durch die Aufnahme in Wasserfilme und Tropfen deutlich niedriger. Dieses Verhalten deckt sich mit den bereits vorgeschlagenen Mechanismen der Wechselwirkung von Wasser und HONO an Oberflächen.

Die Studie hat gezeigt, wie wichtig - gerade für die Betrachtung der heterogenen Bildung von HONO - die Einbeziehung des Vertikaltransports und der (veränderlichen) Oberflächen- eigenschaften ist.

# List of manuscripts

This dissertation consists of three individual manuscripts.

**Published manuscripts:**

**Sörgel, M.**, Regelin, E., Bozem, H., Diesch, J.-M., Drewnick, F., Fischer, H., Harder, H., Held, A., Hosaynali-Beygi, Z., Martinez, M., and Zetzsch, C.: Quantification of the unknown HONO daytime source and its relation to $NO_2$, Atmos. Chem. Phys., 11, 10433-10447, doi:10.5194/acp-11-10433-2011, 2011.

**Sörgel, M.**, Trebs, I., Serafimovich, A., Moravek, A., Held, A., and Zetzsch, C.: Simultaneous HONO measurements in and above a forest canopy: influence of turbulent exchange on mixing ratio differences, Atmos. Chem. Phys., 11, 841–855,doi:10.5194/acp-11-841-2011, 2011.

**Manuscripts to be submitted:**

**Sörgel, M.**, Held, A., Zetzsch, C.: Singular System Analysis of forest observations of HONO and humidity, to be submitted to Atmos. Envion., 2012.

**Publications not included in this thesis:**

Foken, T., Meixner, F. X., Falge, E., Zetzsch, C., Serafimovich, A., Bargsten, A., Behrendt, T., Biermann, T., Breuninger, C., Dix, S., Gerken, T., Hunner, M., Lehmann-Pape, L., Hens, K., Jocher, G., Kesselmeier, J., Lüers, J., Mayer, J.-C., Moravek, A., Plake, D., Riederer, M., Rütz, F., Scheibe, M., Siebicke, L., **Sörgel, M.**, Staudt, K., Trebs, I., Tsokankunku, A., Welling, M., Wolff, V., and Zhu, Z.: ExchanGE processes in mountainous Regions (EGER) – overview of design, methods, and first results, Atmos. Chem. Phys. Discuss., 11, 26245-26345, doi:10.5194/acpd-11-26245-2011, 2011.

# Acknowledgement

# Contents

# Synthesis

## 1  Introduction

Nitrous acid (HONO) is a key compound to understand tropospheric oxidation chemistry. Its photolysis forms OH radicals which are called the "detergent" of the atmosphere due to their oxidizing power. Most compounds emitted into the atmosphere become more hydrophilic (e.g. $NO \rightarrow HNO_3$), less volatile (and then are incorporated into the particulate phase) or are finally oxidized to $CO_2$ and water by this oxidation process. This accelerates the removal of the majority of compounds from the atmosphere by both dry and wet deposition (e.g. Crutzen and Zimmermann, 1991; Ehhalt, 1994). The whole system has been called the "self-cleansing capacity of the atmosphere". HONO has been found to contribute substantially to primary OH formation close to the Earth's surface. HONO typically contributes about one third of OH primary production, but published values range from about 10 to 60 % as summarized by Volkamer et al. (2010) and Sörgel et al. (2011b). Besides its importance for the atmospheric oxidation potential, HONO is part of acid and nutrient deposition to the biosphere. Moreover, growing concern exists about possible health effects due to the formation of nitrosamines (Hanst et al., 1977; Pitts et al., 1978) where HONO acts as the nitrosating agent, especially in indoor environments after wall reactions of HONO with nicotine (Sleiman et al., 2010). HONO is believed to be formed heterogeneously, with the main contribution arising from the ground surface (e.g. Wong et al., 2011a). Thus, HONO mixing ratios are very sensitive to vertical mixing.

In the planetary boundary layer (PBL), turbulent diffusion is about five orders of magnitude faster than molecular diffusion (Foken, 2008). For example, a compound emitted at the surface (like HONO) would need about a month to be uniformly mixed in the lowermost 10 m by molecular diffusion only, whereas it takes only a few seconds by turbulent diffusion (Jacob, 1999). This has important implications for atmospheric chemistry as diffusion brings reactants which have different sources and sinks together. In 1940, Damköhler introduced a dimensionless number (now named Damköhler number), which compares the characteristic transport timescale to the timescale of a chemical reaction (Damköhler, 1940). Thus, the Damköhler number serves as a measure if a trace gas can be considered a quasi-inert tracer during transport (Da $\leq$ 0.01). For larger Damköhler numbers (0.01 < Da < 50) transport and chemistry play a role. According to McRae et al. (1982) above Da = 50 the reaction can be

regarded as diffusion controlled. If the reactants are not well mixed, they are segregated. This means that the effective rate constant is lower than that measured in the laboratory under well mixed conditions. The problem of segregation raised special attention in air chemistry modeling (e.g. Stockwell, 1995; Vila-Guerau de Arellano, 2003; Vinuesa and Vila-Guerau de Arellano, 2005; Ouwersloot et al., 2011). Recent development of fast sensors for reactive species allowed studying the effect of segregation in situ (e.g. Dlugi et al., 2010). Thus, in the real atmosphere a detailed interpretation of the chemistry is not possible without information about the turbulence. This thesis aims to shed light on the distribution of sources and sinks of HONO in forest environments. The identification of sources and sinks is a prerequisite for modeling studies and stimulates new laboratory studies about the nature of these sources and sinks. This work highlights in particular the need to carefully address transport phenomena in deriving source distributions and source strength of reactive species like HONO.

## 1.1  Atmospheric chemistry of HONO

Though HONO is an important compound in the troposphere and has been studied extensively since the unequivocal detection in the atmosphere (Perner and Platt, 1979), the formation pathways are poorly understood. There is a huge body of evidence that the heterogeneous disproportionation of $NO_2$ to HONO and $HNO_3$ is the dominant nighttime formation reaction (also called the "dark heterogeneous reaction"). This reaction was found to be first order in $NO_2$ and water vapor (Sakamaki et al., 1983; Svennson et al., 1987; Pitts et al., 1984; Jenkin et al., 1988). It has been studied on a variety of natural and urban surfaces (Lammel and Cape 1996; Lammel, 1999). Still, the exact mechanism remains unclear. A detailed assessment of the different mechanisms has been given by Finlayson-Pitts et al. (2003) and Finlayson-Pitts (2009). In short:

- The gas phase dimer of $NO_2$ ($N_2O_4$) dissolves in aqueous films (Finlayson-Pitts et al., 2003)

- Chemisorption of water on mineral dust particles produces H, which reacts with $NO_2$ to form HONO (Gustafsson et al., 2008)

- Disproportionation at the droplet surface is anion catalyzed (Yabushita et al., 2009¸ Kinugawa et al., 2011))

Another pathway is the reaction of $NO_2$ with reducing organic compounds (e.g. Gutzwiller et al., 2002a and 2002b). The proposed reactions involving NO (Calvert et al., 1994; Andres-Hernandez et al., 1996; Saliba et al., 2001) were found to be of minor importance (summarized by Finlayson-Pitts et al., 2003 and Kleffmann, 2007). To date, the mechanism still remains unclear. Nevertheless, the nighttime formation rates of HONO measured in urban and rural environments are within a quite narrow range from 0.4 to 2 % $h^{-1}$ with respect to $NO_2$ (summarized by Su et al., 2008a and Sörgel et al., 2011a). The only known relevant gas-phase source of HONO is the reaction of NO with OH, which is the back reaction of HONO photolysis that forms NO and OH. During daytime these reactions form a photostationary state (PSS), whereas during nighttime this HONO formation pathway is not important due to the absence of photochemically produced OH (and NO). All recent studies measured daytime HONO values substantially above the PSS which means that an additional daytime source exists (e.g. Kleffmann et al., 2005 and Kleffmann, 2007). This stimulated laboratory studies, which came up with various proposed mechanisms. These can be summarized as follows (a detailed assessment is given in the review of Kleffmann (2007) and in Appendix B and C of this work):

- Reduction of $NO_2$ on organic photosensitizers (e.g. George et al., 2005 and Stemmler et al., 2006)

- Photolysis of nitrophenols (Bejan et al., 2006)

- Photolysis of adsorbed $HNO_3$ (e.g. Zhou et al., 2002, 2003 and 2011; Ramazan et al. 2004)

- $NO_2$ reduction on irradiated mineral particles (Gustafsson et al., 2006, Ndour et al., 2008)

- Soil emissions from microbiological activity (Su et al., 2011)

A promising pathway to explain HONO daytime production are so-called photosensitized reactions (e.g. George et al., 2005), although, these reactions have been demonstrated to play a minor role regarding the HONO formation on organic aerosols (Stemmler et al., 2007; Sosedova et al., 2011). However, as humic acids are ubiquitous in nature, these reactions may substantially contribute to daytime HONO formation on plant or building surfaces as well as soils (Stemmler et al., 2006). Very recent studies about photolysis of adsorbed $HNO_3$ indeed showed enhanced light absorption of adsorbed $HNO_3$ with respect to gas phase $HNO_3$ (Zhu et al., 2008 and 2010). This makes a substantial contribution of this pathway to daytime HONO formation more realistic. As these laboratory studies found $NO_2$* as main photolysis product,

Zhou et al. (2011) concluded that HONO formation by $HNO_3$ photolysis also follows the photosensitized reduction of $NO_2$ (Stemmler et al.,2006). $HNO_3$ is the final oxidation product of $NO_x$ (Fig.1) and is thus believed to determine the atmospheric lifetime of $NO_x$. $HNO_3$ photolysis therefore provides a pathway back to the atmospheric oxidation cycle of $NO_x$ (Fig.1). This mechanism is especially important for the oxidation capacity in remote areas with low atmospheric $NO_x$ burden. Another "way back" is the proposed HONO emission from soils due to microbiological activity (Kubota and Asami, 1985; Su et al., 2011). The denitrification by microbes is the only pathway to convert reactive nitrogen in the environment back to unreactive $N_2$. The loss of intermediate products is responsible for the emissions of HONO and NO (Fig.1). Via nitrification, also fertilization with reduced nitrogen ($NH_3/NH_4^+$) can form reactive oxidized N- species (NO and HONO).
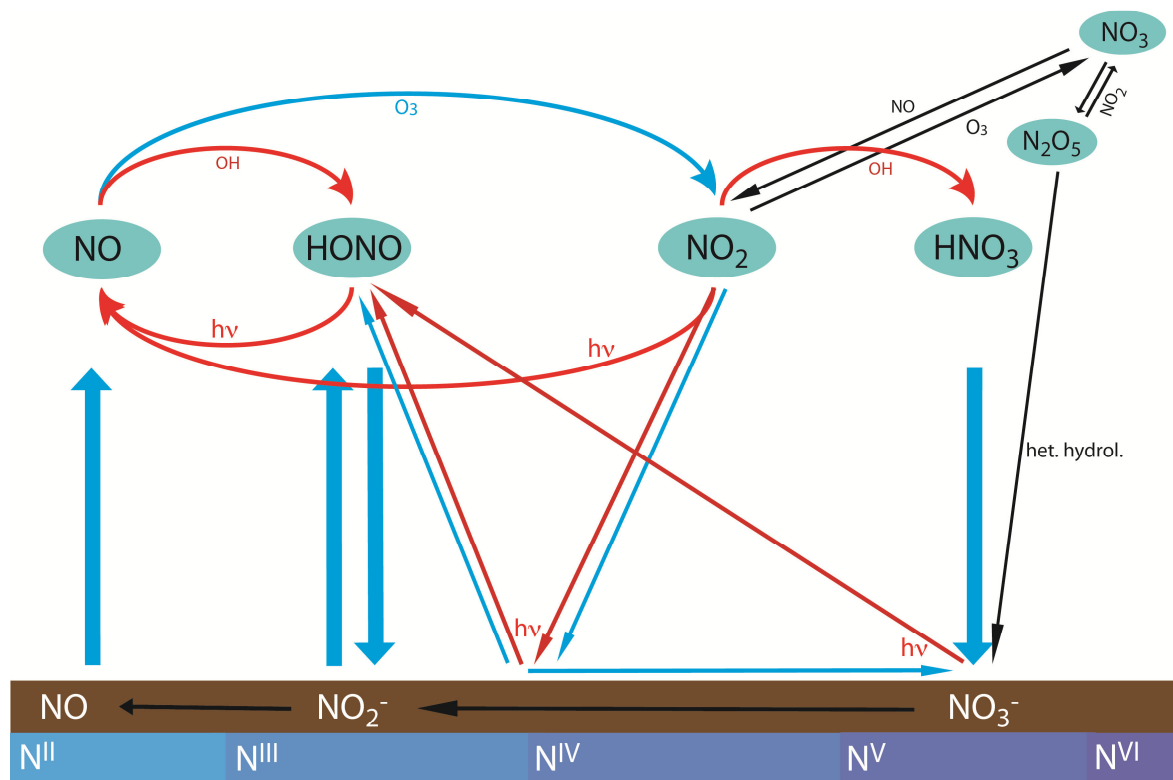


Fig.1: A schematic view (not complete) of the atmospheric chemistry of reactive oxidized nitrogen and its interaction with the ground surface respectively soil (brown layer). Blue arrows denote pathways which are active during the whole day, black arrows contribute only in the absence of light, and red arrows only with light.

Figure 1 presents a schematic view on atmospheric chemistry of oxidized inorganic nitrogen. Anthropogenic and biogenic emissions are mainly in the form of NO. NO is further oxidized in the atmosphere by $O_3$ and OH to be finally deposited as $HNO_3$ (e.g. Lerdau et al., 2000). During night, $HNO_3$ is formed by heterogeneous hydrolysis from $N_2O_5$. $N_2O_5$ is formed only at nighttime because it requires the reaction of $NO_2$ with the $NO_3$ radical (formed by reaction

of $O_3$ with $NO_2$) which is very photolabile. If NO is oxidized to $NO_2$ other than by $O_3$ (e.g. by $HO_2$, $RO_2$ radicals), $O_3$ is formed by this cycle from $NO_2$ photolysis (Finlayson-Pitts and Pitts, 2000). If HONO is formed by other means than through reaction of NO with OH, OH radicals are formed by HONO photolysis. Thus, oxidized nitrogen has an important impact on the self-cleansing capacity of the atmosphere (day and nighttime).

As can be seen in Fig. 1, the formation of HONO is mainly heterogeneous (reactions at surfaces). In principle, these can be both aerosol and ground (building, plant, soil,…) surfaces. There is strong evidence from field measurements that the ground is indeed the major source of HONO (e.g. Febo et al., 1996; Kleffmann et al., 2003; Zhang et al., 2009; Wong et al., 2011a, 2011b). Therefore, HONO mixing ratios are very sensitive to vertical mixing.

Summarizing: The formation pathways of HONO remain unclear, although there are quite a lot mechanisms proposed. In the dark, the heterogeneous disproportionation of $NO_2$ is the most probable source, whereas at daytime an additional light enhanced or photolytic source exists. HONO from microbiological activity may be a source both day and night. According to Su et al. (2011; supporting material) the HONO source strength is dependent inter alia on temperature (HONO equilibrium) and on transfer velocity (from soil to the atmosphere). These parameters exhibit a diurnal cycle which can lead to more efficient HONO transport to the atmosphere during daytime. The most probable HONO sources are located at the ground or in the soil itself. Therefore, as already mentioned above, HONO mixing ratios are very sensitive to vertical mixing.

## 1.2  HONO chemistry and turbulent transport

In rural and remote regions the HONO precursor $NO_2$ is advected from source regions (e.g. cities, roads) and to some extent locally produced by oxidation of soil-emitted NO which reacts with ozone. The $NO_2$ has to be transported to the surface where it reacts to form HONO (or is taken up by plants, e.g. Lerdau et al., 2000; Breuninger et al., 2011). HONO formed at the surface desorbs and is then transported back to the atmosphere. In stable conditions, upward transport is limited, thus HONO accumulates close to the ground. If HONO is predominantly formed by microbes or by $HNO_3$ photolysis, $NO_2$ deposition is of minor importance. During neutral or convective conditions (mostly daytime), vertical gradients are

less pronounced or hardly resolved by current instrumentation (~ 1 ppt detection limit). This can be seen in the vertical profiles of HONO in the boundary layer above a remote forest measured on a small airplane (Zhang et al., 2009). Thus, especially during stable conditions the measured mixing ratios and also the HONO/$NO_2$ ratio depend on the measurement height (Stutz et al., 2002; Veitel, 2002; Wong et al., 2011a). Furthermore, the surface properties are altered by the adsorption of water. This has an influence on solubility (deposition) and on chemistry. Water is required as a reactant for the formation of HONO by heterogeneous disproportionation of $NO_2$. However, with increasing adsorption of water molecules, surface active sites for other reactants ($NO_2$) might be blocked (Lammel and Cape, 1996). Also, Gustafsson et al. (2006) report an inhibition of photocatalytic HONO formation due to adsorption of water. On the other hand, HONO is a weak acid which is taken up into liquid films depending on pH (Hirokawa et al., 2008). Furthermore, HONO can be salted out (become less soluble) in concentrated solutions, which was found for sulfuric acid (Becker et al., 1996) and ammonium sulfate solutions (Becker et al., 1998). A relation between gas phase HONO and relative humidity (RH) was found in many laboratory and field measurements (e.g. Arens et al., 2002; He et al., 2006;Trick, 2004; Stutz et al., 2004; Wainmann et al., 2001; Wojtal et al., 2010; Yu et al, 2009; Sörgel et al., 2011a; Rubio et al., 2008). In accordance with the formation of liquid films or droplets above 95 % RH (Burkhardt and Eiden, 1994; Lammel, 1999), lower HONO and HONO/$NO_x$ values above 95 % RH were reported (Stutz et al., 2004; Yu et al., 2009; Sörgel et al., 2011a). The behavior in the intermediate RH range (~20-95 %) is not well documented. The only mechanism provided so far is a Langmuir type mechanism where co-adsorbing water displaces HONO adsorbed to the surface (Trick, 2004; Stutz, 2005). Up to know it is unclear which role surface humidity plays for tropospheric HONO.

A forest canopy adds more complexity as shown in a simplified scheme of daytime $NO_x$ and HONO chemistry within and above a forest canopy in Fig. 2. A key feature regarding photochemistry is the shading of the canopy which alters photochemical equilibriums. For example, the photolysis of the HONO precursor $NO_2$ is faster above canopy, which results in a net downward flux of NO. In the shaded trunk space this downward mixed NO (together with soil emitted NO) reacts with ozone which was also photochemically produced above the canopy to regenerate $NO_2$. However, $NO_2$ is also deposited to the forest floor and the canopy. There it is taken up by plants (e.g. Lerdau et al., 2000; Breuninger et al., 2011) or reacts to form HONO. HONO itself is also deposited to the forest floor and the canopy, where it is taken up by the stomata (Schimang et al., 2006). As discussed earlier, the emission and

deposition of HONO might depend on RH, which has a distinct vertical gradient and is different within the canopy and at the forest floor. The scheme of $NO_x$ chemistry in forest environments is rather well established (Rummel et al., 2002, Horii et al., 2004; Foken et al., 2011). Investigating the HONO sources and sinks in and above the forest canopy was part of this thesis. Additionally to the differences in chemistry the canopy might act like a gate, which separates these two distinct (photochemical) environments. The coupling between the forest canopy and the air layer above ("control mechanism of the gate") depends on turbulence and might be represented by coupling regimes (Thomas and Foken, 2007).
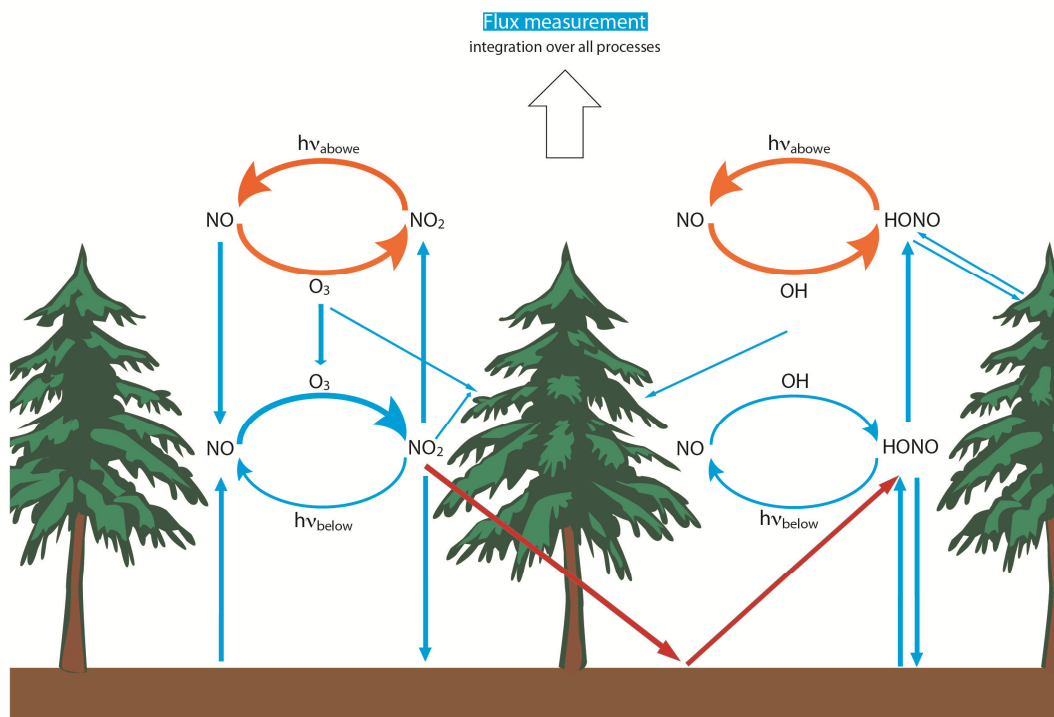


Figure 2: Schematic view of the daytime cycles of $NO_x$ and HONO above and below a canopy.

## *1.3  Surface exchange*

As mentioned above, the exchange of energy and matter between the Earth's surface and the atmosphere is driven by turbulence which is generated by shear and buoyancy forces at the surface. In a first simplified view, a forest canopy can be regarded as a rough wall. Near-wall-turbulence has been studied in hydrodynamics since the 1930s and has been found to be comprised of "classical random turbulence" and "organized motions" = "coherent structures" (Robinson, 1991). Similar to wall turbulence coherent motions were found to contribute significantly or even dominate momentum, heat and scalar exchange in tall canopies (Gao et al., 1989; Bergström and Högström, 1989; Barthlott et al., 2007; Thomas and Foken, 2007; Serafimovich et al., 2010). However, the turbulence structure above tall canopies has been found to differ from that of a rough wall. Due to the high roughness, a layer called roughness sublayer (Garratt, 1978, 1980) which extends to about three times the canopy height (e.g. Cellier and Brunet, 1992; Wenzel et al., 1997) lies between the "classical" boundary layer and the canopy. According to Raupach et al. (1996) the turbulence in the roughness sublayer is better characterized by a plane mixing layer than a boundary layer. These authors compare the instabilities which generate turbulence in the mixing of two air streams with different velocities (plain mixing) with those arising from the inflection point in the wind profile within the canopy. This is another difference to rough walls: Below the dense obstacle (canopy) a more open space (trunk space) exists, before, approaching the surface the horizontal wind speed tends to zero. Thus, the mean wind profile of a canopy is different from that of a boundary layer as it has an inflection point (secondary wind maximum). This inflection point is thought to cause instabilities which produce coherent eddies (Raupach et al., 1996; Finnigan, 2000). Thomas and Foken (2007) used the detection of coherent structures to infer so-called "coupling regimes". The regimes denote which part of the canopy is coupled to the air layer above canopy and thus takes part in the exchange of energy and matter (Thomas and Foken, 2007; Serafimovich et al., 2010). Counter gradient fluxes (Denmead and Bradley, 1985), which violate the flux gradient relationship of classical K-theory, were found to be caused by coherent exchange (Finnigan, 2000). Thus, the classical K-theory is not applicable within a forest canopy. In the roughness sublayer, fluxes are enhanced (with respect to the surface layer), and for the flux gradient relationship correction terms have to be applied (Cellier and Brunet, 1992; Garrett, 1992).

## 1.4  Time scales and spatial scales
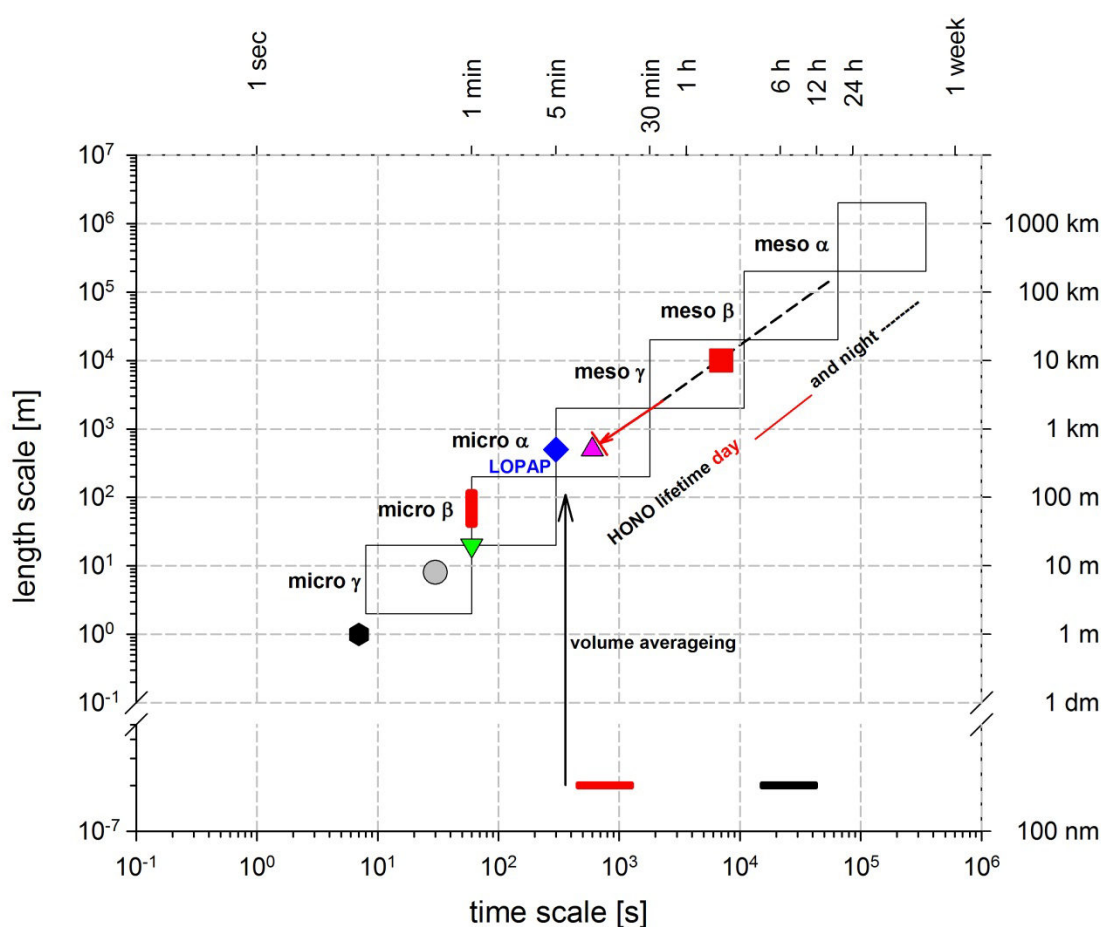


Fig.3: Spatial and temporal scales in the atmosphere adapted from Orlanski (1975). Forest *canopy* related transport processes (adapted from Foken et al., 2011) comprise turbulent transport in the canopy (black hexagon), vertical advection in the canopy (grey circle), transport above canopy (green triangle), coherent structures (red vertical bar), footprint averaged turbulent flux (pink triangle), and horizontal advection at canopy top (red square).The horizontal bars at the bottom mark chemical timescales for heterogeneous nighttime formation (black horizontal bar) and proposed daytime formation rate from $NO_2$ (red horizontal bar). The time resolution of the LOPAP instrument is marked as blue diamond. The range of lifetimes of HONO due to photolysis is marked as red (daytime) and black (nighttime) arrow.

Spatial scales and time scales of atmospheric motion are closely related (Orlanski, 1975; Fig. 3). Studying the distribution or exchange of trace gases with the surface, one has to be aware that chemistry, biological and soil processes occur on spatial and temporal scales different of those of the related transport in the atmosphere. Thus, measurements of trace gases are not directly related to individual (chemical or physical) processes, but integrated via "volume averaging" or in the case of turbulent measurements over a footprint (so called "scale problem"; e.g. Foken et al., 2011). The discrepancy increases with increasing spatial/temporal scales (Foken et al., 2011). To address the problem of the overlapping (or non-overlapping)

scales was one of the major goals of the EGER project. In Fig. 3, canopy related transport phenomena (adapted from Foken et al., 2011) are shown in relation to spatial and temporal scales of atmospheric motion according to Orlanski (1975). Not shown here are the soil and biological processes which were a central part of the investigation of the EGER project. This graph is solely focused on chemical reactions governing the formation and fate of HONO as well as the instrumental limitations (temporal resolution) of the **LO**ng **P**ath **A**bsorption **P**hotometer (LOPAP, blue diamond), which are relevant for this thesis. Timescales of heterogeneous HONO formation (day and nighttime) were inferred from typical (rural) $NO_2$ conversion frequencies and typical $HONO/NO_2$ ratios. These are given for the dark heterogeneous reaction (black horizontal line) as 1.5 % h$^{-1}$ and 10 %, respectively (Su et al., 2008a, Sörgel et al., 2011a), and are about 15 % h$^{-1}$ and 3 %, respectively, for photo-enhanced formation (Sörgel et al., 2011c). An $NO_2$ value of 1 ppb was taken as a typical rural value. Characteristic timescales for these reactions were calculated by taking the time which the conversion of $NO_2$ takes at the given rate to reach 63 % of the final $HONO/NO_2$ ratio. This is similar to the approach used by Dlugi (1993) using the lifetime of a molecule with respect to a certain reaction as a chemical timescale, i.e. the inverse of the reaction rate constant times the concentration of the reaction partner (for bimolecular reactions; $\tau = [x]k^{-1}$). If the lifetime of a molecule with respect to this certain reaction is not the limiting lifetime in a transport volume or, like for the $NO$-$NO_2$-$O_3$ triad, interchange reactions play a role, the approach of Lenschow (1982) is better to use.

The LOPAP has a time resolution of 5 - 10 min. According to the scheme of Fig. 3 this means that each data point reflects a spatial integration of several hundred meters (volume averaging). Thus, only larger scale motions can be directly resolved by the LOPAP instrument. Furthermore, chemical timescales for formation (black and red horizontal bar) and loss (intensity of photolysis/ red and black arrow) are of the same magnitude as the timescales of the transport processes resolved by the LOPAP. Therefore, both chemistry and transport have an influence on HONO mixing ratios. Due to the limited lifetime of HONO due to photolysis, measurements during day are more locally influenced (within few km) than during night.

## *1.5  Challenges measuring HONO*

Especially during daytime and in remote areas, HONO mixing ratios are in the lower ppt range (e.g. Lammel and Cape, 1996; Kleffmann, 2007). The Differential Optical Absorption Spectroscopy (DOAS), a well-established optical method which detects HONO by its specific UV absorptions (Perner and Platt, 1979) was not capable of detecting daytime HONO mixing ratios of up to 200 ppt (in urban areas) until 2002 (Kleffmann, 2007). Nowadays, DOAS instruments are capable of measuring path averaged (up to 10 km) mixing ratios as low as 15 ppt (Wong et al., 2011b). As summarized by Kleffmann (2007), all specific spectroscopic techniques have either too high detection limits (LOD) or suffer from experimental problems, whereas the sensitive wet chemical techniques (mainly denuders) suffer from interferences. Due to these limitations in either sensitivity or selectivity, new techniques have been developed. These include chemical ionization mass spectrometry (Roberts et al., 2010), cavity ringdown spectroscopy (Wang and Zhang, 2000), cavity enhanced spectroscopy (Gherman et al., 2008) and quantum cascade laser absorption spectroscopy (Lee et al., 2011). Still, many of these techniques suffer from high detection limits (> 100 ppt). Very recently, most of the available techniques have been compared in an intercomparison campaign (Formal Intercomparisons of Observations of Nitrous Acid/FIONA) in the atmospheric simulation chamber "EUPHORE" (Ródenas et al., 2011). Up to now the LOPAP is the only commercially available instrument which is a very sensitive wet chemical system where interferences have been minimized.

The LOPAP is a fast (3 - 10 min time resolution) and sensitive (about 1 ppt detection limit) instrument. As wet chemical instruments are known to suffer from interferences, possible interferences of this instrument were studied extensively (Heland et al., 2001; Kleffmann et al., 2002; 2008; Kleffmann, 2006). Interferences in the LOPAP were minimized by an acidic sampling solution, an external sampling unit and a two channel system, which allows for correcting the interferences (Heland et al., 2001; Kleffmann et al., 2002; 2008; Kleffmann, 2006).

Some disadvantages of the LOPAP are the following:

The instrument is calibrated with solutions prepared fom a nitrite standard solution by dilution with the sampling reagent in the field. These are not stable under daylight conditions (Kleffmann, personal communication 2011). Thus, calibrations have to be conducted in low light conditions or with effective shielding. The sampling solution is corrosive (1 mol L$^{-1}$ HCl) and due to the high number of tube connections within the instrument (which often

become loose) often floods the bottom of the instrument. Due to the outgassing of HCl, the electronics in the cover of the instrument may be affected. Furthermore, the loss of solution causes bubbles in the absorption tubes which cause a (continuous) reduction of the sensitivity. Due to the shift in the baseline (diurnal course) and unwanted peaks, the data processing is rather time consuming.

# 2   Experiments and data

The experimental work of this study was part of three Intensive Observation Periods (IOPs) at two different field sites. IOP I and IOP II of the ExchanGE processes in mountainous Regions (EGER) project where conducted at the "Waldstein Weidenbrunnen" field site of the University Bayreuth in the Fichtelgebirge Mountains in south-east Germany. The Diel Oxidant Mechanism In relation to Nitrogen Oxides (Domino) campaign took place at the "Atmospheric Sounding Station - El Arenosillo", a platform of the Atmospheric Research and Instrumentation Branch of the Spanish National Institute for Aerospace Technology (INTA) at the Atlantic coast in south-west Spain. The DOMINO campaign was a "classical" air chemistry field campaign, with a comprehensive set of measurements regarding radicals (OH, $HO_2$, $RO_2$, $NO_3$), radical precursors ($O_3$, HONO, HCHO, $H_2O_2$), reactive nitrogen species (NO, $NO_2$, HONO, PAN, $NO_3$, $N_2O_5$), total OH reactivity, VOCs, and a very extensive set of aerosol parameters. There was also a good meteorological characterization, but no turbulence measurements. This Eulerian kind of experiment ("looking at the air masses passing by") did not directly address interactions with the surface and boundary layer dynamics. In contrast, the EGER project was designed to study the surface interactions (within a tall canopy) in detail, at the expense of a complete set of chemical measurements. Therefore, not only temporal information but also vertical information about some reactive trace gasses ($O_3$, NO, $NO_2$, HONO) was collected. The detailed analysis of fluxes of non-reactive trace gasses ($H_2O$ and $CO_2$), the turbulence structure and the coupling of the forest canopy with the air layers above allowed studying the influence of turbulence on the measured reactive trace gases.

## 2.1 The ExchanGE processes in mountainous Regions (EGER) project

The focus of the EGER project was to study the energy and matter exchange in a "complex" terrain (dense and tall canopy on a mountain slope). During the Intensive Observation Periods (IOPs) of the EGER project simultaneous measurements of micrometeorological and chemical parameters were made in order to investigate the exchange of energy and matter between a forest ecosystem and the atmosphere. The IOPs took place in September 2007 and June/July 2008 to cover different periods of the growing season. The "Weidenbrunnen" research site is located in the Fichtelgebirge Mountains in south-east Germany (50°08 '31''N, 11°52'01'' E, 775 m above sea level) in a rural forested region. The site is covered by a Norway spruce (Picea abies (L.) Karst.) forest with a canopy height of 23 - 25 m (Staudt and Foken, 2007) and a mean leaf area index (LAI) of about 5 (Foken et al., 2011). A detailed description of the aims of the EGER project and the instrumental setup employed during the IOPs has been given by Foken et al. (2011). The measurements were made at three different sites in the forest stand. A slim 36 m high tower ("turbulence tower") located about 60 m southeast of the main tower (31 m walk-up tower) was used for (undisturbed) turbulence measurements. The "forest floor exchange sites" were located about 30 m northwest (IOP I) and 17 m south (IOP II) of the main tower. Figure 4 shows a schematic view of the instrument setup during IOP I. The LOPAPs were set up close to the forest floor (forest floor exchange site) and just above canopy at the main tower. The turbulence measurements, used to investigate the coupling of the forest and the atmosphere, were made on a slim tower ("turbulence tower").
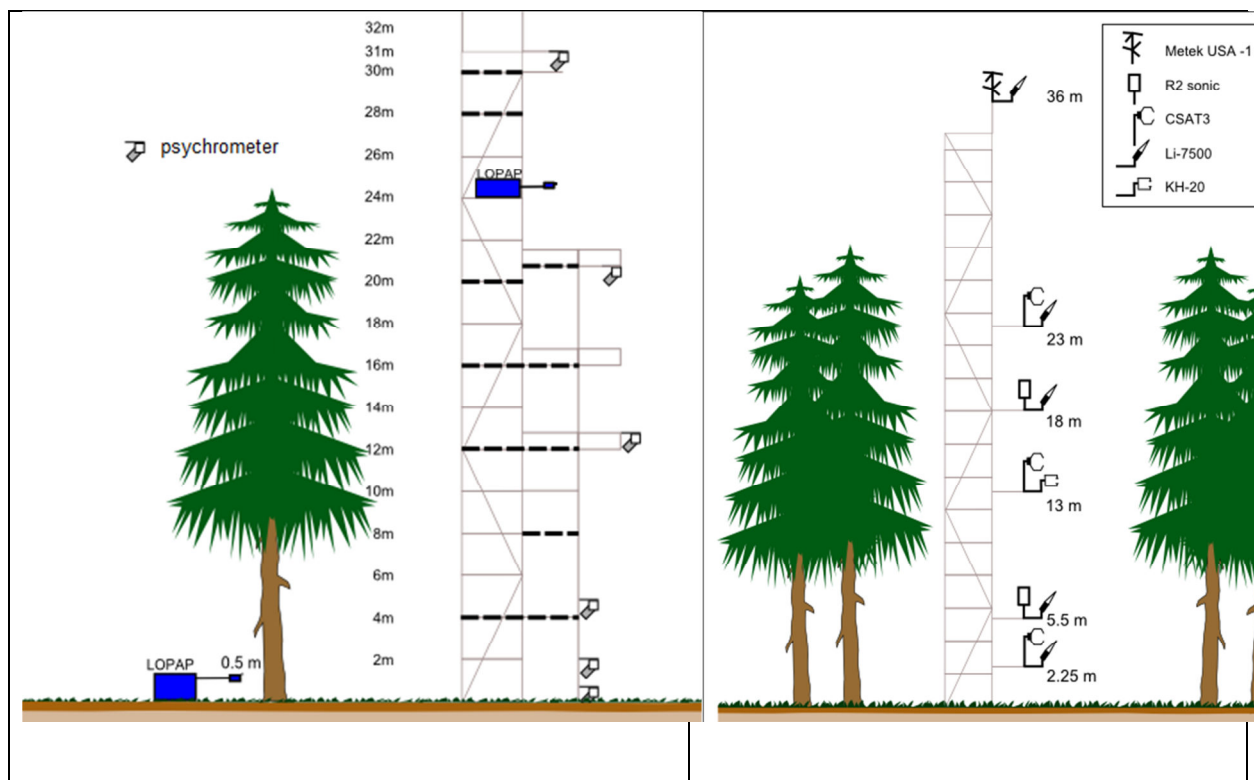
Figure 4: Instrument setup (selection) during IOP I. On the left hand side the main tower with the psychrometer profile for temperature and relative humidity and the positions of the two LOPAPs. The graph on the right hand side shows the setup for the turbulence measurements. The graphs were adapted from Serafimovich et al. (2008).

## 2.2 The Diel Oxidant Mechanism In relation to Nitrogen Oxides (DOMINO) campaign

This international campaign took place at the "Atmospheric Sounding Station - El Arenosillo", a platform of the Atmospheric Research and Instrumentation Branch of the Spanish National Institute for Aerospace Technology (INTA) dedicated to atmospheric measurements in the southwest of Spain (37° 05' 48.03'' N, 6° 44' 07.47'' W). The study was focused on a comprehensive set of measurements regarding air chemistry involving $NO_x$, $HO_x$ and VOCs (http://www.atmos-chem-phys.net/special_issue246.html). The intention of the campaign (based on long term measurements of the prevailing wind direction) was to study the aged urban plume of Seville (~70 km east-north-east) after passing a large area of pine forest with VOC emissions. Unfortunately, during the campaign (mid November to mid December 2008) the prevailing winds were from the north-west and passed the highly industrialized area of Huelva (~ 15-25 km), advecting fresh industrial/vehicle emissions. Also, clean marine air was measured during westerly winds, as the measurement site was about 300 m inland from the coast of the Atlantic Ocean. The canopy of the pine forest

(average height around the measurement platform ~ 6 m; LAI ~ 1.5 (Gonçalves et al., 2010)) was not as dense as the spruce canopy at the EGER site (LAI ~5 (Foken et al., 2011)). The ground consisted mainly of dry sandy soil. The measurement platform was at 10 m height, thus about 4 m above the canopy. No turbulence measurements were available. A detailed assessment of surface exchange was therefore not possible. Fortunately, the comprehensive set of air chemical measurements allowed a detailed analysis of the HONO daytime source and its relation to $NO_2$ and actinic flux.

# 3  Objectives

The overall aim of this thesis was to locate and quantify sources and sinks of HONO in rural forested areas. Other than in prior studies a stronger emphasis was placed on the influence of transport processes. Therefore, simultaneous measurements at different heights, to gain both temporal and spatial information, were planned. To achieve these overall goals, several sub goals have been defined, which are as follows:

1) To characterize the precision of the LOPAP instruments by comparing them under field conditions. This is especially important for the validation of vertical mixing ratio differences.

2) To quantify the HONO daytime source in rural forested environments and to evaluate if it is related (correlated) to a photochemical production of HONO from $NO_2$.

3) To exclude (as far as possible) proposed reactions which have negligible contribution to the HONO daytime source.

4) To study the source and sink distributions within a forest canopy. Are the proposed sources in line with these distributions?

5) To extract (as far as possible) which of the observed effects were caused by transport and which were caused by chemistry.

6) To study the influence of relative humidity on HONO mixing ratios and provide tools to separate this influence from other influencing parameters.

# 4  Results

The results are structured the following:

A prerequisite, especially for studying the vertical mixing ratio differences, was to compare the LOPAPs side by side under field conditions. This is the first section as it contains important information for all other studies. The following three main parts of the thesis, the HONO daytime formation, the HONO vertical exchange and the influence of RH on HONO mixing ratios discuss the main results from the three manuscripts (Appendix B, C, D).

## 4.1  Characterization of the LOPAPs

The two LOPAPs used to measure vertical differences have been compared under field conditions (EGER IOP I¸Sörgel et al., 2011a). This was realized by mounting the external sampling units side-by-side (~ 50 cm distance) perpendicular to the main wind direction. The instruments were fed with the same reagent solutions via a T-piece. Calibrations and data processing (e.g. baseline fit, deleting unwanted peaks) were done by the two operators individually. As shown in Fig. 5 (insert) no systematic error was found (slope 0.97, intercept 2.4 ppt) during dry conditions, thus the calibration and zero fit are robust although being processed by different operators. The instruments agreed within 12 % during dry conditions (two times standard deviation of the relative difference of the two instruments) which is within the estimated instrumental error (10-15 %, Heland et al., 2001). The physical (or chemical) reasons for the huge deviations between the two instruments during rainy and foggy conditions (indicated by visibility < 1000 m Fig. 5) are not clear yet. Potentially, the surfaces of the inlets (first centimeter of the hand-made stripping coils before contact with the sampling reagent) exhibited different wettability due to different roughness of the glass surface. During IOP I, HONO values were always above 15 ppt, which was suspected to be caused by interferences. However, values dropped below the detection limits (~2 ppt under these conditions) during measurements in a clean marine air mass with the same instruments in Spain (DOMINO), showing that in "HONO-free" background air no interferences exist which are not corrected by the two channel system.
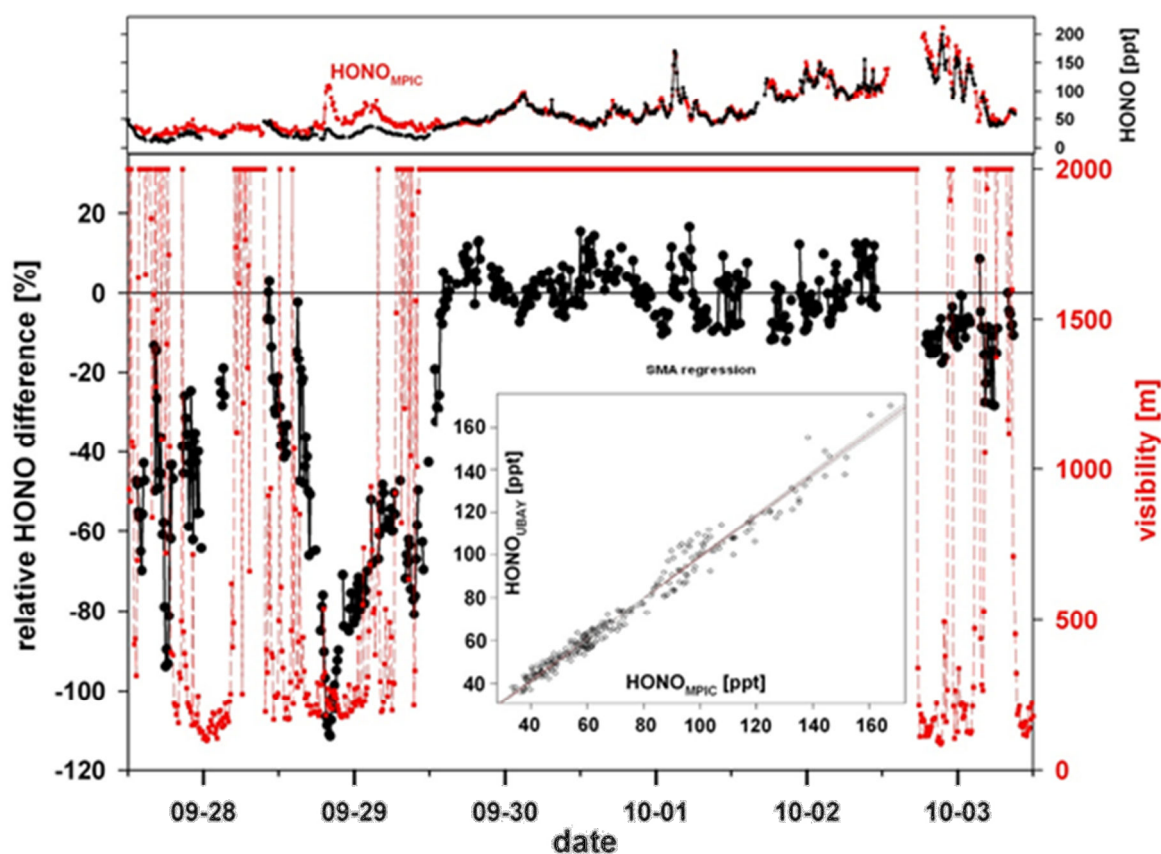
Figure 5: Side-by-side measurements of the two LOPAP instruments from 27 September (noon) to 3 October 2007 (noon) at the "Waldstein-Weidenbrunnen" research site. Relative differences of the HONO signals (black dots) and visibility range (red squares, dashed lines, maximum range 2000 m). The insert shows the regression obtained during dry conditions (N = 247) from 29 September (14:00 CET) to 2 October (10:00 CET) using standard major axis (SMA) regression. The upper panel shows the mixing ratios measured by the two LOPAP instruments. Missing values are due to zero air measurements and calibration of the LOPAP instruments. Taken from Sörgel et al., 2011a.

## *4.2  Daytime source*

During daytime HONO is photolyzed to OH and NO. NO and OH react in a termolecular reaction which regenerates HONO. These reactions reach a photostationary state (e.g. Kleffmann et al., 2005). If the reaction of NO with OH would be the only HONO source during daytime, this cycle would not result in net OH radical formation. All recent studies measured HONO mixing ratios well above the photo stationary state (PSS), although only in few studies all quantities necessary to calculate the PSS were measured directly (summarized by Kleffmann, 2007; Sörgel et al., 2011b). During the DOMINO campaign all required quantities (NO, HONO, OH, *j*(HONO)) were measured directly, and the measurements were collocated. Measured HONO values were more than a factor of three higher than PSS values for most of the data (75 percentile). As OH measurements were possibly influenced by

interferences, the calculated PSS values represent rather upper limits. Thus, this study confirmed the existence of an additional daytime source. Furthermore, in this study the source strength of OH radical formation from HONO photolysis was compared to the "classical" primary OH source from ozone photolysis. Although the contribution of ozone photolysis was higher during intense UV insolation around noon, the integrated OH formation over the day was about 20 % higher from HONO photolysis. HONO was the most important primary OH radical source during the DOMINO campaign (Regelin, 2011).

The additional daytime source can be calculated by combining known sources and sinks to a budget equation (Su et al., 2008b; Sörgel et al., 2011c). From this budget, the unknown HONO daytime source ($P_{unknown}$) was derived, with the assumption dHONO/dt = P(roduction)-L(oss) = 0. The production terms consist of the dark heterogeneous formation ($P_{het}$), the reaction of NO with OH ($P_{NO+OH}$) and the unknown source ($P_{unknown}$) and therefore $P = P_{het} + P_{NO+OH} + P_{unknown}$. The loss terms are the deposition ($L_{dep}$), the photolysis ($L_{phot}$) and the reaction of HONO with OH and therefore $L = L_{dep}+L_{phot}+L_{HONO+OH}$. Thus, the unknown source can be calculated as $P_{unknown}= L - (P_{het}+P_{NO+OH}) + dHONO/dt$. Hence, measured increases in concentrations ($\Delta HONO/\Delta t > 0$) mimic source terms, and decreasing concentrations ($\Delta HONO/\Delta t < 0$) mimic sink terms. As $\Delta HONO/\Delta t$ has a substantial contribution to the HONO budget (see Fig. 6) it was further analyzed. Firstly, to exclude additional source or sink terms simply caused by instrument variations, values of $\Delta HONO/\Delta t$ within the instrumental error ($\pm$ 12 %) of the LOPAP have been omitted. The relative contribution of $\Delta HONO/\Delta t$ to the HONO budget was found to depend on the averaging time with the lowest contribution for 30 min averages as fluctuations are averaged out. Nevertheless, a higher time resolution of 5 min was chosen. Most of the $\Delta HONO/\Delta t$ values larger than the instrumental error of the LOPAP were caused by advection (simultaneous peaks e.g. in $NO_x$, black carbon), where the arrival of the plume mimicked a source term whereas the fading mimicked a sink. Figure 6 shows the mean budget contribution of the different production ($P_{het}$, $P_{NO+OH}$) and loss processes ($L_{dep}$, $L_{HONO+OH}$, $L_{phot}$). $P_{het}$ is the parameterized "dark heterogeneous" formation, which was parameterized from the nighttime increase of HONO mixing ratios (after Alicke et al., 2002). However, as discussed in detail by Sörgel et al. (2011c), it is questionable if these values are transferable to daytime conditions. This is because HONO is formed heterogeneously, and thus, the formation rate depends not only on the precursor ($NO_2$) concentration but also on the available reactive surface in a given volume (surface to volume ratio; S/V). As the mixed volume (V) depends on vertical diffusivity, the S/V ratio in turn depends on atmospheric stability which is different during the

day and nighttime. During day, vertical mixing is typically enhanced (neutral or convective surface layer), which increases the mixed volume, and thus the S/V ratio becomes smaller.

The gas phase reaction of NO with OH ($P_{NO+OH}$) is the most important known formation reaction. The loss of HONO by deposition ($L_{dep}$) was parameterized in a simple way by scaling the deposition flux (deposition velocity times concentration) by the mixed layer height (after Harrison et al., 1996). As the loss by deposition occurs at surfaces (ground or aerosol) $L_{dep}$ can also be regarded as a heterogeneous loss reaction which therefore is also sensitive to S/V. A constant mixed layer height of 1000 m was assumed for the parameterization. This may lead to an underestimation of the relative contribution of HONO loss by deposition in a shallow boundary layer, which might explain a "negative unknown source" in the morning and the afternoon (cf. Fig. 6). If wetting of surfaces in the morning and afternoon may be an alternative explanation is ongoing research. Nevertheless, the contribution of $L_{dep}$ to the HONO budget is negligible during most of the day. Furthermore, the loss of HONO by the reaction of HONO with OH ($P_{HONO+OH}$) is also almost negligible (< 5 % for all data). The dominating loss term during day is therefore photolysis ($P_{phot}$). The most important HONO formation term is $P_{unkown}$.
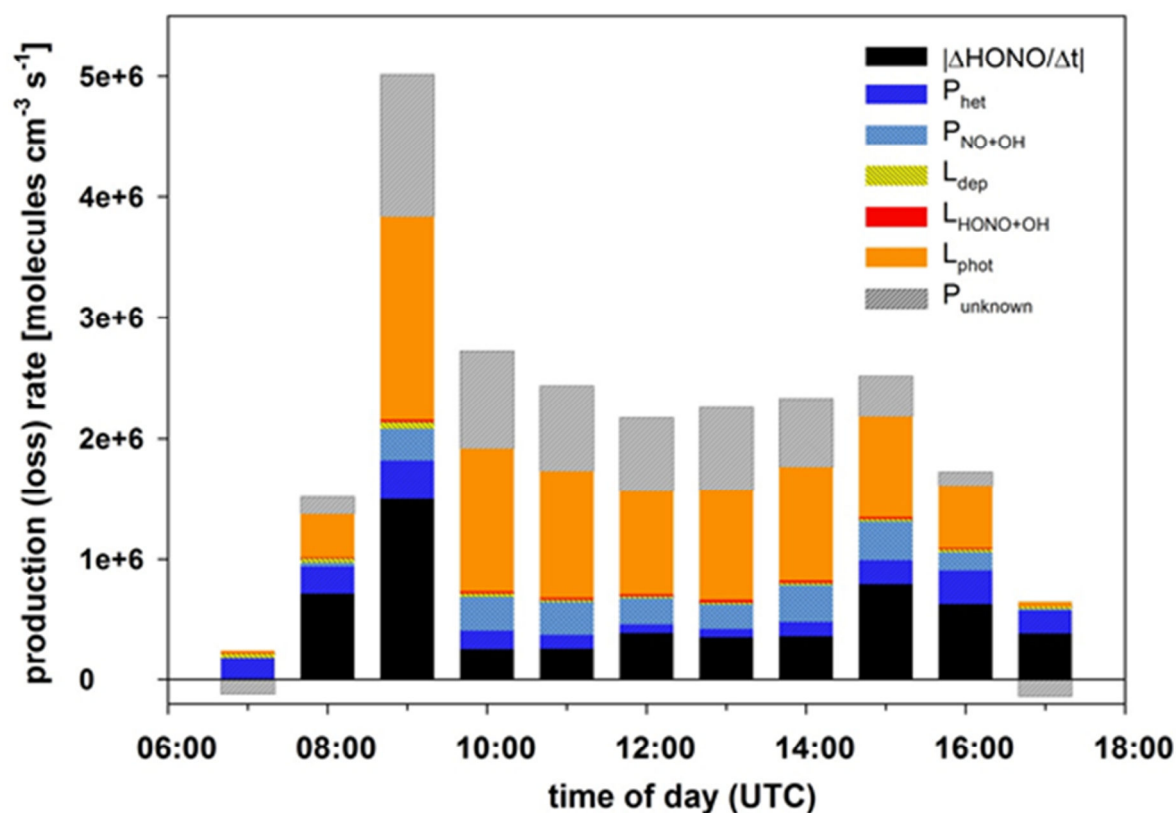


Figure 6: Contributions of production (bluish colours) and loss terms (hourly means 21st Nov. to 5th Dec.) as well as the unknown daytime HONO source $P_{unknown}$. Taken from Sörgel et al., 2011c.

In order to improve the comparability with other studies (urban and remote regions) and to analyze the relation of $P_{unknown}$ to the most probable precursor $NO_2$ and the actinic flux (light-induced conversion) Sörgel et al. (2011c) introduced a normalization of $P_{unknown}$ by $NO_2$. A very recent study about HONO daytime gradients used the same scaling approach (Wong et al., 2011b). It was shown (Fig. 7; Sörgel et al., 2011c) that the scaling efficiently removed the high HONO formation values caused by advection of polluted air in the morning. The normalization led to a slightly better linear correlation with the photolysis frequency of $NO_2$ ($r^2 = 0.38$ instead of 0.16). Furthermore, it provided evidence for the existence of an upper limit for $NO_2$ conversion depending on light intensity (Fig. 7b; Sörgel et al., 2011c). The coefficient of determination could be further improved to 0.47 by restricting the data only to clear (dry) days and excluding the values influenced by advection ($\Delta HONO/\Delta t >$ relative error LOPAP, filled red dots Fig. 7). There might be several reasons for this weak correlation. Firstly, there are other local HONO sources like soil emissions (Su et al., 2011) or photolysis of adsorbed $HNO_3$ (e.g. Zhou et al., 2011) which do not involve direct $NO_2$ conversion. A hint in that direction might be that the highest conversion frequencies ($NO_2$ to HONO in % h$^{-1}$ Fig. 7b) were measured on a quite clean day with low $NO_x$ values. As important parameters (surface nitrate loading, content of photosensitizers on the surfaces, HONO soil emissions and vertical diffusivity) to quantify the source strength of these processes were not measured, only rough estimates of the contribution of these sources could be provided (Sörgel et al., 2011c). Secondly, $NO_2$ and HONO exhibit different temporal variability, due to different chemical time scales. The $NO_2$ lifetime with respect to photolysis is about a factor of three lower than that of HONO. On the other hand, the formation of $NO_2$ by oxidation of NO (by $O_3$ or $HO_2$) is faster than the formation of HONO from $NO_2$. Weaker correlations of HONO and $NO_2$ (both daytime and nighttime) in distance to emission sources (cities) have been observed by Harrison et al. (1996). A very recent PhD thesis by Pöhler (2010) employed a DOAS with different light paths using tomography to infer two-dimensional trace gas distributions of HONO and $NO_2$. HONO displayed a much lower spatial variability than $NO_2$, presumably due to the slow heterogeneous formation (Pöhler, 2010). Thirdly, if HONO mixing ratios are governed by surface water absorption (and thus RH), the HONO signal but not the $NO_2$ signal would be modulated by this effect. A detailed model approach which solves boundary layer dynamics, chemistry and effects of turbulence on chemistry as well as surface modifications (wetting) is required to solve this issue.
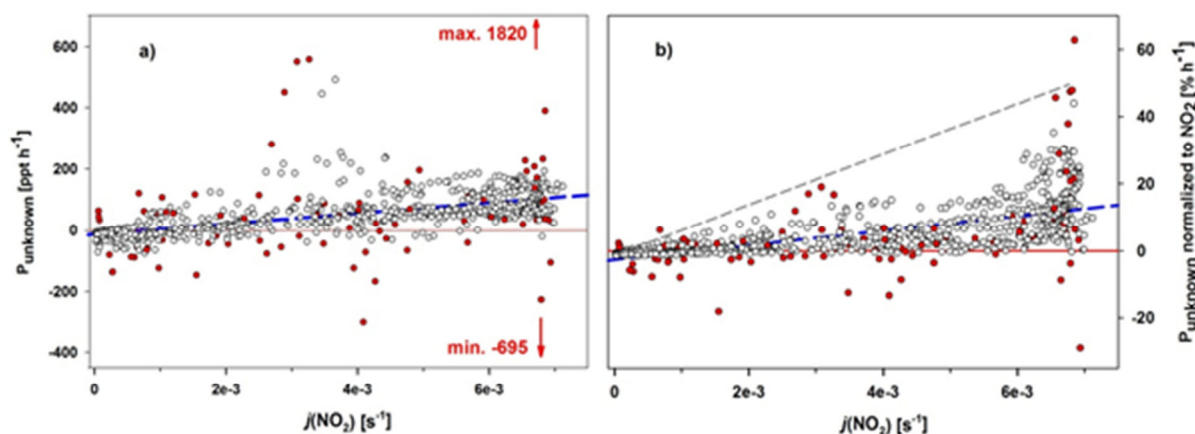
Figure 7: a) Unknown HONO daytime source ($P_{unknown}$) in ppt h$^{-1}$ versus $j$(NO$_2$). b) $P_{unknown}$ normalized by NO$_2$ mixing ratios yielding a conversion frequency (% h$^{-1}$). Figure a) contains only data points (N = 753) which could be normalized to NO$_2$. Points where $\Delta$HONO/$\Delta$t was larger than the relative error of the LOPAP ($\pm$ 12 %) are marked as filled red points. Blue dashed lines are linear fits to the data yielding a) r$^2$ = 0. 16 and b) r$^2$ = 0.38. The grey dashed line in Fig. 7b presents an upper limit based on the mean of the five lowest points at ($j$NO$_2$)$_{min}$ and five highest points at ($j$NO$_2$)$_{max}$. Taken from Sörgel et al. (2011c).

Two reactions forming HONO via light-induced NO$_2$ conversion were investigated in detail, as most parameters to calculate the HONO formation rate by these reactions were measured, i.e. the reduction of NO$_2$ on irradiated soot (Monge et al., 2010) and the reaction of electronically excited NO$_2$ with water vapor (Crowley and Carl, 1997; Li et al., 2008). The latter reaction, which forms HONO and OH in equal amounts, raised special attention and controversial discussion since the publication of Li et al. (2008). These authors found a rate constant for this reaction which was an order of magnitude higher than that originally measured by Crowley and Carl (1997) and confirmed by Carr et al. (2009). This higher value would have a substantial impact on the oxidation potential (Wennberg and Dabdub, 2008; Sarwar et al., 2009; Ensberg et al., 2010). During the DOMINO campaign the reaction of NO$_2$* with water vapor was found to contribute less than 10 % to HONO formation even by taking the value of Li et al. (2008) as an upper limit (Sörgel et al., 2011c). A very recent study (Amedro et al., 2011) confirmed the lower value for the reaction rate constant measured by Crowley and Carl (1997) and Carr et al. (2009). Thus, this reaction contributed less than 1 % to $P_{unknown}$. The same negligible contribution (< 1 %) was calculated for the reaction of NO$_2$ on irradiated soot for the conditions during DOMINO. Thus, for rural conditions (low NO$_x$ and black carbon) both reactions do not substantially contribute to HONO daytime formation.

## *4.3  HONO vertical exchange in a forest environment*

It is highly probable that HONO is formed heterogeneously mainly at ground surfaces both day and night. A forest provides a large surface area and, separated by the canopy, different environments with respect to light and humidity. During IOP I, HONO was measured just above the canopy (24.5 m) and close to the forest floor (0.5 m). The temporal evolution of the mixing ratios at the different heights and the corresponding mixing ratio differences have been analyzed with special emphasis on turbulent mixing (Sörgel et al., 2011a). For this detailed analysis the so called Golden Days of IOP I (20-25$^{th}$ of September 2007) where chosen. This was a warm and dry period between two rain events.

The most astonishing but also clear result was that mixing ratio differences were around zero in the late morning to early afternoon (Fig. 8). Due to a longer lifetime of HONO (by a factor 10 to 30) below canopy because of the shading by the canopy, huge concentration differences had been expected. This discrepancy could be explained by intense vertical mixing as indicated by the coupling regimes. The coupling regimes denote which part of the canopy is coupled to the air layer above, and thus indicates which part of the canopy takes part in the exchange of energy and matter (Thomas and Foken, 2007). During the period when concentration differences were close to zero the canopy was either fully coupled or coupled by sweeps with only intermittent decoupling of the subcanopy. Already in the afternoon (starting at 13:00 CET) the subcanopy becomes decoupled from the air layer above and mixing ratio differences increase. During this period mixing ratio differences were always negative (i.e. below canopy values higher than above) and exhibited low variability (Fig. 8). Around sunset the whole forest became decoupled from the air layer above and during night, wave motion dominated. Thus, vertical exchange was limited and different sources and sinks (above and below canopy) became obvious. After sunset, differences became even more negative (up to – 170 ppt), mainly caused by increasing values below canopy. In the absence of light (photolysis) this was attributed to local HONO formation below canopy (Sörgel et al. 2011a). Around 21:00 CET the sign in mixing ratio differences changed due to increasing values above canopy. For some cases this could be attributed to advection of HONO-enriched air above canopy, which only partly penetrated into the canopy leading to mixing ratio differences up to ~240 ppt. The fact that advection became visible only after sunset can be related to the increasing influencing area due to the increase in HONO lifetime (from about 10 min at noon to >> 1 h at night; cf. Fig. 3). The nearest (~ 30 km) relevant sources are the cities of Kulmbach and Bayreuth and the motorway A9 (9 km). Thus, taking a wind speed of

5 m s$^{-1}$, transport from these sources would require a time of 100 min (> 2 h) and 30 min, respectively. Sörgel et al. (2011a) speculate if the constantly higher HONO values above canopy during the late night (apart from advection events) could be attributed to the wetting of the canopy due to water adsorption, caused by radiative cooling of the canopy top. Co-adsorbing water replaces HONO at the surfaces, according to the mechanism provided by Trick (2004). The only clear influence of surface water was the scavenging of HONO at relative humidities > 95 %, which structured the HONO time series due to rain events associated with the occurrence of synoptic systems. Therefore, the interplay of HONO and RH was studied further with a tool for time series analysis (Sörgel et al., in preparation).



Fig. 8. Box-and-whisker plot for coupling regimes (red open bars) and HONO mixing ratio differences (grey filled bars) for the five-day dry period 20–25 September 2007 at the "Waldstein-Weidenbrunnen" research site. Coupling regimes (right hand side) are: Wa (Wave motion ∼ no turbulent exchange), Dc (decoupled canopy ∼ whole canopy decoupled from the air layer above), Ds (decoupled subcanopy ∼ only subcanopy decoupled), Cs (coupled by sweeps ∼ canopy and subcanopy coupled by sweep motion) and C (fully coupled canopy). The upper panel shows the specific humidity difference between 21 m and the forest floor for comparison. The upper end of the boxes represents the 75th percentile, the lower end the 25th percentile and the line within the boxes the median. Whiskers denote the 10th (lower whisker) and 90th (upper whisker) percentiles. Outliers are marked as points (HONO difference) or squares (coupling regimes). If only whiskers appear, there are no other values between the values marked by the whiskers. For the boxes at 10:00 and 14:00 CET the median falls in line with the lower end of the boxes (Ds). Taken from Sörgel et al., 2011a.

## 4.4  Influence of RH on HONO mixing ratios
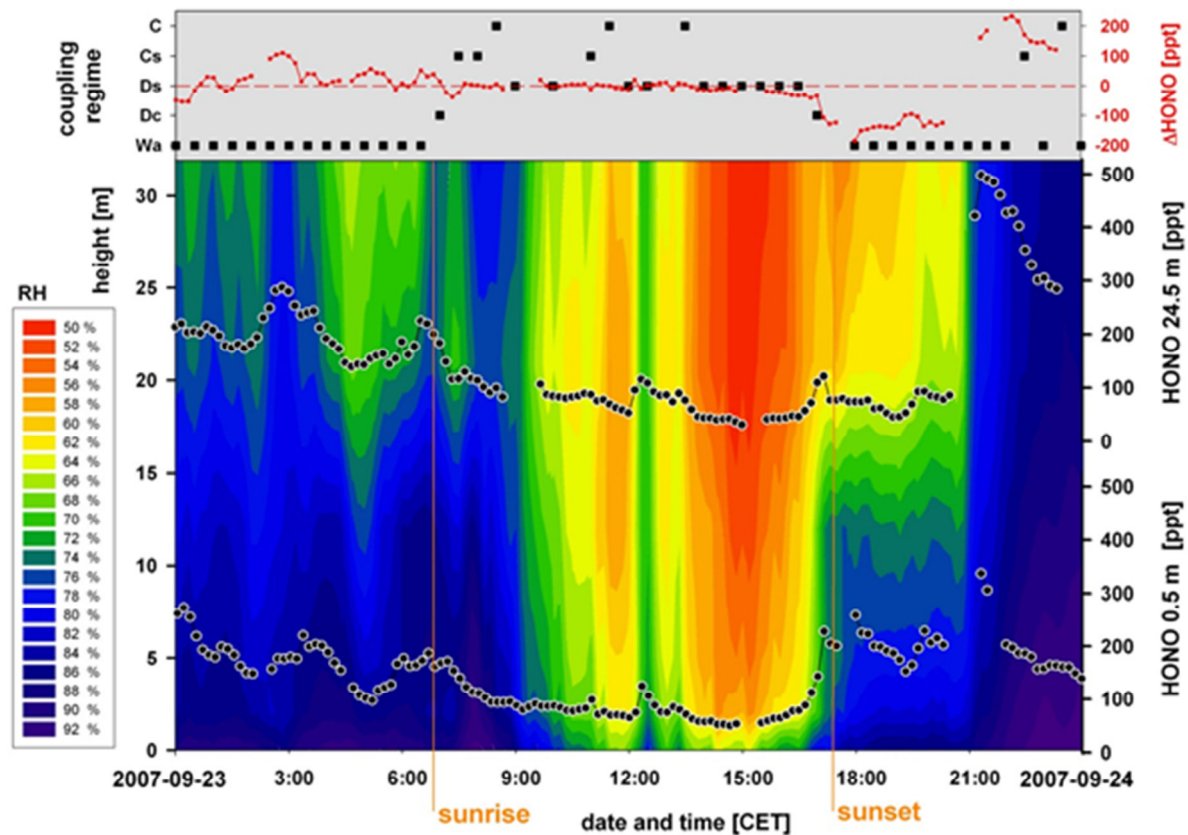


Fig. 9. Simultaneous time series of HONO (right hand scales) at 0.5 m (lower graph, circles and lines) and 24.5m (upper graph, circles and lines), overlaid with a contour plot of the vertical profile of measured RH (left hand scale and color coded 50–92 %) for 23 September 2007 at the "Waldstein-Weidenbrunnen" research site. Missing values in the HONO measurements are due to zero air measurements. Sunrise and sunset (inferred from $j(NO_2)$ and global radiation measurements) are marked as vertical (orange) lines. The upper panel shows the mixing ratio differences between 24.5 m and 0.5 m (1HONO) and the coupling regimes in the forest. Taken from Sörgel et al. (2011a).

In all time series (IOP I, IOP II and DOMINO) HONO seemed to be influenced by RH (co-variation, signal dampening, increase or decrease correlated). An example is given in Fig. 9, where HONO measurements at two different heights were overlaid with a contour plot of the relative humidity profile on a clear and dry day (IOP I). The canopy height was 23 m. During night, HONO features at both heights seemed to be correlated to features in RH which extend throughout the canopy. In the morning, RH and HONO decrease due to increasing radiation. HONO mixing ratios decrease due to photolysis and RH due to surface heating. The peak in HONO and RH around noon was associated with passing clouds and a change in wind direction. The increase in HONO and RH in the late afternoon was caused by the decoupling of the forest and subsequent accumulation of HONO and water vapor emitted at the ground. The sharp increase of both quantities at 21:00 CET was caused by an air mass change. Thus,

for only one day several different correlations could be identified for different reasons (Sörgel et al., 2011a). This result stressed the importance to use tools for time series analysis in order to investigate causality between HONO and RH.

Starting with "classical statistics" and taking all values from all campaigns, the linear correlation of HONO and RH was low (r=0.01). A first statistical analysis revealed that HONO values were log-normally distributed, whereas RH values were normally distributed or showed a bimodal distribution. Thus, for a linear correlation after Pearson the logarithmic HONO values have to be correlated with the RH values. This indeed improves the correlation, but mainly due to daytime data. Further improvement in the coefficient of determination was achieved by excluding HONO values measured in marine air masses during DOMINO which might be influenced by equilibrium with the sea surface (Wojtal et al., 2010). Nevertheless, taking only nighttime data, the coefficient of determination is still low ($r^2 \sim 0.13$).

Part of the influence on the relation of HONO and RH might arise from variations of the HONO precursor $NO_2$, but correlations of HONO and $NO_2$ were weak as well, especially for IOP I ($r^2 = 0.14$ at 24 m and $r^2 = 0.05$ at 0.5 m). The very weak correlation of HONO with its precursor $NO_2$ was the main motivation to think about the influence of RH. Although correlations of HONO with $NO_2$ were higher for IOP II and particularly good for DOMINO ($r^2 = 0.44$), this reflects more a tendency (higher $NO_2$ = higher HONO) than a strong correlation. This might be attributed to the rather slow formation of HONO from $NO_2$ (max. 2 % $h^{-1}$). This means that HONO mixing ratios build up slowly are thus more evenly distributed, whereas $NO_2$ values might be quite variable as indicated by the results of Pöhler (2010) and Harrison et al. (1996). Therefore, HONO values were not normalized to $NO_2$ to avoid disturbances of the HONO to RH correlation due to variations in $NO_2$. Usually, normalization to $NO_2$ is done to account for changes in boundary layer height and precursor concentration. Some shortcomings of this scaling approach have already been discussed by Su et al. (2008 a). By applying Singular System Analysis (SSA), correlations on different time scales can be found and may possibly allow for a separation of HONO and $NO_2$ and HONO and RH correlations. SSA (e.g. Elsner and Tsonis, 1996) was chosen for this analysis as it provides the opportunity to reconstruct the time series by using signal contributions associated to certain time scales. This is necessary to remove the signal contributions of the diurnal cycle of HONO and RH and the long term trends in order to identify correlations on shorter time scales which might be a hint at the interaction due to fast physical processes (adsorption/desorption).

The SSA analysis of the HONO and RH time series revealed that the main signal contributions were the long term trends and the diurnal cycle (about 98 % for RH and 50-80 % for HONO). Therefore, it was rather challenging to extract correlations from the remaining signal as this contained both signal and noise. However, as can be seen in Fig. 10, the diurnal cycle and the long term trends are effectively removed by this technique. Only during the rainy periods (RH > 95 %) with almost constant values (RH ~ 98 - 100 %, HONO ~ 15 – 40 ppt) this method induced a non-existent diurnal cycle (Fig. 10, 18.09 - 19.09). Filtered time series (without long term trends and diurnal cycle) of HONO were weak but positively correlated to the filtered RH signals pointing to at least some influence of RH on HONO apart from diurnal cycle and long term trends.
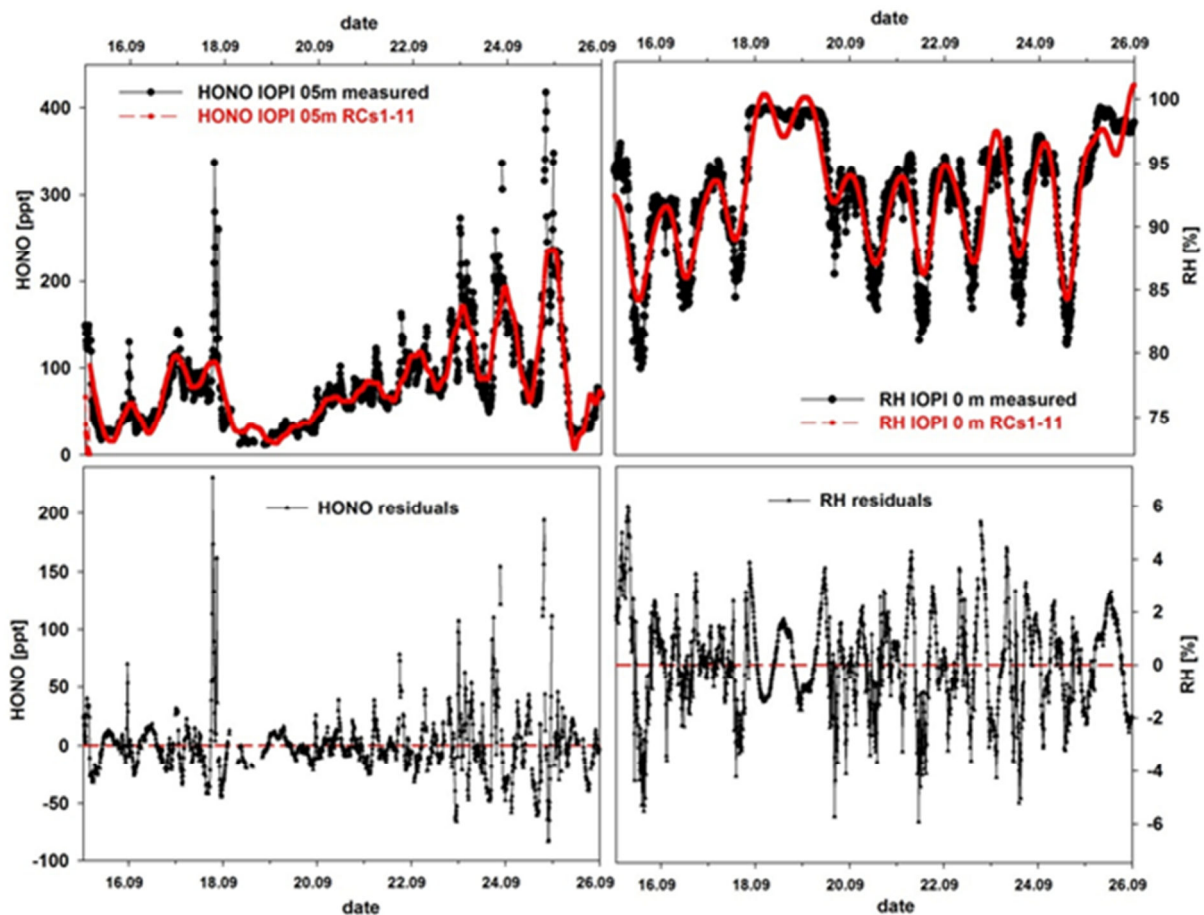


Figure 10: Upper left panel: HONO measured (black dots) and reconstructed time series (red line) using the long term trends and the diurnal cycle; upper right panel: measured RH (black dots) and reconstructed time series (red line) using the first 11 EOFs; lower panels: residuals after subtracting the reconstructed time series from the measured time series for HONO (left) and RH (right). Taken from Sörgel et al. (2012).

# 5  Conclusions and outlook

It has been demonstrated that two different LOPAP instruments agreed within 12 % under field conditions with no systematic deviation and reached a detection limit of about 2 ppt. Therefore, these instruments can be regarded as reliable to study the vertical distribution of HONO (especially small mixing ratio differences during daytime). However, these instruments exhibited large relative deviations (up to 100 %) during rainy and foggy conditions. Thus, the LOPAP is not reliable under these conditions. Further experiments to ascertain the possible causes (physical or chemical) are needed.

A detailed budget analysis (sources and sinks) for HONO has been conducted for the DOMINO campaign (Sörgel et al., 2011c). This analysis put special emphasis on discussing the uncertainties in the parameterization of the dark heterogeneous HONO formation for daytime conditions. As this reaction is heterogeneous, measured mixing ratios depend on the surface to volume ratio (S/V). This ratio itself depends on vertical diffusivity and thus on atmospheric stability. Another prerequisite is the deposition of the HONO precursor $NO_2$ which is also influenced by vertical diffusivity, but presumably in the opposite direction. As the reaction mechanisms and the reaction rates on most natural surfaces are not exactly known, they have to be parameterized from the nighttime conversion rates (Alicke et al. 2002). These conversion rates are quite similar (0.4 -2 % $h^{-1}$) for different environments (summarized by Su et al., 2008a; Sörgel et al., 2011a). The deposition of HONO in turn can be regarded as a heterogeneous loss process and therefore, also as sensitive to S/V. Furthermore, both formation and deposition might be influenced by the amount of water adsorbed on surfaces. Presumably, such changes in S/V and surface wetness were responsible for the "negative" unknown source in the early morning and the late afternoon, as this could be either caused by overestimation of the source or underestimation of the loss processes. As the contribution of these terms to the budget might be higher in the morning and evening, they may change the shape of the diurnal profile of $P_{unknown}$. This may be critical for studies which try to identify the photochemical processes by correlation of HONO formation with different geometries of light (like for example Wong et al. (2011b) with irradiance and actinic flux). Therefore, the relative contribution of the dark heterogeneous HONO source and the deposition sink to the HONO budget during daytime should be addressed by modeling studies resolving vertical diffusivity.

The most important HONO loss term during DOMINO was photolysis, and the most important source term was the unknown source, followed by the combination reaction of NO

with OH, which contributed less than one third of the HONO formation. The unknown daytime source has been further analyzed with respect to its light dependence and the influence of the most probable precursor $NO_2$ (light-induced $NO_2$ conversion). It was confirmed that the HONO daytime source is light-dependent, but correlations were found to be weak. A normalization of the unknown source with $NO_2$ values was introduced, which improved the correlation. This indicates an influence of $NO_2$ availability. The maximum coefficient of determination that was achieved by restricting the data to clear days and excluding values associated to advection events was 0.47. The weak correlation ($r^2_{max} = 0.47$) of the normalized unknown source with light intensity might be caused by the presence of additional HONO sources which do not involve direct $NO_2$ conversion such as $HNO_3$ photolysis (e.g. Zhou et al., 2011) and soil emissions from microbiological activity (Su et al., 2011). Again, a model approach is required which can estimate the "real" source strength by taking vertical mixing and loss by photolysis (and to aerosols) into account. This source strength can then be compared to the source strength of possible ground sources. These include light-induced $NO_2$ conversion on humic acids (Stemmler et al., 2006), $HNO_3$ photolysis at surfaces (e.g. Zhou et al., 2011), and HONO soil emissions (Su et al., 2011).

Although the correlation of the normalized unknown source with light intensity was quite low ($r^2 \sim 0.4$), an upper limit for light intensity dependent conversion was proposed. Two possible HONO formation pathways of light-induced $NO_2$ conversion (Li et al., 2008; Monge et al., 2010) were found to be negligible HONO sources (< 1 % contribution) for the conditions during DOMINO (median $NO_2$ < 1 ppb and median black carbon < 500 ng m$^{-3}$), and therefore most rural sites. Furthermore, this study confirmed that reactions for nighttime formation of HONO involving NO were not of atmospheric relevance. The integrated primary OH formation due to HONO photolysis was about 20 % higher than that of ozone, thus confirming the importance of HONO as an OH radical precursor.

The influence of vertical mixing on HONO mixing ratio differences was investigated in detail during EGER IOP I in and above a dense (LAI ~ 5) and tall (~ 23 m) forest canopy. Despite the light dependence of daytime HONO formation and the different HONO lifetimes above and below canopy due to photolysis, mixing ratio differences were around zero at noon. As the differences in lifetimes (about 10 min above and up to 250 min below canopy around noon) were rather large, this unexpected result stressed the importance of the influence of vertical mixing on HONO mixing ratios. Identification of the coupling regimes (Thomas and Foken, 2007) has been found to be a very useful tool to study the influence of vertical exchange on mixing ratio differences. Even though the original paper about coupling regimes

(Thomas and Foken, 2007) already recognized the potential influence of coupling on reactive trace-gas species, this was the first study to use the coupling tool for interpretation of vertical mixing ratio differences. The importance of considering coherent exchange for the interpretation of gradients of trace gases in forests was recently highlighted by Steiner et al. (2011). Also recently, Foken et al. (2011) extended the use of this coupling scheme for the interpretation of other reactive and non-reactive trace-gas gradients as well as trace-gas fluxes and provided a more general discussion.

It has been shown by this study (Sörgel et al., 2011a), that the mixing ratio differences of HONO were caused by different sources and sinks within and above the forest canopy, but that the magnitude of the differences depends on the vertical mixing. For example, around noon large differences were expected due to light dependent sources and sinks and shading by the canopy, but they were offset by efficient vertical exchange. The decoupling of the subcanopy in the early afternoon led to a faster increase in mixing ratios below canopy. The mixing ratio differences increased further around sunset when the whole forest was decoupled from the air layers above. HONO mixing ratios were up to 170 ppt higher below canopy, which was attributed to local formation below canopy. In the later night the sign of the mixing ratio differences changed due to increasing values above canopy. For some cases, especially extremely high mixing ratio differences of up to 240 ppt, this could be attributed to advection of HONO enriched air which only partly penetrated the canopy due to decoupling of the forest canopy. Therefore, the coupling regimes can be denoted as an essential tool for studying vertical trace gas profiles in tall vegetation. Furthermore, these results have important implications for above-canopy concentration and flux measurements, as it has been shown that sources and sinks below canopy or in the canopy are often decoupled from the measurements above canopy.

Advection of HONO enriched or HONO depleted air masses can cause misinterpretations if attributed to local chemistry or physical processes. The analysis of the temporal and the corresponding spatial scales is useful to identify possible sources (e.g. traffic, industry) and sinks (e.g. ocean surface) other than the local sources and sinks. The area of influence increases with increasing lifetime and horizontal wind speed. The lifetime of HONO is limited by photolysis during daytime, whereas during nighttime it is only limited by deposition (which is comparatively slow). Only around noon when HONO lifetimes are 10 to 15 min the measurements reflect local conditions. Decoupling of the subcanopy was identified as an opportunity to study local HONO formation despite long lifetimes of HONO in the early night (Sörgel et al. 2011a). Under these conditions, local formation below the

canopy has been observed in the early night (Sörgel et al., 2011a). However, decoupling only limits but does not prevent vertical exchange, and therefore, advection in the later night can also be observed at the forest floor. Therefore, considering the HONO lifetimes and the corresponding spatial scales is necessary to elucidate "how local" the measurements are.

The influence of relative humidity on HONO mixing ratios could not be fully elucidated and is subject to ongoing research. A prerequisite to study correlations of HONO and RH on timescales less than a day is to remove the diurnal cycle from the time series. Both HONO and RH are correlated due to the diurnal cycle but this is simply caused by radiation (photolysis for HONO and heating for RH). Removing the diurnal cycle and long term trends was achieved by using Singular System Analysis (SSA), a statistical tool for time series analysis. SSA was found to effectively remove the long term trends and the diurnal cycle, but the remaining signal also contains all noise components of the original signal. Therefore, correlations might be disturbed by the noise. HONO values were log-normally distributed, and RH values followed a normal or bimodal distribution. Thus, for a linear correlation after Pearson the logarithm of HONO values has to be correlated with RH. SSA clarified that the main signal contributions arise from the long term trends on time scales of synoptic systems and it was possible to quantify these contributions. For RH it was about 98-99 %, whereas for HONO it was about 80 %, maybe due to the more complex structure of the HONO signal.

This study demonstrates the importance of considering atmospheric transport phenomena like vertical diffusion and horizontal advection for the interpretation of HONO measurements. If only one measurement height and thus only the temporal evolution is available, the interpretation of chemistry alone is ambiguous. For quantifying the source strength of HONO at the ground surface flux measurements are needed. Up to now, only a few studies measured HONO fluxes over grassland by the gradient method (Harrison et al., 1996; Stutz et al., 2002). Two very recent studies (Zhou et al., 2011; Ren et al., 2011) employed relaxed eddy accumulation (REA) to measure HONO surface fluxes, but both used inlet lines which may cause problems due to interactions of HONO with the surface of the inlet (Heland et al., 2001; Kleffmann et al., 2002). However, even with a "perfect" flux measurement the flux above a forest does not represent the surface source as there are various sources and sinks within the canopy. An "ideal" approach would be a flux profile consisting of eddy covariance (EC) measurements, but to date HONO measurement techniques are not sufficiently fast for EC measurements. Although experimentally and technically challenging, REA techniques will be available in the near future and will provide HONO flux measurement capabilities. If these

measurements are applied above tall vegetation the coupling regime of the canopy to the atmosphere has to be considered. Furthermore, in order to verify the budget terms of HONO during daytime, air chemistry models which parameterize heterogeneous HONO formation and take boundary layer dynamics as well as surface modifications (i.e. wetting) into account have to be developed.

# References

Alicke, B., Platt, U., and Stutz, J.: Impact of nitrous acid photolysis on the total hydroxyl radical budget during the Limitation of Oxidant Production Pianura/Padana Produzione di Ozono study in Milan, J. Geophys. Res., 107, 8196, doi:10.1029/2000JD000075, 2002.

Amedro, D., Parker, A. E., Schoemaecker, C., and Fittschen, C.: Direct observation of OH radicals after 565 nm multi-photon excitation of $NO_2$ in the presence of $H_2O$, Chem. Phys. Lett., 513, 12–16, 2011.

Andres-Hernandez, M. D., Notholt, J., Hjorth, J., and Schrems, O.: A DOAS study on the origin of nitrous acid at urban and non-urban sites, Atmos. Environ., 30, 175-180, 1996.

Arens, F., Gutzwiller, L., Baltensperger, U., Gäggler, H. W., and Ammann, M.: Heterogeneous reaction of $NO_2$ on diesel soot particles, Environ. Sci. Technol., 35, 2191-2199, 2001.

Barthlott, C., Drobinski, P., Fesquet, C., Dubos, T. and Pietras, C.: Long-term study of coherent structures in the atmospheric surface layer, Bound.-Lay. Meteorol, 125, 1-24, 2007.

Becker, K. H., Kleffmann, J., Kurtenbach, R. and Wiesen, P.: Solubility of nitrous acid (HONO) in sulfuric acid solutions, J. Phys. Chem., 100, 14984-14990, 1996.

Becker, K. H., Kleffmann, J., Negri, R. M. and Wiesen, P.: Solubility of nitrous acid (HONO) in ammonium sulfate solutions, J. Chem. Soc., Faraday Trans., 94(11), 1583-1586, 1998.

Bejan, I., Abd el Aal, Y., Barnes, I., Benter, T., Bohn, B., Wiesen, P., and Kleffmann, J.: The photolysis of ortho-nitrophenols: a new gas phase source of HONO, Phys. Chem. Chem. Phys., 8, 2028–2035, doi: 10.1039/b516590c, 2006.

Bergström, H. and Högström, U.: Turbulent exchange above a pine forest. II, Organized structures, Bound.-Lay.Meteorol, 49, 231–263, 1989.

Breuninger, C., Oswald, R., Kesselmeier, J. and Meixner, F. X.: The dynamic chamber method: trace gas exchange fluxes (NO, NO2, O3) between plants and the atmosphere in the laboratory and in the field, Atmos. Meas. Tech. Discuss., 4, 5183–5274, 2011.

Bröske, R., Kleffmann, J. and Wiesen, P.: Heterogeneous conversion of $NO_2$ on secondary organic aerosol surfaces: A possible source of nitrous acid (HONO) in the atmosphere? Atmos. Chem. Phys., 3, 469-474, 2003.

Burkhardt, J. and Eiden, R.: Thin water films on coniferous needles, Atmos. Environ., 28 (12), 2001-2011, 1994.

Calvert, J. G., Yarwood, G., and Dunker, A. M.: An evaluation of the mechanism of nitrous acid formation in the urban atmosphere, Res. Chem. Intermediat., 20, 463-502, 1994.

Carr, S., Heard, D. E., and Blitz, M. A.: Comment on "Atmospheric Hydroxyl Radical Production from Electronically Excited $NO_2$ and $H_2O$", Science, 324, 336 b, doi: 10.1126/science.1166669, 2009.

Cellier, P. and Brunet, Y.: Flux-gradient relationships above tall plant canopies, Agr. Forest Meteorol. , 58, 93-117, 1992.

Crowley, J. N., and Carl, S. A.: OH formation in the photoexcitation of $NO_2$ beyond the dissociation threshold in the presence of water vapor, J. Phys. Chem. A, 101, 4178-4184, 1997.

Damköhler, G.: Der Einfluss der Turbulenz auf die Flammengeschwindigkeit in Gasgemischen. Z. Elektrochem. Angew. P., 46 (11), 601–652, 1940.

Denmead, O. T. and Bradley, E. F.: Flux-gradient relationships in a forest canopy, in: The forest atmosphere interaction, edited by: Hutchison, B. A. and Hicks, B. B., D. Reidel Publ. Comp., Dordrecht, Boston, London, 421–442, 1985.

Dlugi, R.: Interaction of NOx and VOC's within vegetation, in: Proceedings EUROTRAC-Symposium 92, edited by: Borrell, P. M., Borrell, P., Cvitaš, T., Seiler, W., SPB Acad. Publ., Den Haag, 682–688, 1993.

Dlugi, R., Berger, M., Zelger, M., Hofzumahaus, A., Siese, M., Holland, F., Wisthaler, A., Grabmer, W., Hansel, A., Koppmann, R., Kramm, G., Möllmann-Coers, M. and Knaps, A.: Turbulent exchange and segregation of HOx radicals and volatile organic compounds above a deciduous forest, Atmos. Chem. Phys., 10, 6215-6235, 2010.

Ehhalt, D. H.: On the photochemical oxidation of natural trace gases and man-made pollutants in the troposphere,Sci.Total Environ. , 143, 1-15, 1994.

Ensberg, J. J., Carreras-Sospedra, M., and Dabdub, D.: Impacts of electronically photo-excited $NO_2$ on air pollution in the South Coast Air Basin of California, Atmos. Chem. Phys., 10, 1171–1181, 2010.

Febo, A., Perrino, C., and Allegrini, I.: Measurement of nitrous acid in Milan, Italy, by DOAS and diffusion denuders, Atmos. Environ., 30 3599-3609, 1996.

Finlayson-Pitts, B. J. and Pitts, J. N., Jr.: Chemistry of the upper and lower atmosphere: Theory, experiments, and applications, Academic Press, San Diego, CA, USA, 940p, 2000.

Finlayson-Pitts, B. J., Wingen, L. M., Sumner, A. L., Syomin, D., and Ramazan, K. A.: The heterogeneous hydrolysis of $NO_2$ in laboratory systems and in outdoor and indoor atmospheres: An integrated mechanism, Phys. Chem. Chem. Phys., 5, 2003.

Finlayson-Pitts, B. J.: Reactions at surfaces in the atmosphere: integration of experiments and theory as necessary (but not necessarily sufficient) for predicting the physical chemistry of aerosols, Phys. Chem. Chem. Phys., 11, 7760–7779, 2009.

Foken, T: Micrometeorology, Springer, Heidelberg, 308 p, 2008.

Foken, T., Meixner, F. X., Falge, E., Zetzsch, C., Serafimovich, A., Bargsten, A., Behrendt, T., Biermann, T., Breuninger, C., Dix, S., Gerken, T., Hunner, M., Lehmann-Pape, L., Hens, K., Jocher, G., Kesselmeier, J., Lüers, J., Mayer, J.-C., Moravek, A., Plake, D., Riederer, M., Rütz, F., Scheibe, M., Siebicke, L., Sörgel, M., Staudt, K., Trebs, I., Tsokankunku, A., Welling, M., Wolff, V., and Zhu, Z.: ExchanGE processes in mountainous Regions (EGER) – overview of design, methods, and first results, Atmos. Chem. Phys. Discuss., 11, 26245-26345, doi:10.5194/acpd-11-26245-2011, 2011.

Garratt, J. R.: Flux profile relations above tall vegetation, Q. J. Roy. Meteorol.Soc., 104, 199–211, 1978.

Garratt, J. R.: Surface influence upon vertical profiles in the atmospheric near surface layer, Q. J. Roy. Meteorol.Soc., 106, 803–819, 1980.

Garratt, J. R.: The atmospheric boundary layer, Cambridge Univ. Press., Cambridge, 316 pp., 1992.

George, C., Strekowski, R. S., Kleffmann, J., Stemmler, K., and Ammann, M.: Photoenhanced uptake of gaseous $NO_2$ on solid organic compounds: a photochemical source of HONO?, Faraday Discuss., 130, 195–210, 2005.

Gherman, T., Venables, D. S., Vaughan, S., Orphal, J. and Ruth, A. A.: Incoherent broadband cavity-enhanced absorption spectroscopy in the near-ultraviolet: Application to HONO and $NO_2$, Environ. Sci. Technol., 42, 890–895, 2008.

Gonçalves, M ., Dabdub, D., Chang, W. L. , F. Saiz, F., O. Jorba, O., and Baldasano, J. M.: The impact of different nitrous acid sources in the air quality levels of the Iberian Peninsula, Atmos. Chem. Phys. Discuss., 10, 28183–28230, 2010.

Gustafsson, R. J., Orlov, A., Griffiths, P. T., Cox, R. A., and Lambert, R. M.: Reduction of $NO_2$ to nitrous acid on illuminated titanium dioxide aerosol surfaces: implications for photocatalysis and atmospheric chemistry, Chem. Commun., 37, 3936–3938, 2006.

Gustafsson, R. J., Kyriakou, G., and Lambert, R. M.: The molecular mechanism of tropospheric nitrous acid production on mineral dust surfaces, ChemPhysChem, 9, 1390-1393, 2008.

Gutzwiller, L., Arens, F., Baltensberger, U., Gäggler, H. W., and Ammann, M.: Significance of semivolatile diesel exhaust organics for secondary HONO formation, Environ. Sci. Technol., 36, 677-682, 2002a.

Gutzwiller, L., George, C., Rössler, E., and Ammann, M.: Reaction kinetics of $NO_2$ with resorcinol and 2,7-naphthalenediol in the aqueous phase at different pH, J. Phys. Chem. A, 106, 12045-12050, 2002b.

Hanst, P. L., Spence, J. W., and Miller, M.: Atmospheric chemistry of n-nitroso dimethylamine, Environ. Sci. Technol., 11, 403-405, 1977.

Harrison, R. M., Peak, J. D., and Collin, G. M.: Tropospheric cycle of nitrous acid, J. Geophys. Res., 101, 14429–14439, 1996.

Heland, J., Kleffmann, J., Kurtenbach, R., and Wiesen, P.: A new instrument to measure gaseous nitrous acid (HONO) in the atmosphere, Environ. Sci. Technol., 35, 3207–3212, 2001.

Hirokawa, J., Kato, T. and Mafune, F.: Uptake of gas-phase nitrous ccid by pH-controlled aqueous solution studied by a wetted wall flow tube, J. Phys. Chem. , 112, 12143-12150, 2008.

Horii, C. V., Munger, J. W., Wofsy, S. C., Zahniser, M., Nelson, D., and McManus, J. B.: Fluxes of nitrogen oxides over a temperate deciduous forest, J. Geophys. Res., 109, D08305, doi:10.1029/2003JD004326, 2004.

Jacob, D. J.: Introduction to Atmospheric Chemistry, Princeton University Press, 264 pp, 1999.

Jenkin, M. E., Cox, R. A., and Williams, D. J.: Laboratory studies of the kinetics of formation of nitrous acid from the thermal reaction of nitrogen dioxide and water vapour, Atmos. Environ., 22 487-498, 1988.

Kinugawa, T., Enami, S., Yabushita, A., Kawasaki, M., Hoffmann, M. R., and Colussi, A. J.: Conversion of gaseous nitrogen dioxide to nitrate and nitrite on aqueous surfactants, Phys. Chem. Chem. Phys., 13, 5144-5149,DOI: 10.1039/C0CP01497D, 2011.

Kleffmann, J., Heland, J., Kurtenbach, R., Lörzer, J., and Wiesen,P.: A new instrument (LOPAP) for the detection of nitrous acid (HONO), Environ. Sci. Pollut. R., 4, 48–54, 2002.

Kleffmann, J., Kurtenbach, R., Lörzer, J., Wiesen, P., Kalthoff, N., Vogel, B., and Vogel, H.: Measured and simulated vertical profiles of nitrous acid—Part I: Field measurements, Atmos. Environ., 37, 2949–2955, 2003.

Kleffmann, J., Gavriloaiei, T., Hofzumahaus, A., Holland, F., Koppmann, R., Rupp, L., Schlosser, E., Siese, M., and Wahner, A.: Daytime formation of nitrous acid: A major source of OH radicals in a forest, Geophys. Res. Lett., 32, L05818, 2005.

Kleffmann, J.: Manual LOPAP-3, version 1.3.0, Bergische Universität Wuppertal, QUMA Elektronik & Analytik GmbH, Wuppertal, Germany, 2006.

Kleffmann, J.: Daytime sources of nitrous acid (HONO) in the atmospheric boundary layer, ChemPhysChem, 8, 1137 − 1144, 2007.

Kleffmann, J. and Wiesen, P.: Technical Note: Quantification of interferences of wet chemical HONO measurements under simulated polar conditions, Atmos. Chem. Phys., 8, 6813–6822, 2008.

Kubota, M., Asami, T.: Source of nitrous acid volatilized from upland soils, Soil Sci. Plant Nutr., 31, 35-42, 1985.

Lammel, G., and Cape, J. N.: Nitrous acid and nitrite in the atmosphere, Chem. Soc. Rev., 25, 361-369, 1996.

Lammel, G.: Formation of nitrous acid: Parameterization and comparison with observations, Max Planck Institute for Meteorology, Hamburg, Germany, report No. 286, 36, 1999.

Lee, B.H., Wood, E.C., Zahniser, M.S. , McManus, J.B., Nelson, D.D., Herndon, S.C., Santoni, G.W., Wofsy, S.C. and Munger, J.W.: Simultaneous measurements of atmospheric HONO and $NO_2$ via absorption spectroscopy using tunable mid-infrared continuous-wave quantum cascade lasers, Appl. Phys. B, 102, 417–423, 2011.

Lenschow, H. D.: Reactive trace species in the boundary layer from a micrometeorological perspective, J. Meteorol. Soc. Jpn., 60, 472 − 480, 1982.

Lerdau, M. T., Munger, J.W. and Jacob, D. J.: The $NO_2$ flux conundrum, Science, 289, 2291-2293, 2000.

Li, S., Matthews, J., and Sinha, A.: Atmospheric hydroxyl radical production from electronically excited $NO_2$ and $H_2O$, Science, 319, 1657-1660, doi: 10.1126/science.1151443, 2008.

McRae, G. J., Gooden, W. R., Seinfeld, J. H.: Mathematical modeling of photochemical air pollution, EQL Report No. 18, Environmental Quality Laboratory, California Institute of Technology, Pasadena, California, United States, 690pp, 1982.

Monge, M. E., D'Anna, B., Mazri, L., Giroir-Fendler, A., Ammann, M., Donaldson, D. J., and George, C.: Light changes the atmospheric reactivity of soot, P. Natl. Acad. Sci. USA, 107, 6605–6609, 2010.

Ndour, M., D'Anna, B., George, C., Ka, O., Balkanski, Y., Kleffmann, J., Stemmler, K., and Ammann, M.: Photoenhanced uptake of $NO_2$ on mineral dust: Laboratory experiments and model simulations, Geophys. Res. Lett., 35, L05812, doi:10.1029/2007GL032006, 2008.

Orlanski, I.: A rational subdivision of scales for atmospheric processes, B. Am. Metrol.Soc., 56(5), 527-530, 1975.

Perner, D., and Platt, U.: Detection of nitrous acid in the atmosphere by differential optical absorption, Geophys. Res. Lett., 6, 917-920, 1979.

Pitts Jr., J.N., Biermann, H. W., Winer, A. M., and Tuazon, E. C.: Spectroscopic identification and measurement of gaseous nitrous acid in dilute auto exhaust, Atmos. Environ., 18, 847-854, 1984.

Pitts Jr,, J. N., Grosjean, D., Cauwenberghe, K. V., Schmid, J. P., and Fitz, D. R.: Photooxidation of aliphatic amines under simulated atmospheric conditions: formation of nitrosamines, nitramines, amides, and photochemical oxidant, Environ. Sci. Technol., 12 946-953, 1978.

Pöhler, D.: Determination of two dimensional trace gas distributions using tomographic LP-DOAS measurements in the city of Heidelberg, Germany, Ph.D. thesis, University Heidelberg, Germany, 334 pp., 2010.

Ouwersloot, H. G., Vilà-Guerau de Arellano, J., van Heerwaarden, C. C., Ganzeveld, L. N., Krol, M. C., and Lelieveld, J.: On the segregation of chemical species in a clear

boundary layer over heterogeneous land surfaces, Atmos. Chem. Phys., 11, 10681-10704, doi:10.5194/acp-11-10681-2011, 2011.

Ramazan, K. A., Syomin D. and Finlayson-Pitts, B. J.: The photochemical production of HONO during the heterogeneous hydrolysis of $NO_2$, Phys.Chem.Chem.Phys., 6, 3836–3843, 2004.

Regelin, E.: Räumliche und jahreszeitliche Verteilung von OH- und $HO_2$-Radikalen in der Troposphäre über Europa, Ph.D. thesis, University Mainz, Germany, 194 pp., 2011.

Ren, X., Sanders, J. E., Rajendran,A. , Weber, R. J., Goldstein, A. H., Pusede, S. E., Browne, E. C., Min, K.-E. and Cohen, R. C.: A relaxed eddy accumulation system for measuring vertical fluxes of nitrous acid, Atmos. Meas. Tech., 4, 2093–2103, 2011.

Roberts, J.M., Veres, P., Warneke, P., Neuman, J. A., Washenfelder, R. A., Brown, S. S., Baasandorj, M., Burkholder, J. B., Burling, I. R., Johnson, T. J., Yokelson, R. J., and de Gouw, J.: Measurement of HONO, HNCO, and other inorganic acids by negative-ion proton-transfer chemical ionization mass spectrometry (NI-PT-CIMS): application to biomass burning emissions, Atmos. Meas. Tech., 3, 981–990, 2010.

Robinson, S. K.: Coherent motions in the turbulent boundary layer, Annu. Rev. Fluid Mech., 23, 601-639, 1991.

Ródenas, M., Munoz, A., Alacreu, F. and the FIONA Team.: The FIONA campaign (EUPHORE): Formal Intercomparison of Observations of Nitrous Acid, Geophysical Research Abstracts, Vol. 13, EGU2011-8736, 2011.

Rummel, U., Ammann, C., Gut, A., Meixner, F. X. and Andreae, M. O.: Eddy covariance measurements of nitric oxide flux within an Amazonian rain forest, J. Geophys. Res., 107 (D20), 8050, doi:10.1029/2001JD000520, 2002.

Sakamaki, F., Hatakeyama, S., and Akimoto, H.: Formation of nitrous acid and nitric oxide in the heterogeneous dark reaction of nitrogen dioxide and water vapour, Int. J. Chem. Kinet., 15, 1013 -1029, 1983.

Saliba, N. A., Yang, H., and Finlayson-Pitts, B. J.: Reaction of gaseous nitric oxide with nitric acid on silica surfaces in the presence of water at room temperature, J. Phys. Chem. A, 105, 10339-10346, 2001.

Sarwar, G., Pinder, R. W., Appel, K. W., Mathur, R., and Carlton, A. G.: Examination of the impact of photoexcited $NO_2$ chemistry on regional air quality, Atmos. Environ., 43, 6383–6387, 2009.

Schimang, R., Folkers, A., Kleffmann, J., Kleist, E., Miebach, M. and Wildt, J.: Uptake of gaseous nitrous acid (HONO) by several plant species, Atmos. Envi., 40, 1324–1335, 2006.

Serafimovich, A., Siebicke, L., Staudt, K., Lüers, J., Biermann, T., Schier, S., Mayer, J.-C., Foken, T.: ExchanGE processes in mountainous Regions (EGER) Documentation of the Intensive Observation Period (IOP1) September, 6th to October, 7th 2007, Arbeitsergebnisse Nr. 36, Bayreuth, Germany, print ISSN 1614-8916; internet ISSN 1614-8924, 2008.

Serafimovich, A., Thomas, C., and Foken, T.: Vertical and horizontal transport of energy and matter by coherent motions in a tall spruce canopy, Bound.-Lay. Meteorol., 140, 429–451, DOI 10.1007/s10546-011-9619-z, 2011.

Sleiman, M., Gundel, L. A., Pankow, J. F., Jacob, P., Singer, B. C., and Destaillats, H.: Formation of carcinogens indoors by surface-mediated reactions of nicotine with nitrous acid, leading to potential thirdhand smoke hazards, P. Natl. Acad. Sci. USA, 107, 6576–6581, 2010.

Sörgel, M., Trebs, I., Serafimovich, A., Moravek, A., Held, A., and Zetzsch, C.: Simultaneous HONO measurements in and above a forest canopy: influence of turbulent exchange on mixing ratio differences, Atmos. Chem. Phys., 11, 841–855, 2011a.

Sörgel, M., Regelin, E., Bozem, H., Diesch, J.-M., Drewnick, F., Fischer, H., Harder, H., Held, A., Hosaynali-Beygi, Z., Martinez, M., and Zetzsch, C.: Quantification of the unknown HONO daytime source and its relation to NO$_2$, Atmos. Chem. Phys. Discuss., 11, 15119-15155, doi:10.5194/acpd-11-15119-2011, 2011b.

Sörgel, M., Regelin, E., Bozem, H., Diesch, J.-M., Drewnick, F., Fischer, H., Harder, H., Held, A., Hosaynali-Beygi, Z., Martinez, M., and Zetzsch, C.: Quantification of the unknown HONO daytime source and its relation to NO$_2$, Atmos. Chem. Phys., 11, 10433-10447, doi:10.5194/acp-11-10433-2011, 2011c.

Sörgel, M., Held, A., Zetzsch, C.: Singular System Analysis of forest observations of HONO and humidity, to be submitted to Atmos. Envi., 2012.

Stemmler, K., Ammann, M., Donders, C., Kleffmann, J., and George, C.: Photosensitized reduction of nitrogen dioxide on humic acid as a source of nitrous acid, Nature, 440, 195-198, 2006.

Stemmler, K., Ammann, M., Elshorbany, Y., Kleffmann, J., Ndour, M., D'Anna, B., George, C., and Bohn, B.: Light-induced conversion of nitrogen dioxide into nitrous acid on submicron humic acid aerosol, Atmos. Chem. Phys., 7, 4237–4248, 2007.

Steiner, A. L., Pressley, S. N., Botros, A., Jones, E., Chung, S. H. and Edburg, S. L.: Analysis of coherent structures and atmosphere-canopy coupling strength during the CABINEX field campaign, Atmos. Chem. Phys., 11, 11921–11936, 2011.

Stockwell, W. R.: Effects of turbulence on gas-phase atmospheric chemistry: Calculation of the relationship between time scales for diffusion and chemical reaction, Meteorol. Atmos. Phys. 57, 159-171, 1995.

Stutz, J., Alicke, B., and Neftel, A.: Nitrous acid formation in the urban atmosphere: Gradient measurements of NO$_2$ and HONO over grass in Milan, Italy, J. Geophys. Res., 107 doi:10.1029/2001JD000390, 2002.

Stutz, J., Alicke, B., Ackermann, R., Geyer, A., Wang, S., White, A. B., Williams, E. J., Spicer, C. W., and Fast, J. D.: Relative humidity dependence of HONO chemistry in urban areas, J. Geophys. Res., 109, D03307, doi:10.1029/2003JD004135, 2004.

Stutz, J.: Final report "Nitrogen oxides in the nocturnal boundary layer: Chemistry of nitrous acid and the nitrate radical", U.S. Department of Energy Project Number: DE-FG02-01ER63094, University California Los Angeles, Los Angeles, California, USA, 159 pp., 2005.

Su, H., Cheng, Y. F., Cheng, P., Zhang, Y. H., Dong, S., Zeng, L. M., Wang, X., Slanina, J., Shao, M., and Wiedensohler, A.: Observation of nighttime nitrous acid (HONO) formation at a non-urban site during PRIDE-PRD2004 in China, Atmos. Environ., 42, 6219–6232, 2008a.

Su, H., Cheng, Y. F., Shao, M., Gao, D. F., Yu, Z. Y., Zeng, L. M., Slanina, J., Zhang, Y. H., and Wiedensohler, A.: Nitrous acid (HONO) and its daytime sources at a rural site during the 2004 PRIDE-PRD experiment in China, J. Geophys. Res., 113, doi:10.1029/2007JD009060, 2008b.

Su, H., Cheng,Y., Oswald, R., Behrendt, T., Trebs, I., Meixner, F.-X., Andreae, M. O., Cheng, P., Zhang,Y., and Pöschl, U.: Soil Nitrite as a Source of Atmospheric HONO and OH Radicals, Science, 333 (6049), 1616-1618, DOI: 10.1126/science.120768, 2011.

Svennson, R., Ljungstrom, E., and Lindqvist: Kinetics of the reaction between nitrogen dioxide and water vapour, Atmos. Environ., 21 1529-1539, 1987.

Trick, S.: Formation of nitrous acid on urban surfaces - a physical-chemical perspective-, Ph.D. thesis, University Heidelberg, Germany, 290 pp., 2004.

Veitel, H.: Vertical profiles of NO$_2$ and HONO in the boundary layer, Ph.D. thesis, University, Heidelberg, Germany, 270 pp., 2002.

Vila-Guerau de Arellano, J.: Bridging the gap between atmospheric physics and chemistry in studies of small-scale turbulence, B. Am. Meteorol. Soc., 84, 51-56, 2003.

Vinuesa, J.-F., Vila-Guerau de Arellano, J.: Introducing effective reaction rates to account for the inefficient mixing of the convective boundary layer, Atmospheric Environment, 39, 445–461, 2005.

Volkamer, R., Sheehy, P., Molina, L. T., and Molina, M. J.: Oxidative capacity of the Mexico City atmosphere − Part 1: A radical source perspective, Atmos. Chem. Phys., 10, 6969–6991, 2010.

Volpe Horii, C., Munger, J. M., Wofsy S. C., Zahniser, M., Nelson, D., McManus, J. B.: Fluxes of nitrogen oxides over a temperate deciduous forest, J. Geophys. Res., 109, D08305, doi:10.1029/2003JD004326, 2004.

Wang, L. and Zhang, J.: Detection of nitrous acid by cavity ring-down spectroscopy, Environ. Sci. Technol., 34, 4221-4227, 2000.

Wennberg, P., O., and Dabdub, D.: Rethinking ozone production, Science, 319, 1624-1625, 2008.

Wenzel, A., Kalthoff, N. and Horlacher, V.: On the profiles of wind velocity in the roughness sublayer above a coniferous forest, Bound.-lay. Meteorology, 84, 219–230, 1997.

Wojtal, P., Halla, J.D. and McLaren, R.: Pseudo steady states of HONO measured in the nocturnal marine boundary layer: a conceptual model for HONO formation on aqueous surfaces, Atmos. Chem. Phys., 11, 3243–3261, 2011.

Wong, K. W., Oh, H.-J. , Lefer, B. L. , Rappenglück, B. , and Stutz, J.: Vertical profiles of nitrous acid in the nocturnal urban atmosphere of Houston, TX, Atmos. Chem. Phys., 11, 3595–3609, 2011a.

Wong, K. W., Tsai, C., Lefer, B., Haman, C., Grossberg, N., Brune, W. H., Ren, X., Luke, W.and Stutz, J.: Daytime HONO Vertical Gradients during SHARP 2009 in Houston, TX , Atmos. Chem. Phys. Discuss., 11, 24365–24411, 2011b.

Yabushita, A., Enami, S., Sakamoto, Y., Kawasaki, M., Hoffmann, M. R., and Colussi, A. J.: Anion-catalyzed dissolution of $NO_2$ on aqueous microdroplets, J. Phys. Chem. A, 113, 4844–4848, 2009.

Yu, Y., Galle, B., Hodson, E., Panday, A., Prinn, R., and Wang, S.: Observations of high rates of $NO_2$ – HONO conversion in the nocturnal atmospheric boundary layer in Kathmandu, Nepal, Atmos. Chem. Phys., 9, 6401–6415, 2009.

Zhang, N., Zhou, X., Shepson, P. B., Gao, H., Alaghmand, M., and Stirm, B.: Aircraft measurement of HONO vertical profiles over a forested region, Geophys. Res. Lett., 36, L15820, doi:10.1029/2009GL038999, 2009.

Zhou, X., He, Y., Huang, G., Thornberry, T. D., Carroll, M. A., and Bertman, S. B.: Photochemical production of nitrous acid on glass sample manifold surface, Geophys. Res. Lett., 29, 1681, 10.1029/2002GL015080, 2002.

Zhou, X., Gao, H., He, Y., Huang, G., Bertman, S. B., Civerolo, K., and Schwab, J.: Nitric acid photolysis on surfaces in low-NOx environments: Significant atmospheric implications, Geophys. Res. Lett., 30(23), 2217, doi:10.1029/2003GL018620, , 2003.

Zhou, X., Zhang, N., TerAvest, M., Tang , D., Hou, J., Bertman, S., Alaghmand, M., Shepson, P. B., Carroll, M. A., Griffith, S., Dusanter, S., and Stevens, P. S.: Nitric acid photolysis on forest canopy surface as a source for tropospheric nitrous acid, Nat. Geosci., 4, 440–443, doi:10.1038/ngeo1164, 2011.

Zhu, C., Xiang, B., Zhu, L. and Cole, R.: Determination of absorption cross sections of surface-adsorbed $HNO_3$ in the 290–330 nm region by Brewster angle cavity ring-down spectroscopy, Chem. Phys. Lett., 458, 73–377, 2008.

Zhu, C., Xiang, B., Chu, L. T. and Zhu, L.: Photolysis of nitric acid in the gas phase, on aluminum surfaces, and on ice films, J. Phys. Chem. A, 114, 2561–2568, 2010.

# List of appendices

Appendix A:

Individual contributions to the publications

Appendix B:

Sörgel, M., Regelin, E., Bozem, H., Diesch, J.-M., Drewnick, F., Fischer, H., Harder, H., Held, A., Hosaynali-Beygi, Z., Martinez, M., and Zetzsch, C.: Quantification of the unknown HONO daytime source and its relation to $NO_2$, Atmos. Chem. Phys., 11, 10433-10447, doi:10.5194/acp-11-10433-2011, 2011.

Appendix C:

Sörgel, M., Trebs, I., Serafimovich, A., Moravek, A., Held, A., and Zetzsch, C.: Simultaneous HONO measurements in and above a forest canopy: influence of turbulent exchange on mixing ratio differences, Atmos. Chem. Phys., 11, 841–855,doi:10.5194/acp-11-841-2011, 2011.

Appendix D:

Sörgel, M., Held, A., Zetzsch, C.: Singular System Analysis of forest observations of HONO and humidity, to be submitted to Atmos. Envion., 2012.

# Appendix A

## Individual contributions to the publications

This cumulative thesis consists of several manuscripts which originate from a close collaboration with other researchers. In this section the individual contributions are specified.

Appendix B

Sörgel, M., Regelin, E., Bozem, H., Diesch, J.-M., Drewnick, F., Fischer, H., Harder, H., Held, A., Hosaynali-Beygi, Z., Martinez, M., and Zetzsch, C.: Quantification of the unknown HONO daytime source and its relation to $NO_2$, Atmos. Chem. Phys., 11, 10433-10447, doi:10.5194/acp-11-10433-2011, 2011.

- I myself had the idea, did the calculations, made the graphs and wrote the manuscript. I also performed the HONO measurements. Furthermore, I responded to the referee comments and wrote the revised manuscript.
- Eric Regelin performed the OH measurements together with Hartwig Harder and Monica Martinez. He also calculated the photolysis frequency of ozone with a radiation transfer model (TUV). Furthermore, Monica Martinez proposed corrections to the manuscript and provided helpful suggestions.
- Heiko Bozem did the $j(NO_2)$ measurements.
- Jovana Diesch and Frank Drewnick measured the meteorological parameters (RH, wind speed, wind direction, atmospheric pressure), black carbon, ozone and water vapor mixing ratios. Additionally, Frank Drewnick helped to improve the manuscript with suggestions and questions as well as language corrections.
- Andreas Held substantially helped to improve the structure and language of the manuscript. He participated consistently with discussions. He also helped to improve the replies to the referees as well as the revised manuscript.
- Zeinab Hosaynali-Beygi performed the $NO_x$ measurements and wrote the experimental part regarding the $NO_x$ measurements. Additionally, Horst Fischer provided helpful comments to the manuscript.

- Cornelius Zetzsch supported my participation in the DOMINO campaign. He also contributed to the preparation of the manuscript with discussions and suggestions and also helped to improve it by language corrections.
- Two anonymous referees provided critical questions and suggestions to further improve the manuscript.

Appendix C

Sörgel, M., Trebs, I., Serafimovich, A., Moravek, A., Held, A., and Zetzsch, C.: Simultaneous HONO measurements in and above a forest canopy: influence of turbulent exchange on mixing ratio differences, Atmos. Chem. Phys., 11, 841–855,doi:10.5194/acp-11-841-2011, 2011.

- I myself had the idea, did the calculations, made the graphs and wrote the manuscript. I also performed the HONO measurements at the forest floor. Furthermore, I replied to the referee comments and wrote the revised manuscript. Several discussions and suggestions led to the ideas of the manuscript. The input given during discussion by people who are not coauthors of this paper but are acknowledged in the manuscript (Ralph Dlugi, Thomas Foken, Jörg Kleffmann and Franz Meixner) helped developing the ideas. Also Eva Falge gave important input to several aspects of the manuscript.
- Ivonne Trebs performed the HONO measurements above canopy and furthermore contributed to the manuscript with discussions, suggestions and corrections. She also provided the final data of the $j(NO_2)$ and SMPS measurements which were performed by Jörg Sintermann and Daniel Plake.
- Andrei Serafimovich performed the measurements of the eddy-covariance profile and the subsequent calculations of the coupling regimes.
- Alexander Moravek performed the $NO_x$ and $O_3$ measurements.
- Andreas Held substantially helped to improve the structure and language of the manuscript. He participated consistently with discussions. He also helped to improve the comments to the referees as well as the revised manuscript.
- Cornelius Zetzsch proposed the original project to the DFG, supported the preparation of the manuscript with discussions and suggestions. He also helped to improve the manuscript by language corrections.

- Data for temperature, relative humidity, precipitation and visibility are courtesy of the Department of Micrometeorology of the University of Bayreuth. SODAR data were provided by Stephanie Schier.
- Two anonymous referees provided critical questions and suggestions to further improve the manuscript.

Appendix D

Sörgel, M., Held, A., Zetzsch, C.: Singular System Analysis of forest observations of HONO and humidity, to be submitted to Atmos. Envion., 2012.

- I myself developed the idea, did the calculations, made the graphs and wrote the manuscript. I also performed the HONO measurements at the forest floor in IOP I and in the other campaigns. The idea to use Singular System Analysis for this kind of investigation was provided by Michael Hauhs.
- Andreas Held substantially helped to improve the structure and language of the manuscript. He participated consistently with discussions.
- Cornelius Zetzsch proposed the original project to the DFG, supported the preparation of the manuscript with discussions and suggestions. He also helped to improve the manuscript by language corrections.
- Data for relative humidity (RH) during IOP I and IOP II are courtesy of the department of micrometeorology of the University of Bayreuth. RH data for DOMINO are courtesy of Jovana Diesch and Frank Drewnick from the Max Planck Institute for Chemistry, Mainz. During IOP I, HONO data above the canopy (IOP I 24.5 m) were provided by Ivonne Trebs, Max Planck Institute for Chemistry, Mainz.

# Appendix B

# Quantification of the unknown HONO daytime source and its relation to NO$_2$

M. Sörgel[1,2], E. Regelin[3], H. Bozem[3*], J.-M. Diesch[4], F. Drewnick[4], H. Fischer[3], H. Harder[3], A. Held[2], Z. Hosaynali-Beygi[3], M. Martinez[3] and C. Zetzsch[1,5]

1 University of Bayreuth, Atmospheric Chemistry Research Laboratory, Bayreuth, Germany

2 University of Bayreuth, Junior Professorship in Atmospheric Chemistry, Bayreuth, Germany

3 Max Planck Institute for Chemistry, Atmospheric Chemistry Department, P. O. Box 3060, 55020 Mainz, Germany

4 Max Planck Institute for Chemistry, Particle Chemistry Department, P. O. Box 3060, 55020 Mainz, Germany

5 Fraunhofer Institute for Toxicology and Experimental Medicine, Hannover, Germany

* now at University Mainz, Institute for Atmospheric Physics, Mainz, Germany

## Abstract

During the DOMINO (**D**iel **O**xidant **M**echanism **I**n relation to **N**itrogen **O**xides) campaign in southwest Spain we measured simultaneously all quantities necessary to calculate a photostationary state for HONO in the gas phase. These quantities comprise the concentrations of OH, NO, and HONO and the photolysis frequency of NO$_2$, $j$(NO$_2$) as a proxy for $j$(HONO). This allowed us to calculate values of the unknown HONO daytime source. This unknown HONO source, normalized by NO$_2$ mixing ratios and expressed as a conversion frequency (% h$^{-1}$), showed a clear dependence on $j$(NO$_2$) with values up to

43 % h$^{-1}$ at noon. We compared our unknown HONO source with values calculated from the measured field data for two recently proposed processes, the light-induced $NO_2$ conversion on soot surfaces and the reaction of electronically excited $NO_2$* with water vapour, with the result that these two reactions normally contributed less than 10 % (< 1% $NO_2$ + soot + h$\nu$; and < 10 % $NO_2$* + $H_2O$) to our unknown HONO daytime source. OH production from HONO photolysis was found to be larger (by 20 %) than the "classical" OH formation from ozone photolysis (O($^1$D)) integrated over the day.

# 1   Introduction

Nitrous acid (HONO) is an important OH radical precursor which serves as the "detergent" of the atmosphere due to its oxidizing power. Besides its importance for the atmospheric oxidation potential, HONO is part of acid and nutrient deposition to the biosphere. Moreover, growing concern exists about possible health effects due to the formation of nitrosamines (Hanst et al., 1977; Pitts et al., 1978) where HONO acts as the nitrosating agent, especially in indoor environments after wall reactions of HONO with nicotine (Sleiman et al., 2010). Despite three decades of research since the first unequivocal detection of HONO in the atmosphere (Perner and Platt, 1979), HONO formation processes in the atmosphere are still under discussion, especially during daytime where large discrepancies were found between mixing ratios calculated from known gas phase chemistry and measured daytime mixing ratios (Kleffmann et al., 2005). In the absence of light, the most favoured formation reaction is the heterogeneous disproportionation of nitrogen dioxide ($NO_2$):

$$2NO_2 + H_2O \rightarrow HONO + HNO_3 \qquad\qquad (R1)$$

This reaction has been extensively studied on different materials like fluorinated polymers and different types of glass as reviewed by Lammel and Cape (1996), but also on building materials like concrete (Trick, 2004). It was found to be first order in $NO_2$ and water vapour (Sakamaki et al., 1983; Svennson et al., 1987; Pitts et al., 1984; Jenkin et al., 1988). A mechanism involving the formation of the $NO_2$ dimer ($N_2O_4$) in the gas phase was proposed (Finlayson-Pitts et al., 2003), but is not important in the real atmosphere (Kleffmann et al., 1998; Gustafsson et al., 2008). Recently, evidence for a mechanism involving reaction between adsorbed $NO_2$ and H ($NO_2$ (ads) + H(ads) $\rightarrow$ HONO (ads)) present on the surface

following the dissociation of chemisorbed $H_2O$ was found in a study on mineral dust particles with isotopically labelled water (Gustafsson et al., 2008), but the results are probably not transferable from laboratory to field conditions (Finlayson-Pitts, 2009). The disproportionation reaction (R1) was found to be catalysed by anions at the surface of droplets (Yabushita et al., 2009; Kinugawa et al., 2011). In the absence of light, HONO formation from $NO_2$ on soot deactivates quite rapidly and thus was concluded to be less important for atmospheric HONO formation except for freshly emitted soot (Kleffmann et al., 1999, Arens et al., 2001; Aubin and Abbatt, 2007). The mechanism was summarized as the reaction (R2) of reducing organic compounds $\{C-H\}_{red}$ with $NO_2$ (Gutzwiller et al., 2002a). A reaction similar to (R2) was postulated for the aqueous phase (Gutzwiller et al., 2002b; Ammann et al., 2005), but only proceeds at a relevant rate at high pH levels, since it is based on the well-known charge transfer reaction of phenolate with $NO_2$.

$$NO_2 + \{C-H\}_{red} \rightarrow HONO + \{C\}_{ox} \qquad\qquad (R2)$$

$$NO + NO_2 + H_2O \rightarrow 2\ HONO \qquad\qquad (R3)$$

$$HNO_3\ (ads) + NO\ (g) \rightarrow HONO + NO_2 \qquad\qquad (R4)$$
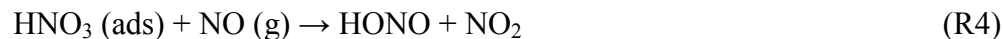
The reactions (R3) (via the intermediate $N_2O_3$) and (R4) proposed from field measurements (Calvert et al., 1994; Andres-Hernandez et al., 1996; Saliba et al., 2001) could neither explain laboratory results under low $NO_x$ conditions (Svensson et al., 1987; Jenkin et al., 1988; Kleffmann et al., 1998; Kleffmann et al., 2004;) nor field experiments with low NO mixing ratios (Harrison and Kitto, 1994; Alicke et al., 2003; this study).

During daytime the dominant sink for HONO is photolysis according to (R5), which forms OH.

$$HONO + h\nu \rightarrow NO + OH \qquad\qquad (R5)$$

An additional sink is the reaction of HONO with OH (R6).

$$HONO + OH \rightarrow NO_2 + H_2O \hspace{4cm} (R6)$$

The back reaction (R7) regenerates HONO.

$$NO + OH + M \rightarrow HONO + M \hspace{4cm} (R7)$$

At high insolation, (R5)-(R7) are supposed to be in a photostationary state (PSS) (Cox, 1974; Kleffmann et al., 2005). Only few studies (Kleffmann et al., 2005; Acker et al., 2006) measured all quantities necessary to calculate the photostationary state (no net OH formation), some with $j$(HONO) calculated from UV measurements (Ren et al., 2003; Ren et al., 2006). In all these studies measured HONO values exceeded the HONO values calculated from PSS. The "dark" heterogeneous formation (via (R1)/(R2)) was too slow (20-60 times) to explain this discrepancy (Kleffmann et al., 2003; Kleffmann et al., 2005). This stimulated laboratory studies about a light-induced conversion of $NO_2$ to HONO or other photolytic sources of HONO as recently summarized by Kleffmann (2007). There are a variety of proposed sources dealing with light-induced $NO_2$ reduction including $NO_2$ reduction on irradiated mineral surfaces like $TiO_2$ (Gustafsson et al., 2006; Ndour et al., 2008). Many studies focussed on the reduction of $NO_2$ involving organic photosensitizers (George et al., 2005) like hydrocarbons on soot (Monge et al., 2010) or humic acids (Stemmler et al., 2006; Stemmler et al., 2007).

As already proposed from smog chamber experiments (Killus and Whitten, 1990), photolysis of deposited $HNO_3$/nitrate on surfaces was suggested as a daytime HONO source for rural forested environments by Zhou et al. (2002a, 2002b, 2003) and Raivonnen et al. (2006). This mechanism is still controversial since the photolysis of $HNO_3$ was not found to be a photolytic source of HONO in chamber experiments (Rohrer et al., 2005), and quantum yields for $HNO_3$/nitrate photolysis are too low in the gas phase and in solution (Kleffmann, 2007). The photolysis of $HNO_3$ might be enhanced at surfaces (Finlayson-Pitts, 2009) or via organic photosensitizers as speculated by Kleffmann (2007). Recent studies showed the enhanced light absorption of surface adsorbed $HNO_3$ compared to the gas phase (Zhu et al., 2008; Zhu et al., 2010), and thus higher photolysis rates of adsorbed $HNO_3$. These laboratory studies identified $NO_2$* as the main photolysis product. Zhou et al. (2011), who found that their HONO daytime source is correlated to the product of surface nitrate loading and the

photolysis frequency of $HNO_3$, concluded that HONO formation by $HNO_3$ photolysis at the surface occurs via the mechanism proposed by Stemmler at al. (2006).

A direct HONO source is the photolysis of nitrophenols (Bejan et al., 2006) depending on pollution levels which govern the formation of nitrophenols.

The contribution of the reaction of electronically excited $NO_2^*$ with water vapour (R8) to the oxidation capacity of the troposphere was investigated in recent modelling studies (Wennberg and Dabdub, 2008; Sarwar et al., 2009; Ensberg et al., 2010). These studies focussed on ozone formation and concluded that there is an impact on oxidant formation for high $NO_x$ emissions when using the rate constant of Li et al. (2008) for reactive quenching of $NO_2^*$. Even with low $NO_x$ emissions the influence is still noticeable, whereas using the rate constant of Crowley and Carl (1997) the impact is negligible. The portion of the reactive quenching of $NO_2^*$ by $H_2O$ (and thus the rate constant of (R8), $k_8$) is still under discussion (Carr et al., 2009; Li et al., 2009; Fang et al., 2010; Blitz, 2010). In their laboratory study, Crowley and Carl (1997) did not observe any OH production via (R8) and thus derived an upper limit for the reactive quenching of $NO_2^*$ by $H_2O$ of $k_8 = 1.2 \times 10^{-14}$ cm³ molecules$^{-1}$ s$^{-1}$. A recent study by Carr et al. (2009) confirmed these findings. In contrast to these studies which used unfocused laser beams, Li et al. (2008) observed OH production and report a one order of magnitude higher value for $k_8 = 1.7 \times 10^{-13}$ cm$^3$ molecules$^{-1}$ s$^{-1}$.

$$NO_2^* + H_2O \rightarrow HONO + OH \qquad\qquad\qquad (R8)$$

In this study we quantify the gas phase photostationary state for HONO from measured values in Spain, calculate the values of the unknown HONO daytime source, and compare the latter with HONO formation from (R8) and the light-induced $NO_2$ conversion on soot (Monge et al., 2010).

# 2  Experimental

The **D**iel **O**xidant **M**echanism **I**n relation to **N**itrogen **O**xides (DOMINO) campaign took place at the "Atmospheric Sounding Station - El Arenosillo", a platform of the Atmospheric Research and Instrumentation Branch of the Spanish National Institute for Aerospace Technology (INTA) dedicated to atmospheric measurements in the southwest of Spain (37° 05' 48.03'' N, 6° 44' 07.47'' W). The measurement site was about 300 m inland from the coast of the Atlantic Ocean in a large area of uniform pine (Pinus pinea L.) forest with sandy soil. Only sparse buildings and streets were located around the site. The average canopy height was about 6 m. The leaf area index (LAI) for this forested area is about 1-1.5 (Gonçalves et al., 2010). About 15 kilometres to the northwest is the industrial area of Huelva, with refineries and other heavy industry. The metropolitan area of Seville is about 70 km to the east-north-east. The campaign took place from mid November to mid December 2008.

Measurements of HONO were conducted at a height of 10 m above ground (~ 4 m above canopy) on a scaffold and at 1 m above ground, by commercial LOPAP instruments (**LO**ng **P**ath **A**bsorption **P**hotometer, QUMA Elektronik & Analytik, Wuppertal, Germany). The LOPAP is based on a wet chemical technique, with fast sampling of HONO as nitrite in a stripping coil and subsequent detection as an azo dye using long path absorption in 2.4 m long Teflon AF tubing. A detailed description of the instrument has been given by Heland et al. (2001) and Kleffmann et al. (2002). The instruments were placed outside directly on the scaffolds in ventilated aluminium boxes without temperature control. The temperature of the stripping coils was kept constant at 20 °C by thermostats to assure constant sampling conditions. The overall relative error of the LOPAP instruments was found to be 12 % in a recent side by side intercomparison in the field (Sörgel et al., 2011). Detection limits during DOMINO, calculated as 3 σ of the noise during zero air measurements, were between 1 and 2.5 ppt.

The instrument used to measure $NO_x$ was a high resolution and high sensitivity chemiluminescence detector (ECO-Physics CLD 790 SR, ECO-Physics, Dürnten, Switzerland) which carries out simultaneous in situ measurements of NO and $NO_2$. NO is measured directly, however, $NO_2$ is measured indirectly after conversion to NO using a blue light converter which is a solid state photolytic converter (Droplet Measurement Technologies, Boulder, Co, USA). A detailed description of the instrument, the calibration

techniques and the error calculation has been given by Hosaynali-Beygi et al. (2011). Air was sampled through a polytetrafluoroethylene (PTFE) inlet line which was mounted on top of a scaffold at the measurement site at a height of 10 m above the ground. From there an inlet line which consisted of 1/2" PTFE tubing was installed to the container. The last meter of the inlet line consisted of 1/4" PTFE tubing. The total uncertainty for the original 1 s data (at 2σ) based on the calculations of precision and accuracy is 6.04 ppt + 5 % of reading for NO and 8.29 ppt + 8 % of reading for $NO_2$ measurements. The residence time in the tubing was about 3 seconds. The shift in the tubing due to the reaction of NO with $O_3$ was thus less than 5 % for NO and less than 2 % for $NO_2$ during the campaign.

OH was measured by Laser Induced Fluorescence (LIF) with the "HORUS" (**H**ydr**O**xyl **R**adical measurement **U**nit based on fluorescence **S**pectroscopy) instrument (Martinez et al., 2010). The detection system was placed next to the LOPAP on top of the scaffold (10 m). The measurement uncertainty was ±18 %. Measured OH values present an upper limit due to interferences which can be up to a factor of two for some conditions (H. Harder, personal communication, 2011). The inlets for HONO, $NO_x$ and $HO_x$ measurements were collocated at 10 m above ground on the scaffold.

$NO_2$ photolysis frequencies $j(NO_2)$ were measured by filter radiometers (Meteorologie consult, Königstein, Germany) on top of the scaffold, with an uncertainty of ± 5%. The HONO photolysis frequency ($j(HONO)$) was calculated by multiplying $j(NO_2)$ with a factor of 0.175 (Trebs et al., 2009). By comparing different parameterizations (Kraus and Hofzumahaus, 1998; Trebs et al., 2009), the uncertainty for the calculation of $j(HONO)$ was estimated to be 5 %. The overall (4 π) photolysis frequency was calculated by increasing values of the downwelling radiation by 5 %, i.e. the portion of the upwelling radiation (albedo of UV radiation) at this site (Cancillo et al., 2005).

Photolysis frequencies for $O(^1D)$ formation ($j(O(^1D))$) were calculated using the TUV model (Version 4.1, e.g. Madronich et al., 1998) taking the ozone column from the NASA webpage (http://jwocky.gsfc.nasa.gov/teacher/ ozone_overhead.html).We firstly derived a factor for scaling modelled $j(NO_2)$ to measured $j(NO_2)$. This factor was then applied for scaling modelled $j(O^1D)$.

Meteorological parameters like temperature, relative humidity (RH), atmospheric pressure, wind speed and wind direction were measured with a Vaisala WXT510 (Vaisala, Helsinki, Finnland) meteorological station on top of the MoLa (**Mo**bile **La**boratory) inlet system, which was at 10 m height 10 m southeast of the scaffold. For details see Diesch et al. (2011).

MoLa measured ozone by UV absorption with the "Airpointer" (Recordum, Mödling, Austria), water vapour mixing ratios by infrared absorption (LICOR 840, Li-COR, Lincol, USA) and black carbon with a Multi Angle Absorption Photometer (MAAP, Model 5012, Thermo Fischer Scientific, Whatman, USA).

# 3  Results and discussion

## 3.1  Meteorological and chemical conditions

Figure 1 gives an overview of meteorological and chemical measurements during the experiment in November/December 2008. In the beginning of the campaign there was a fair weather period with moderate (about 3 m s$^{-1}$) north-easterly winds (from inland Seville region). On November 24, the wind direction changed to northwest (along the coast from Huelva). From the 28$^{th}$ to 30$^{th}$ November, clean marine air with some plumes arrived at the site from the west. This was also the only period with rainfall, and HONO values were often around the detection limit (2 ppt). Ozone mixing ratios were about 30 ppb and showed a diurnal variation except for the clean air period with higher values (40 ppb) and no diurnal variation. A more detailed analysis of the ozone behaviour and the different wind sectors has been given by Diesch et al. (2011).
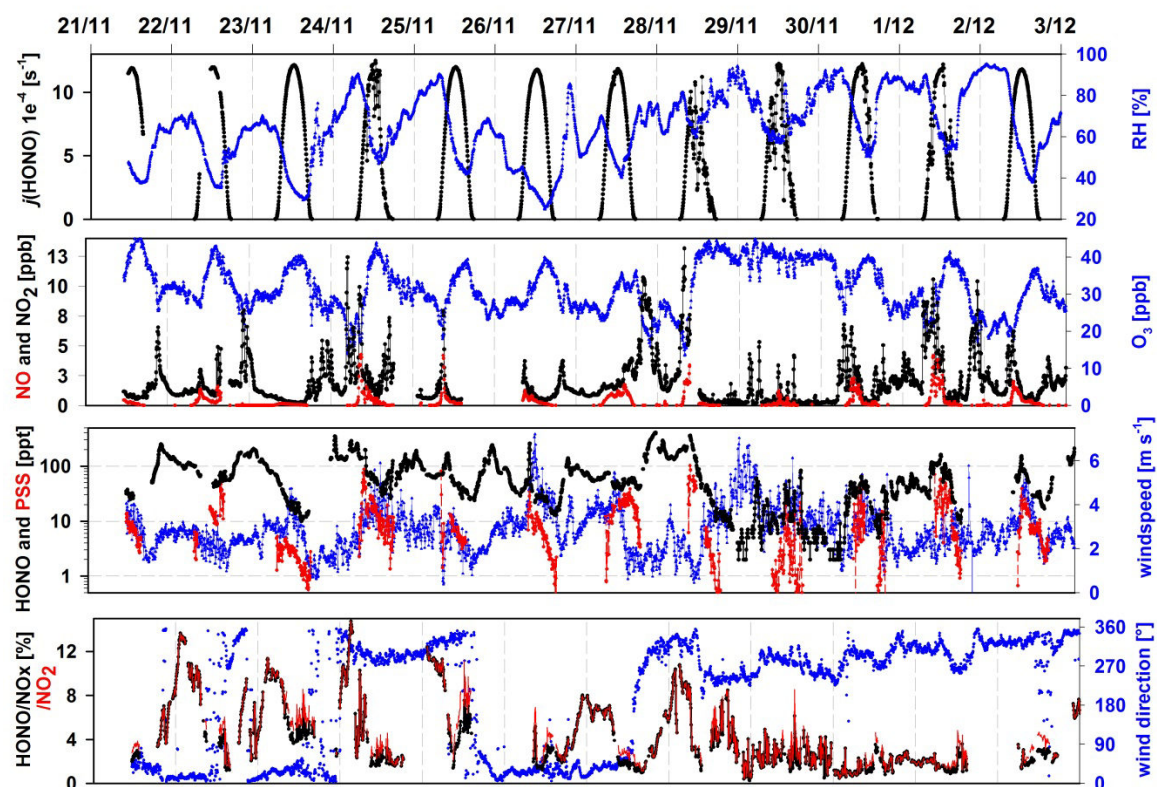
Figure 1: Overview of meteorological (RH, wind speed and wind direction) and chemical quantities (O₃, NO, NO₂, HONO, HONO$_{PSS}$ (calculated), HONO/NO$_x$ and HONO/NO₂ ratios and $j$(HONO)).

## 3.2  Photostationary state (PSS)

### 3.2.1  Calculating the photostationary state/gas phase

Regarding only the well-established gas phase formation (R7) and gas phase sink processes ((R5) and (R6)) one can calculate the photostationary state (PSS) mixing ratio of HONO (Cox, 1974; Kleffmann et al., 2005),

$$[HONO_{PSS}] = \frac{k_7[NO][OH]}{k_6[OH] + j(HONO)}$$

(1)

[HONO$_{PSS}$] is the equilibrium concentration, [NO] and [OH] are the measured NO and OH concentrations, and $j$(HONO) is the photolysis frequency of HONO. Rate constants for the termolecular reaction (R7) were calculated at atmospheric pressure from the fall-off curves (high and low pressure limit rate constants) according to the formulas given by the respective references (Atkinson et al., 2004; Sander et al., 2006). Values of k₇ differed by 24 %

(constantly over the temperature and pressure range of our study): from IUPAC (Atkinson et al., 2004) $k_{7,(298\ K)}$ = 9.8 x $10^{-12}$ $cm^3$ molecules$^{-1}$ s$^{-1}$ and from JPL (Sander et al., 2006) $k_{7,(298\ K)}$ = 7.4 x $10^{-12}$ $cm^3$ molecules$^{-1}$ s$^{-1}$ . The calculated JPL value is consistent with the value ($k_{7,(\sim298\ K)}$ = (7.4 ± 1.3 ) x $10^{-12}$ $cm^3$ molecules$^{-1}$ s$^{-1}$) measured directly at atmospheric pressure by Bohn and Zetzsch (1997). We therefore prefer this value and use it for our calculations of the PSS. For the bimolecular reaction of HONO and OH (R6), a rate constant of $k_{6,298\ K}$ = 6.0 x $10^{-12}$ $cm^3$ molecules$^{-1}$ s$^{-1}$ was taken from Atkinson et al. (2004).

Uncertainties in the PSS mainly originate from OH measurements with an accuracy of ± 18 %. This has some influence on HONO formation via (R7) but not much influence on the loss term, since HONO loss via (R7) was mostly less than 5 % of the total loss ((R5) + (R6)) during the whole campaign. As OH measurements may possibly suffer from interferences, the [HONO$_{PSS}$] values are rather an upper limit. As a consequence, the unknown HONO source discussed in Sect. 3.3 is rather a lower limit. There is also some uncertainty in the $j$(HONO) values since the portions of the upwelling part of the radiation measured at the site were about 0.3-0.5 of the downwelling (direct + diffuse). These high albedo values were presumably caused by the white container roofs and the aluminium scaffold below the sensor. As the minimum HONO lifetime (inverse photolysis frequency) is about 15 min around noon, our measurements at the 10 m scaffold do not reflect the local situation but an integration over a "footprint area" (Schmid, 2002; Vesala et al., 2008). Therefore, we chose an albedo value for UV radiation of the surrounding pine forest of 0.05 (Cancillo et al., 2005) which is more representative.
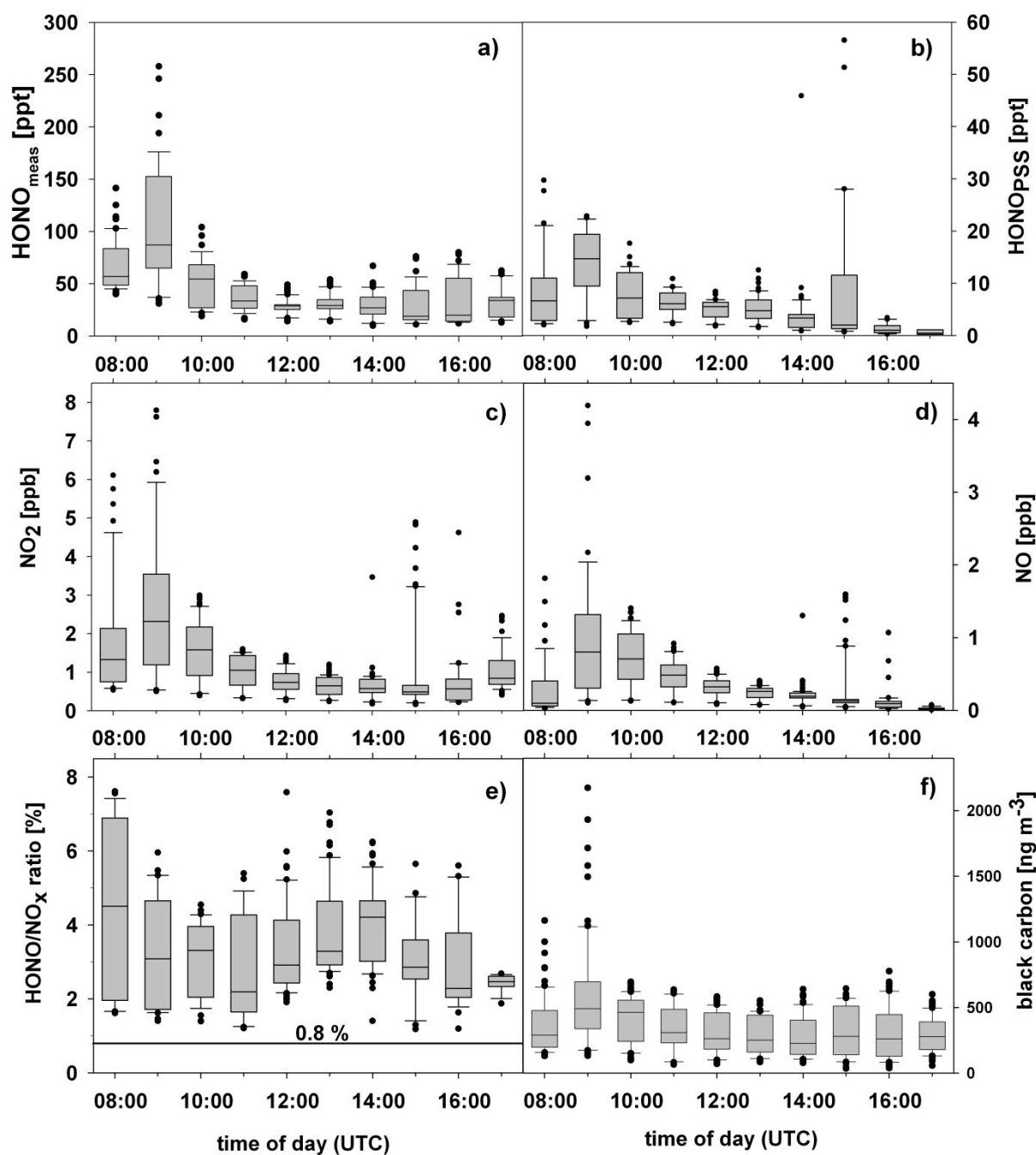
Figure 2: Daytime cycles of a) measured HONO mixing ratios, HONO$_{meas}$ b) calculated HONO mixing according to Eq. (1), HONO$_{PSS}$ c) NO$_2$ and d) NO mixing ratios as well as e) HONO/NO$_x$ ratios with the value of 0.8 % for direct emissions (Kurtenbach et al., 2001) marked as black line and black carbon concentration f). The boxes and whiskers represent a one hour time interval (centred in the middle) of five minute data (22-72 data points) of 7 cloud free days (21 ,22, 23, 25, 26, 27th November and 2nd December). The upper ends of the boxes represent the 75th percentile, the lower bounds the 25th percentile and the line within the boxes the median. The upper whisker marks the last point within the 90th percentile and the lower whisker that of the 10th percentile. Data points outside the 10th and 90th percentile are marked individually as dots.

Figure 2 summarizes the diurnal courses of HONO and $NO_x$ for 7 cloud free days. On the 27th around noon, fair weather clouds were passing. These data points were rejected for further analysis to exclude effects from fluctuations in $j$(HONO). On 2nd of December, data was taken from a second LOPAP at 1 m height as there were no data available from the 10 m instrument. Both instruments have been demonstrated to agree within 12 % under dry field conditions in side-by-side measurements (Sörgel et al. 2011). Assuming efficient vertical mixing during the day, HONO mixing ratios at 1 m and 10 m height can be expected to be similar (Sörgel et al., 2011).

The portion of HONO formed by known reactions in the gas phase ([$HONO_{PSS}$], Fig. 2 b) is not negligible. The median contribution is 20 % (25 percentile is 13 %) of the measured HONO mixing ratios. On the other hand, the gas phase formation can explain only part of the measured HONO, as 75 % of the [$HONO_{PSS}$] values contribute less than 30 % to the measured values. $HONO_{meas}$, $HONO_{PSS}$, NO and $NO_2$ have a similar diurnal cycle with the most pronounced feature being the maximum values around 9:00 UTC. This could be explained by local emissions which were trapped in the stable boundary layer before the breakup of the inversion in the morning. In the afternoon (15:00-16:00), this peak occurs less pronouncedly in NO and $NO_2$ but very clearly in the PSS values, as OH values are about twice ($\sim 3 \times 10^6$ molecules $cm^{-3}$) those at 9:00. From Figs. 2 b and d one can infer that [$HONO_{PSS}$] values are correlated to NO mixing ratios ($r^2 = 0.78$). Correlations to other input parameters of the PSS are low ([OH] $r^2 = 0.006$; $j$(HONO) $r^2 = 0.01$). Therefore, NO availability seems to be a driving force for HONO gas phase chemistry. Measured HONO mixing ratios (Fig. 2a) have a coefficient of determination

$r^2 = 0.49$ with [$NO_2$], and $r^2 = 0.36$ with [NO]. The relation of the HONO formation rate (which is more appropriate than HONO mixing ratios) and $NO_2$ is discussed in detail in chapter (3.3).

HONO/$NO_x$ ratios reach their daytime maximum in the early afternoon with median values around 4 % (Fig. 2 e), implying efficient $NO_x$ conversion. On the other hand, the maximum can also be attributed to sources independent from ambient $NO_x$ values such as soil emissions (Su et al., 2011), and $HNO_3$ photolysis at surfaces (Zhou et al., 2011), which are not affected by the declining $NO_x$ values in the early afternoon.

### 3.2.2 Including the parameterized heterogeneous HONO formation into PSS calculations

To sum up known HONO formation pathways, the heterogeneous formation ((R1)/(R2)) which was measured during nighttime may be included as an additional source in the PSS (e.g. Alicke et al., 2002; Alicke et al., 2003) with the assumption that ((R1)/(R2)) continue at daytime in the same manner as at night.

This assumption may not be true because even at night HONO formation (release) is not proceeding at the same rate all night. Studies about HONO fluxes (Harrison and Kitto, 1994; Harrison et al., 1996; Stutz et al., 2002; Stutz et al., 2004) explained that measured HONO formation is a net process (pseudo steady state) of release and deposition (see also discussion in Vogel et al. (2003)). A recent study by Wong et al. (2011) provides detailed information about HONO formation and deposition in the **N**octurnal **B**oundary **L**ayer (NBL) by combining vertical gradient measurements with 1-D model calculations. According to their results the ground surface accounts for most (~70%) of the HONO formation by $NO_2$ conversion but also for most of the loss (~70%). This confirms previous results from ground based field measurements (Harrison and Kitto, 1994; Stutz et al., 2002; Veitel, 2002; Kleffmann et al., 2003; Zhang et al., 2009; Sörgel et al., 2011), aircraft profiles (Zhang et al., 2009) and modelling (Vogel et al., 2003) that the ground surface is a major source of HONO. Hence, turbulent exchange has a significant impact on near surface HONO mixing ratios as already proposed by Febo et al. (1996). These authors found a good correlation of HONO with radon, which is exclusively emitted from the ground. Furthermore, profiles from recent aircraft measurements were closely related to atmospheric stability with higher HONO values close to the ground and steeper gradients during stable conditions (Zhang et al., 2009). Therefore, mixing ratios are also expected to be controlled by the mixed volume which determines the surface to volume ratio (S/V). The conventional way to account for changes in S/V is the scaling of HONO or HONO production ($P_{HONO}$) by $NO_2$ or $NO_x$ (e.g. Alicke et al., 2002; Alicke et al., 2003). It is assumed that $NO_x$ is also emitted close to the ground, and therefore is also sensitive to S/V and $NO_2$ is the precursor of HONO. As local sources/sinks of the compounds used for scaling (e.g. $NO_x$) may disturb the HONO/$NO_x$ ratio, Su et al. (2008a) proposed a combined scaling using also black carbon (BC) and carbon monoxide (CO). To our knowledge, only two recent studies (Yu et al., 2009; Sörgel et al., 2011) tried to address S/V (ground and aerosol) directly by using inversion layer heights from SODAR

measurements to estimate mixed volumes. However, at night a stable boundary layer is formed where only intermittent turbulence provides some mixing (Stull, 1988). Therefore, a mixed volume cannot easily be defined. Apart from that, $NO_2$ conversion frequencies measured in different environments around the world are all within a quite narrow range from 0.4 to 1.8 % $h^{-1}$ as summarized by Su et al. (2008a) and Sörgel et al. (2011). Conversion frequencies ($F_{HONO, night}$) of 0.9-2 % $h^{-1}$ for individual nights and a mean value of 1.5 ± 0.6 % $h^{-1}$ were derived in this study using the approach of Alicke et al., (2002).

In our study, nighttime HONO formation occurs presumably by (R1) and (R2). Formation through (R3), (R4) and (R7), all involving NO, is not considered to be important since HONO typically increased from sunset (17:30 UTC) to midnight, when NO mixing ratios were mostly (93 %) below the detection limit (LOD) of 6 ppt. Only 87 of 1232 five-minute mean values were above the LOD with median mixing ratios of 8 ppt, respectively. Therefore, a linear regression of the HONO/$NO_x$ ratio and HONO/$NO_2$ ratio for all night time data yields a slope of 1.0 and an intercept of 0.02 % ($r^2$=0.9986). Thus, both ratios can be regarded as equivalent during nighttime. There are no clear indications about the contribution of direct emissions. The closest emissions sources were the industrial area of Huelva (shortest distance ~15 km) and the city of Huelva (city centre about 20 km). Thus, transport times are in the range from one to two hours. Applying a conversion frequency for $NO_2$ to HONO of about 1 % $h^{-1}$, which is within the range of published values (see above), yields a 1-2 % increase in HONO/NOx during the transport. Thus, HONO mixing ratios reaching the site are already two to threefold those originally emitted (HONO/NOx ~0.8 %, Kurtenbach et al., (2001)). Using the wind sector classification for the DOMINO site of Diesch et al. (2011) we found indeed lower HONO/NOx values at night for air masses passing Huelva than for other air masses from the continent. If this can be attributed to direct emissions is unclear. The transport occurs along the coast and therefore also mixing with HONO depleted marine air can cause lower HONO/NOx. HONO/NOx values for Huelva are indeed within the range of those for the "clean" marine sector. Therefore, we assume that (R1)/(R2) is the dominant nightime HONO formation pathway at the DOMINO site.


Generally, a stable boundary layer is formed at nighttime in which turbulence is suppressed, whereas during daytime a mixed layer develops which is much more turbulent (e.g. Stull, 1988). This has two opposing effects on (R1) and (R2) (especially if the ground surface is the dominant source).

1) During daytime turbulence is enhanced which means that $NO_2$ is efficiently transported to the reactive surface.

2) The surface to volume ratio (S/V) is lower during daytime, as the mixed volume increases (mixed layer), thus less reactive surface area per volume is available.

If no deposition or advection occurs, HONO/$NO_x$ will rise continuously from sunset to sunrise, as photolysis is absent. We found decreasing HONO/$NO_x$ in the late night until sunrise which may point to the dominance of loss processes of HONO, e.g. deposition. Therefore, it is questionable if (R1) and (R2), i.e. heterogeneous formation, can simply be transferred to daytime conditions. As will be shown in Sect. 3.3 (Figs. 3 and 4), including this dark heterogeneous source as a daytime source in Eq. (3) to calculate the magnitude of the unknown daytime source $P_{unknown}$ yields mainly negative values in the early morning. This points to a missing sink like deposition (or a smaller source or both). Therefore, we did not consider this heterogeneous source for the PSS calculations.

## 3.3  Missing daytime source

As shown in Sect. 3.2 (Fig. 2) measured HONO values ($HONO_{meas}$) almost always exceed the $[HONO]_{PSS}$ values. Thus, an additional (unknown) HONO daytime source exists. Equation (2), which is similar to that of Su et al. (2008b), sums up the processes influencing HONO mixing ratios.

$$\frac{dHONO}{dt} = sources - \sin ks =$$
$$= (P_{NO+OH} + P_{emis} + P_{het} + P_{unknown}) - (L_{phot} + L_{HONO+OH} + L_{dep}) + T_v + T_h$$

(2)

The source/production ($P_x$) terms consist of the gas phase formation ($P_{NO+OH}$, (R7)), the dark heterogeneous formation ($P_{het}$, via (R1)/(R2)) and direct emissions ($P_{emis}$). $P_{unknown}$ is the unknown HONO daytime source. The sink/loss processes ($L_y$) are photolysis ($L_{phot}$, (R5)), reaction of HONO with OH ($L_{HONO+OH}$, (R6)), and dry deposition ($L_{dep}$). Note that the terms for vertical ($T_v$) and horizontal advection ($T_h$) can mimic source or sink terms depending on the HONO mixing ratios of the advected air relative to that of the measurement site (and

height). If HONO has a ground source (or near surface aerosol source), $T_v$ mimics a sink term, as vertical mixing dilutes HONO formed near the ground (see also discussion 3.2.2). The magnitude of $T_v$ (without the contribution of the rising boundary layer in the morning) can be estimated by using a parameterization for dilution by background air provided by Dillon et al. (2002), i.e. $T_v = k_{(dilution)}$ ([HONO]-[HONO]$_{background}$). Assuming a $k_{(dilution)}$ of 0.23 $h^{-1}$ (Dillon et al., 2002), a [HONO]$_{background}$ value of about 10 ppt (Zhang et al., 2009) and taking mean noontime [HONO] values of 35 ppt we can derive that $T_v$ is about 4 ppt $h^{-1}$. This value is about the same magnitude as $L_{dep}$ as already suggested by Su et al. (2008b).

$L_{dep}$ can be parameterized by multiplying the measured HONO concentration with the dry deposition velocity and then scaling by the mixing height, in order to scale the loss at the ground to its contribution to total HONO loss in the mixed volume. Taking a deposition velocity of 2 cm $s^{-1}$ (Harrison et al., 1996, Su et al., 2008b) and a mixing height of 1000 m, $L_{dep}$ is in the order of a few ppt $h^{-1}$ in our study which is indeed small (<3 % of $L_{phot}$ 09:00-15:30 UTC for 7 clear days N=312) compared to $L_{phot}$. As is discussed in more detail later, the relative contribution of $L_{dep}$ might be higher in the morning and evening hours, as $L_{phot}$ is smaller and a stable boundary layer is formed (mixed height << 1000 m, or stable conditions). Overall, $T_v$ and $L_{dep}$ are small loss terms (compared to $L_{phot}$). If their contributions are larger than assumed (especially in the morning and evening), $P_{unknown}$ is underestimated during these periods.

$P_{emis}$ cannot easily be determined, because its contribution varies with the source strength, the HONO lifetime, the horizontal wind speed and wind direction. Again, this contribution is assumed to be highest in the morning and in the evening (longer lifetimes = longer transport range). As there were no collocated emission sources, directly emitted HONO only contributed to the horizontal advection term ($T_h$). Measured HONO/NO$_x$ ratios were always higher than those reported for direct emissions (max. reported 0.8 %) (Pitts et al., 1984; Kirchstetter et al., 1996; Kurtenbach et al., 2001; Kleffmann et al., 2003). Thus, no pure direct emissions were measured. Therefore, the contribution of directly emitted HONO to the HONO budget is uncertain, but $P_{emis}$ can be assumed to be of minor importance around noon, as NO$_x$ values exhibit a minimum and show low variability. Furthermore, HONO lifetime is only about 15 min, so at typical wind speeds of about 3 m $s^{-1}$, emissions have to occur within 3 km to reach the site within their lifetime. Additionally, minimum values of HONO/NO$_x$, which indicate fresh emissions, are independent of wind direction.

Simplifying Eq. (2), we can derive the unknown HONO daytime source, $P_{unknown}$, from Eq.( 3).

$$P_{unknown} = L_{HONO+OH} + L_{phot} + L_{dep} - P_{NO+OH} - P_{het} + \frac{\Delta HONO}{\Delta t} \tag{3}$$

$P_{unknow}$ is not equal to OH production from HONO as for net OH formation a simple balancing of gas phase sources and sinks without further assumptions is applicable ($P_{OH}$ = $L_{phot}$-$L_{HONO+OH}$-$P_{NO+OH}$). Mean diurnal contributions of the single terms and the values of $P_{unknown}$ are presented in Fig.3. $P_{NO+OH}$, $L_{phot}$, $L_{HONO+OH}$ were calculated from measured values as already described for the PSS (Sect. 3.2.1). $P_{het}$ was parameterized from the nighttime $NO_2$ conversion by $P_{het}(t) = \overline{F_{HONO,night}}[NO_2]$ (Alicke et al., 2002) using $F_{HONO,night}$ = 1.5 % $h^{-1}$ (Sect. 3.2.2). The differential dHONO/dt was substituted by the difference $\Delta HONO/\Delta t$, which is the mixing ratio difference from the centre of the interval (5 min) to the centre of the next interval (LOPAP has 5 min time resolution) and accounts for changes in mixing ratio levels. It became obvious that point to point changes in HONO ($\Delta HONO/\Delta t$) were mostly smaller than the relative error of the instrument (± 12 %), and so we could not account for these changes. Values above this threshold were mainly caused by sharp HONO peaks which were accompanied with peaks in NO and BC. These plumes passed the site mainly in the morning hours (see Figs. 2, 3 and 4) with maximum HONO values comparable to the nighttime maxima (Fig.1). This indicates that especially in the morning, the advective term $T_h$ does play a role and the arrival of plumes at the site mimics a source term ($\Delta HONO/\Delta t > 0$), whereas their fading ($\Delta HONO/\Delta t < 0$) mimics a sink (Figs. 3 and 4). Also, the contribution of $\Delta HONO/\Delta t$ to the HONO budget depends on the integration time of the HONO signal. Comparing 5, 15, 30 and 60 min values, the highest contribution is associated with the 5 min values and the lowest with the 30 min values (60 min values are possibly already influenced by the diurnal cycle). Besides less influence from advection, the lower contribution of $\Delta HONO/\Delta t$ to the source and sink terms during the PRIDE-PRD-2004 experiment (Su et al., 2008b) compared to our study could at least partly be caused by the lower time resolution for HONO measurements in that study.
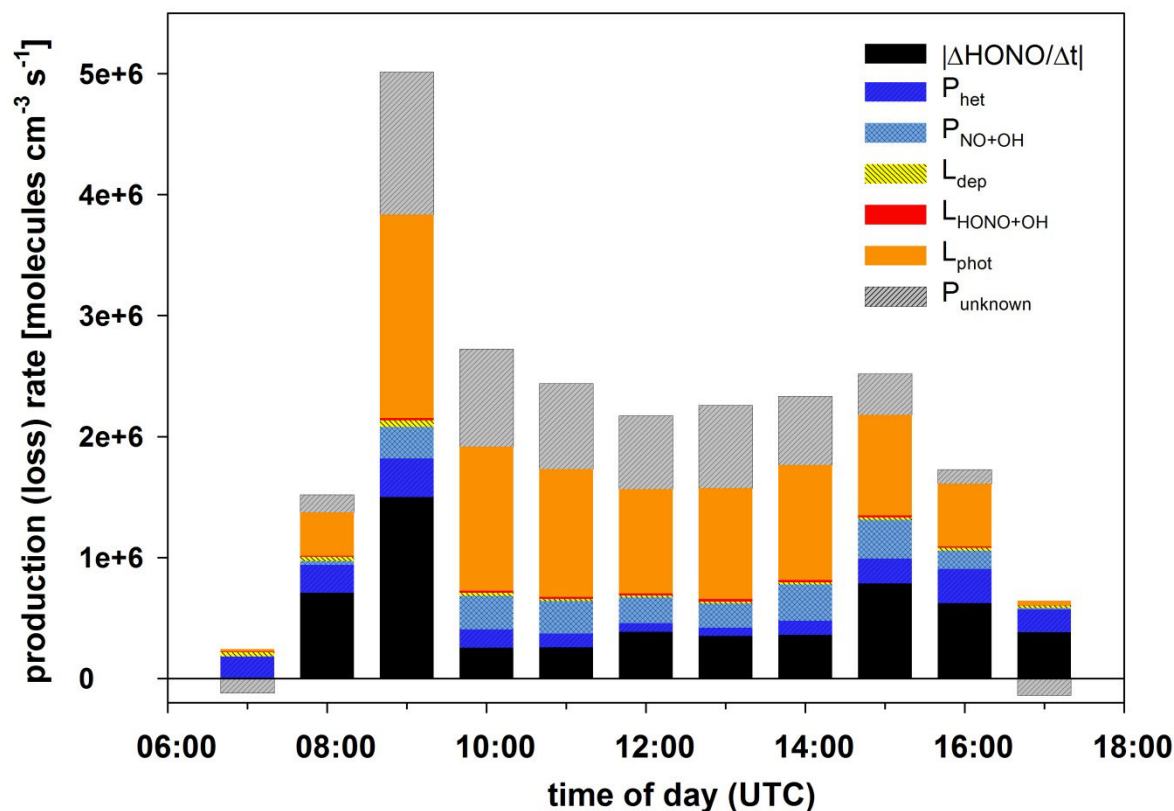
Figure 3: Contributions of production (bluish colours) and loss terms (hourly means 21st Nov. to 5th Dec.) as well as the unknown daytime HONO source $P_{unknown}$ from Eq. (3).

The contributions of the terms of Eq (3) to the HONO budget (Fig.3) are as follows. The reaction between HONO and OH ($L_{HONO+OH}$) has a very small contribution to HONO loss (mostly less than 5 % of $L_{phot}$). Dry deposition ($L_{dep}$) is also very small (mostly less than 3 % of $L_{phot}$). Around noon the main known HONO source is $P_{NO+OH}$. Due to low $NO_2$ levels around noon (see Fig.2) $P_{het}$ is also very low during that period. The noon period is clearly dominated by loss via $L_{phot}$ (the overall dominant loss process) and formation by the unknown HONO source ($P_{unknown}$). $P_{het}$ is higher in the morning and evening, respectively, provided that the parameterization (Sect. 2.3.2) is valid. $P_{unknown}$ is negative (Figs. 3 and 4) in the early morning and evening indicating a missing sink, since more HONO is formed by the "known sources" than is destroyed via photolysis. A likely sink is non-negligible deposition of HONO, whose relative contribution might be higher in the morning and evening hours (mixed height <<1000m).
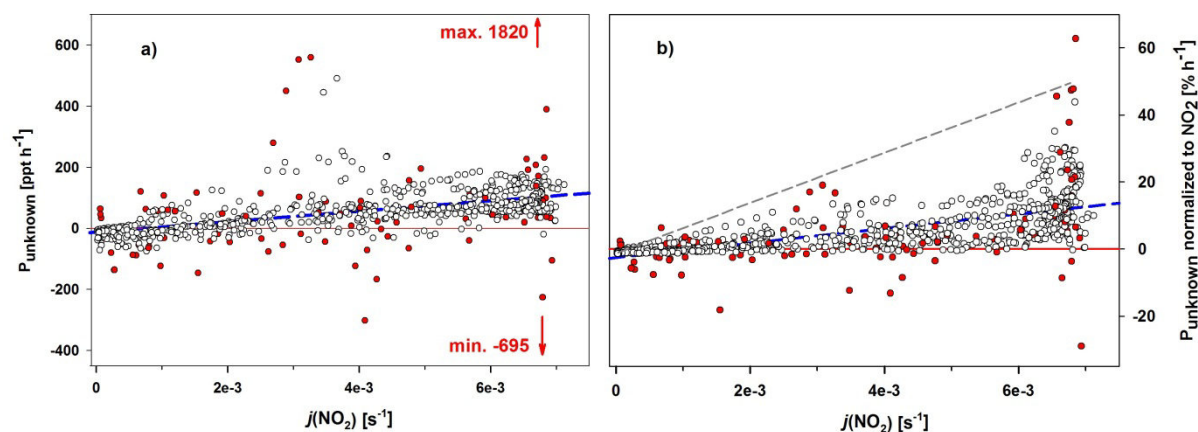
Figure 4: a) unknown HONO daytime source ($P_{unknown}$) in ppt h$^{-1}$ for all days versus $j(NO_2)$. b) $P_{unknown}$ normalized by $NO_2$ mixing ratios yielding a conversion frequency (% h$^{-1}$). Figure a) contains only data points (N= 753) which could be normalized to $NO_2$. Points where $\Delta HONO/\Delta t$ was larger than the relative error of the LOPAP ($\pm$ 12 %) are marked as filled red points. Blue dashed lines are linear fits to the data with a) r$^2$ = 0. 16 and b) r$^2$ = 0.38. The grey dashed line in Fig. 4a presents an upper limit based on the mean of the five lowest points at $(jNO_2)_{min}$ and five highest points at $(jNO_2)_{max}$.

Figure 4a shows all calculated values of the unknown HONO source ($P_{unknown}$) in ppt h$^{-1}$ (= 7.37 x 10$^3$ molecules cm$^{-3}$ s$^{-1}$ at 1000 hPa and 273.15 K) versus $j(NO_2)$, as former studies (e.g. Vogel et al., 2003; Su et al., 2008b) proposed a correlation of this source to $j(NO_2)$. Values for $P_{unknown}$ range from about -700 to 1800 ppt h$^{-1}$ (at noontime 10:00-14:00 UTC: 105 $\pm$ 39 ppt h$^{-1}$ for 7 clear days N= 195) which is within the range of other rural and urban studies (Kleffmann, 2007). The filled red dots in Fig. 4 are points where $\Delta HONO/\Delta t$ values were larger than the respective relative errors of the HONO measurements, and thus included in Eq.( 3). Applying a linear fit to the data in Fig. 4 a yields a coefficient of determination (r$^2$) of 0.16, and thus a rather weak linear correlation of $P_{unknown}$ versus $j(NO_2)$.

As light-induced conversion of $NO_2$ is thought to be the most probable source of HONO daytime formation, we normalized the unknown source by the $NO_2$ mixing ratios to improve comparability to other environmental conditions (remote, urban, laboratory). This normalized $P_{unknown}$ presented in Fig. 4b has the same units (% h$^{-1}$) as the nightime conversion frequency ($F_{HONO,night}$) and can be referred to as a daytime conversion frequency assuming $NO_2$ is the direct precursor as indicated by recent studies of light-induced $NO_2$ conversion (e.g. Stemmler et al., 2006). Figure 4b indicates that $NO_2$ levels indeed play an important role, as peak values of the daytime source, when scaled by $NO_2$ mixing ratios, fall below an upper limit of conversion of $P_{unknown,norm,max}$ = (7490*$j(NO_2)$-1.2) % h$^{-1}$ . The coefficient of determination of the linear fit to all values (Fig. 4b blue dashed line) increased from 0.16 without to 0.38 with $NO_2$ scaling. The correlation further improved to r$^2$ = 0.47 if only data from clear days were

taken and advection events were excluded (Fig. 5 insert). Nevertheless, this means that less than 50 % of the variance is explained by the linear model of the normalized unknown HONO source increasing linearly with $j(NO_2)$. A possible reason are HONO sources which are independent of the $NO_x$ values such as $HNO_3$ photolysis (Zhou et al., 2011) or soil emissions (Su et al., 2011). These sources would cause an overestimation of the conversion frequencies at low ambient $NO_x$ levels. Nevertheless, normalizing by $NO_2$ values seems to efficiently remove peak values in HONO formation during advection events.
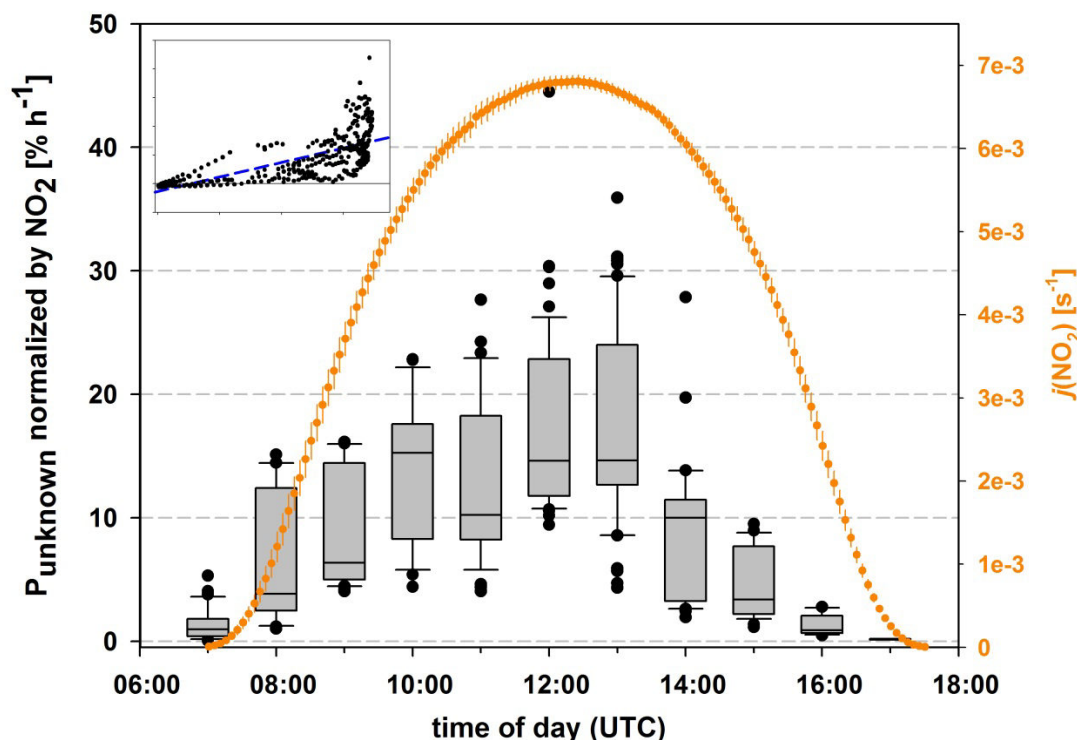


Figure 5: Diurnal cycle (only daytime) of the unknown HONO source ($P_{unknown}$), normalized by $NO_2$ mixing ratios from 7 cloud-free days (same as Fig. 2). To reflect more stationary conditions, only values where $\Delta HONO/\Delta t$ was lower than the relative error of the LOPAP were included in this graph. The upper ends of the bars reflect the $75^{th}$ percentiles, the lower bounds the $25^{th}$ percentiles and the line in between the medians. The upper whiskers represents the $90^{th}$ percentiles and the lower the $10^{th}$ percentiles. The minimum number of data points per hour is 17 (7:00), the maximum is 59 (13:00), except for the values close to sunset (17:00) with only 8 data points. Orange dots and bars represent the mean and standard deviation of $j(NO_2)$ for these days, respectively. The insert shows the same data, but as correlation plot of normalized $P_{unknown}$ versus $j(NO_2)$. The $r^2$ of the regression line is 0.47.

As can be seen from a comparison with the diurnal cycle of the normalized $P_{unknown}$ in Fig. 5, the contribution of $P_{het}$ to daytime HONO is very low during most of the day. While the maximum dark heterogeneous conversion rates are around 2 % $h^{-1}$, the normalized unknown source (presumably daytime $NO_2$ conversion frequency) reaches median values of about 14 % $h^{-1}$ around noontime, with maximum values up to 43 % $h^{-1}$. Around noon $P_{unknown}$ is thus about 7 to 20 times faster than the parameterized nighttime conversion, which is in agreement

with Kleffmann et al. (2003), but a factor of three lower than found by Kleffmann et al. (2005).

## *3.4  Potential contributions to the unknown HONO daytime source*

In this section we investigate the contributions of two possible reaction pathways recently investigated in laboratory studies following a light-induced conversion of $NO_2$.

### 3.4.1  $NO_2$ conversion on irradiated soot

We calculated HONO production rates from the reaction of $NO_2$ on irradiated soot surfaces by extrapolating the reactive uptake coefficients ($\gamma$-values) derived in a laboratory study (Monge et al., 2010) to conditions we measured in the field. These $\gamma$-values were normalized to the Brunauer-Emmett-Teller surface (BET-surface) of the soot samples yielding a mass independent uptake ($\gamma$-BET). This $\gamma$-BET for $NO_2$ was found to increase with increasing irradiance and with decreasing $NO_2$ mixing ratios (Monge et al. 2010). Therefore, we used an extrapolation to lower $NO_2$ values (<< 16 ppb) provided by D'Anna et al. (personal communication, 2010) leading to higher reactive $NO_2$ uptake in our study (median daytime $NO_2$= 0.9 ppb). For simplicity, we took a value of 100 $m^2$ $g^{-1}$ as the BET surface for soot, which is between the values (120-140 $m^2$ $g^{-1}$ from a propane flame) used by Monge et al. (2010) and a value of 97 $m^2$ $g^{-1}$ published for freshly emitted (81 $m^2$ $g^{-1}$ for oxidized) soot (Daly and Horn, 2009). It can be regarded as an upper limit for soot from natural and anthropogenic combustion (Rockne et al., 2000, Fernandes et al., 2003). Black carbon (BC) measurements were taken as proxy soot values. As a further simplification, we used a constant upper limit integrated (300-420 nm) photon flux of 1.91 x $10^{16}$ photons $cm^{-2}$ $s^{-1}$ instead of varying it with the solar zenith angle. Therefore, the diurnal variation of the calculated values (Fig. 6) has to be viewed with caution. High values in the morning hours due to $NO_2$ and BC peaks are actually lower due to lower irradiance values in the morning, and thus lower reactivity. Following Monge et al. (2010), we assumed a HONO production of 60 % of the reactive $NO_2$ uptake. Although we used upper limits for all calculations, the resulting values for the HONO production by this source (Fig. 6) are below 0.6 % of $P_{unknown}$ in 75 % of all cases (25 percentile = 0.2 % and median = 0.3 %). Thus, for conditions encountered during our campaign (daytime $BC_{median} \sim 300$ ng $m^{-3}$ and $NO_{2,median} \sim 0.9$ ppb) this reaction has no noticeable influence on HONO daytime values.

### 3.4.2 Electronically excited NO$_2$ reacting with water vapour

In order to study the potential contribution of the controversially discussed reaction of electronically excited NO$_2$ with water vapour (R8), we calculated its contribution to HONO and OH formation using the expression for OH production (= HONO production) from Crowley and Carl (1997).

$$R_{OH} = j_{ex}(NO_2)[NO_2]/(1 + k_{air}[M]/k_8[H_2O])  \qquad (4)$$

$j_{ex}(NO_2)$ is the frequency of electronic excitation of NO$_2$ beyond the dissociation threshold (> 420 nm), and k$_{air}$ (~3*10$^{-11}$, Crowley and Carl, 1997) the rate constant for non- reactive quenching with air. k$_8$ is the rate constant for the reactive quenching with H$_2$O, k$_{8,Crowley}$ = 1.2 x 10$^{-14}$ cm$^3$ molecules$^{-1}$ s$^{-1}$ according to Crowley and Carl (1997) and k$_{8,Li}$ = 1.7 x 10$^{-13}$ cm$^3$ molecules$^{-1}$ s$^{-1}$ according to Li et al. (2008). We estimated $j_{ex}$(NO$_2$) from measured $j$(NO$_2$) by multiplying with a factor of 3.5 (Crowley and Carl, 1997) which is consistent with solar zenith angles < 70° (~ 60° around noontime).
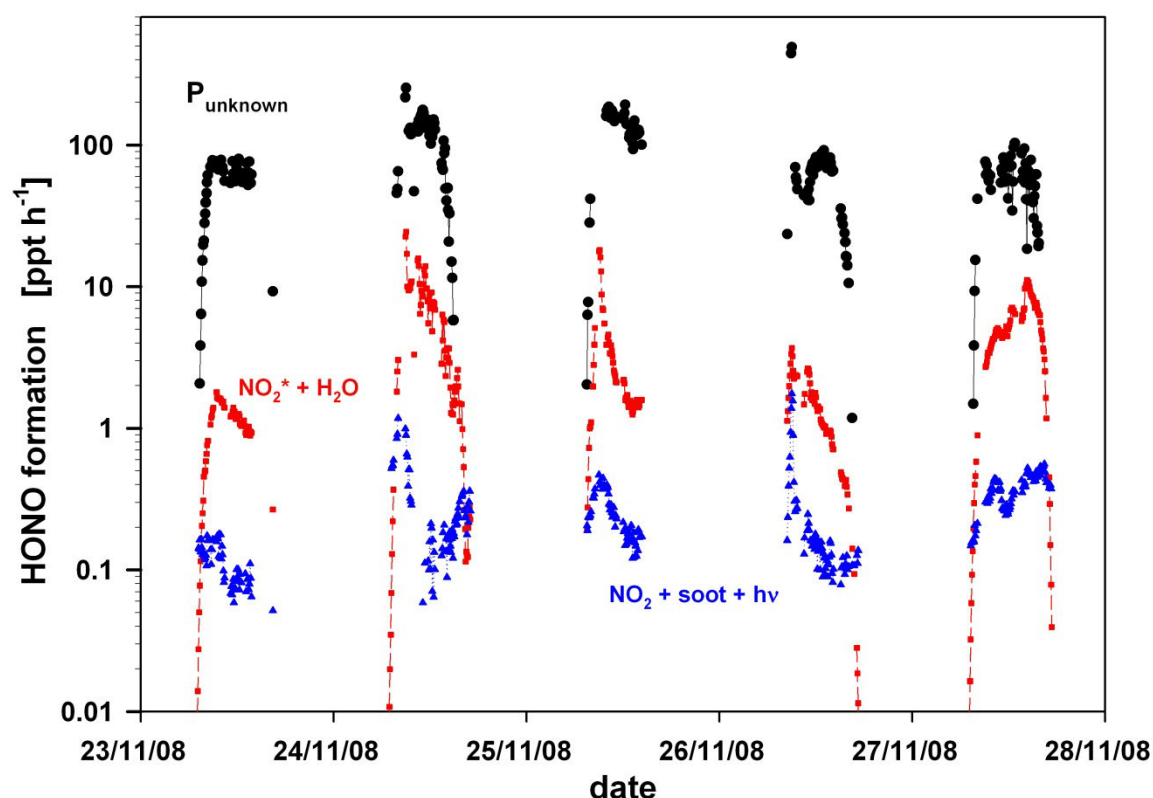


Figure 6: Comparison of different HONO daytime source strengths (blue: NO$_2$ + soot + hv (Monge et al., 2010); red: NO$_2$* + H$_2$O (Li et al., 2008)) with the unknown HONO daytime source (black).

Referring to $k_{8,Li}$ as an upper limit, HONO and OH production rates calculated via Eq. (4) are in the order of a few ppt $h^{-1}$. This contribution to $P_{unknown}$ is less than 8 % for 75 % of our data, with a median contribution of 4 %. Using $k_{8,Crowley}$, the values are one order of magnitude lower and thus negligible. These findings are in line with calculations from Crowley and Carl (1997) and with recent modelling studies (Wennberg and Dabdub, 2008; Sarwar et al., 2009; Ensberg et al., 2010) where this reaction was found to have a noticeable impact only at very high pollution levels, when using $k_{8,Li}$. As we do not expect the value for $k_8$ to be higher than reported by Li et al. (2008), we do not follow the approach of Wentzell et al. (2010) to explain the unknown HONO source by (R8) with varying $k_8$ alone. A very recent paper by Amedro et al. (2011) confirms that the reaction of Li et al. (2008) followed a multi photon absorption process, and provides an upper limit for reactive quenching which is even lower than that of Crowley and Carl (1997).

### 3.4.3  Important ground sources

The proposed formation of nitrous acid on the ground follows two major pathways. The light-induced $NO_2$ conversion via organic photosensitizers (George et al., 2005; Stemmler et al., 2006) and the microbiological formation of nitrite in the soil and the volatilization to the atmosphere as HONO (Kubota and Asami 1985; Su et al., 2011). As recent measurements of the photolysis of adsorbed $HNO_3$ (Zhu et al., 2010) found $NO_2^*$ as the main photolysis product, Zhou et al. (2011) assume that HONO formation by $HNO_3$ photolysis also follows the mechanism of $NO_2$ conversion provided by George et al.(2005) and Stemmler et al. (2006). Adsorbed $HNO_3$ therefore acts as a reservoir or a source of $NO_x$ in rural environments (Zhou et al., 2002b, 2003, 2011). One might speculate if the reaction of $NO_2^*$ formed by $HNO_3$ photolysis at the surface with adsorbed water is also enhanced with regard to the gas phase reaction (R8), and thus can act as source of HONO from $HNO_3$ photolysis. The relative contribution of $HNO_3$ photolysis to direct $NO_2$ conversion increases with surface nitrate loading and decreasing $NO_x$ values. This might be reflected in our measurements as some of the highest conversion frequencies (Fig. 4b) were measured on a "clean day" ($NO_x < 0.5$ ppb). For a rough estimate of the contribution of direct $NO_2$ conversion (on aerosol and ground surfaces) we took the estimates of Stemmler et al. (2007) which are about 1 ppt $h^{-1}$ for humic acid aerosol and about 700 ppt $h^{-1}$ for conversion at the soil surface in a 100 m mixed height

at 20 ppb $NO_2$. We scaled these values to 1 ppb $NO_2$ (observed $NO_2$ values). As already concluded by Stemmler et al. (2007) the contribution of the aerosol is negligible ($\sim$0.05 ppt h$^{-1}$). The ground source would contribute about 35 ppt h$^{-1}$, i.e. one third of the missing source, applying a linear scaling with $NO_2$.

Regarding the soil emissions, there are no soil acidity and nitrate loading data available for the DOMINO campaign. Therefore, it is at best speculative to derive a HONO source based on the numbers given by Su et al. (2011) as the resulting HONO fluxes vary by orders of magnitude. But as HONO soil flux values in the lowest range (low nitrogen loading and rather high pH) can already produce source strength in the right order of magnitude for $P_{unknown}$, this HONO source might be a substantial contribution during DOMINO.

All calculations about source strength at the ground are very sensitive to vertical mixing. Thus, as already addressed by Zhou et al. (2011), vertical transport determines the discrepancy between the effective source strength relative to that calculated at the measurement height. We conclude that only modelling which takes vertical transport into account can yield reliable estimates of the ground source contribution to the missing HONO source.

## 3.5 Comparison of OH radical production from ozone and HONO photolysis

OH production rates from ozone photolysis were calculated from ozone, $H_2O$ measurements and modelled $jO(^1D)$ values which were scaled by the ratio of measured and modelled $j(NO_2)$. OH production from $O(^1D)$ was calculated according to Crowley and Carl (1997) using the rate constants for $O(^1D)$ quenching by $O_2$, $N_2$ and $O_3$ and the reaction with $H_2O$ taken from the IUPAC recommendations (Atkinson et al., 2004 and updated values from the IUPAC homepage, http://www.iupac-kinetic.ch.cam.ac.uk/). These values are in good agreement ($\sim$ 3 % higher) with the same calculations using the recommendations from Sander et al. (2006). The net OH production by HONO was calculated by balancing source and sink terms of OH by HONO in the gas phase (for k values see Sect. 3.2):

$$P_{OH} = j(HONO)[HONO] - k_7[NO][OH] - k_6[HONO][OH] \qquad (5)$$

Although HONO mixing ratios (mean: 30 ppt) are three orders of magnitude lower than $O_3$ mixing ratios (mean: 35 ppb) around noon and OH production rates by $O(^1D)$ exceed those of HONO photolysis by about 50 % around noon (11:00-13:00), the integrated daily OH production is about 20 % lower than that of HONO. Figure 7 shows the higher contribution of HONO photolysis to the OH formation in the morning and evening hours due to longer wavelengths (up to ~ 400 nm) associated with HONO photolysis. A special feature of our measurement site are the very high HONO values between 8:00 and 11:00, which can be attributed to advection (see Sect. 3.2 and 3.3). This leads to high $P_{OH}$ values from HONO photolysis during that period.



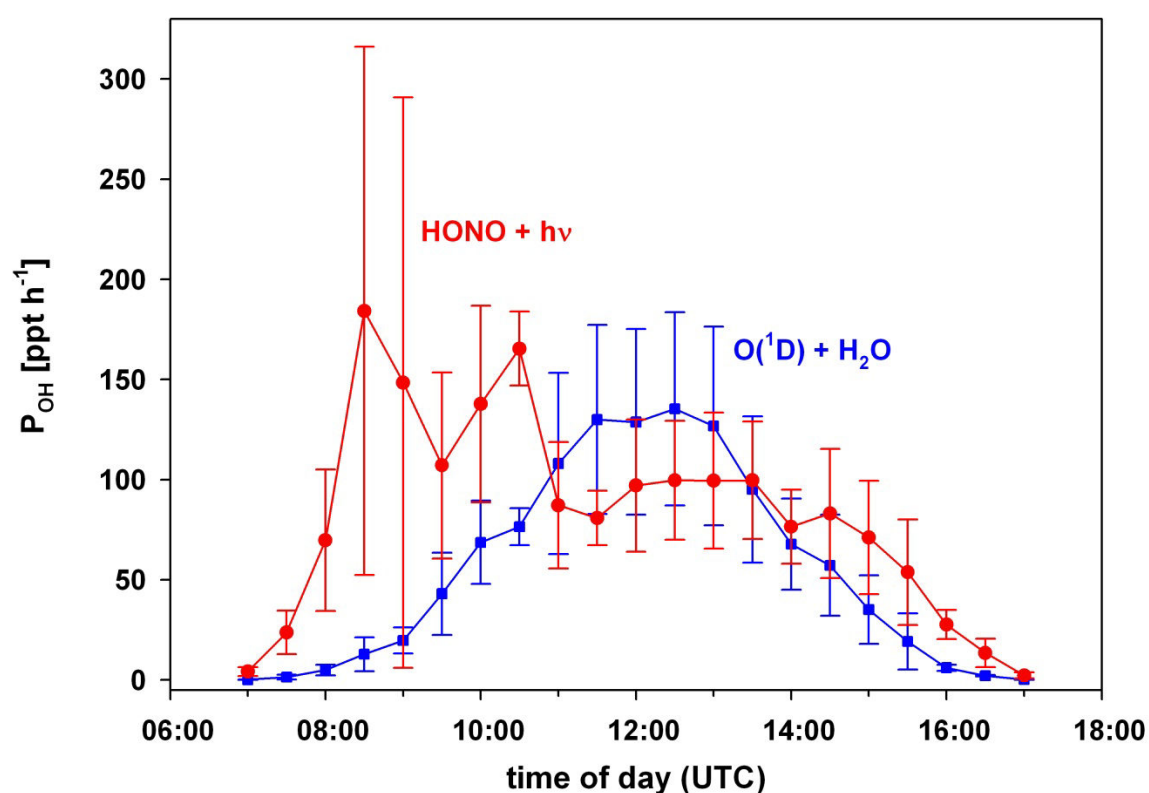Figure 7: Comparison for the seven clear days of the campaign of calculated primary OH production by HONO and ozone photolysis (means and standard deviations).

# 4  Conclusions

The unknown HONO daytime source derived from our measurements was normalized by $NO_2$ mixing ratios to improve comparability of HONO source strengths in different environmental and laboratory conditions. For the nighttime formation of HONO, we can

exclude that NO plays an important role as NO was mostly below the detection limit of about 6 ppt. Inclusion of the parameterized nighttime HONO formation from $NO_2$ (1.5 % $h^{-1}$ in this study) as an additional source into the calculations of the unknown HONO daytime source ($P_{unknown}$) yields mainly negative values in the early morning. This indicates the relevance of loss terms not taken into account (e.g. deposition) or overestimation of the dark heterogeneous formation in the morning and evening. Restricting the analysis only to cloud free days and the time around noon, when faster HONO photolysis leads to lifetimes around 15 min and other loss processes for HONO are small compared to loss by photolysis, establishment of a PSS can be assumed. The mean source strength of $P_{unknown}$ under these conditions was about 100 ppt $h^{-1}$ and thus in the lower range of values reported in the literature. Nevertheless $P_{unknown}$ was the dominant HONO source during day. The normalized unknown HONO source (or $NO_2$ conversion frequency, if we assume that $NO_2$ is the precursor) varied from slightly negative values in the morning and evening to an upper limit correlated with $j(NO_2)$. High median daytime $NO_2$ conversion frequencies of ~14 % $h^{-1}$ were found around noon, in addition to the 1.5 % $h^{-1}$ HONO formation rate observed during night.

Our results indicate light-induced HONO formation, possibly via conversion of $NO_2$ as indicated by lab experiments. This source is about an order of magnitude stronger than HONO formation during nighttime. We compared the HONO net source to values calculated for light-induced $NO_2$ uptake on soot (Monge et al., 2010) and the reaction of electronically excited $NO_2^*$ with water vapour. The contribution of these reactions to HONO daytime values was mostly less than 10 % and cannot explain the HONO source strength derived in our study. Other processes like light-induced conversion of $NO_2$ on irradiated organic materials like humic acids (Stemmler et al., 2006), or soil emissions (Su et al., 2011) might be more important. Additional measurements including detailed speciation of organic aerosols and determination of humic acids on ground and canopy surfaces are needed to quantify their contribution. Furthermore, a detailed assessment of the contribution of the ground sources requires profound knowledge of boundary layer processes. The unknown HONO daytime source is essential contribution to primary OH production, as photolysis of HONO exceeded the OH formation by ozone photolysis by 20 %.

# References:

Acker, K., Möller, D., Wieprecht, W., Meixner, F. X., Bohn, B., Gilge, S., Plass-Dülmer, C., and Berresheim, H.: Strong daytime production of OH from HNO$_2$ at a rural mountain site, Geophys. Res. Lett., 33, L02809, doi:10.1029/2005GL024643, 2006.

Alicke, B., Platt, U., and Stutz, J.: Impact of nitrous acid photolysis on the total hydroxyl radical budget during the Limitation of Oxidant Production Pianura/Padana Produzione di Ozono study in Milan, J. Geophys. Res., 107, 8196, doi:10.1029/2000JD000075, 2002.

Alicke, B., Geyer, A., Hofzumahaus, A., Holland, F., Konrad, S., Pätz, H. W., Schäfer, J., Stutz, J., Volz-Thomas, A., and Platt, U.: OH formation by HONO photolysis during the BERLIOZ experiment, J. Geophys. Res., 108, 8247, doi:10.1029/2001JD000579, 2003.

Amedro, D., Parker, A. E., Schoemaecker, C., and Fittschen, C.: Direct observation of OH radicals after 565 nm multi-photon excitation of NO$_2$ in the presence of H$_2$O, Chem. Phys. Lett., 513, 12-16, 2011.

Ammann, M., Rössler, E., Strekowski, R., and George, C.: Nitrogen dioxide multiphase chemistry: Uptake kinetics on aqueous solutions containing phenolic compounds, Phys. Chem. Chem. Phys., 7, 2513 – 2518, 2005.

Andres-Hernandez, M. D., Notholt, J., Hjorth, J., and Schrems, O.: A DOAS study on the origin of nitrous acid at urban and non-urban sites, Atmos. Environ., 30, 175-180, 1996.

Arens, F., Gutzwiller, L., Baltensperger, U., Gäggler, H. W., and Ammann, M.: Heterogeneous reaction of NO$_2$ on diesel soot particles, Environ. Sci. Technol., 35, 2191-2199, 2001.

Atkinson, R., Baulch, D. L., Cox, R. A., Crowley, J. N., Hampson, R. F., Hynes, R. G., Jenkin, M. E., Rossi, M. J., and Troe, J.: Evaluated kinetic and photochemical data for atmospheric chemistry: Volume I – gas phase reactions of Ox, HOx, NOx and SOx species, Atmos. Chem. Phys., 4, 1461–1738, 2004.

Aubin, D. G., and Abbatt, J. P. D.: Interaction of NO$_2$ with hydrocarbon soot: focus on HONO yield, surface modification, and mechanism, J. Phys. Chem. A, 111, 6263-6273, 2007.

Bejan, I., Abd el Aal, Y., Barnes, I., Benter, T., Bohn, B., Wiesen, P., and Kleffmann, J.: The photolysis of ortho-nitrophenols: a new gas phase source of HONO, Phys. Chem. Chem. Phys., 8, 2028–2035, doi: 10.1039/b516590c, 2006.

Blitz, M. A.: Comment on "The conical intersection dominates the generation of tropospheric hydroxyl radicals from NO$_2$ and H$_2$O", J. Phys. Chem. A, 114, 8016, 2010.

Bohn, B., and Zetzsch, C.: Rate constants of HO$_2$ + NO covering atmospheric conditions. 1. HO$_2$ formed by OH + H$_2$O$_2$, J. Phys. Chem. A, 101, 1488-1493, 1997.

Calvert, J. G., Yarwood, G., and Dunker, A. M.: An evaluation of the mechanism of nitrous acid formation in the urban atmosphere, Res. Chem. Intermediat., 20, 463-502, 1994.

Cancillo, M. L., Serrano, A., Antón, M., García, J. A., Vilaplana, J. M., and de la Morena, B.: An improved outdoor calibration procedure for broadband ultraviolet radiometers, Photochem. Photobiol., 81, 860-865, 2005.

Carr, S., Heard, D. E., and Blitz, M. A.: Comment on "Atmospheric Hydroxyl Radical Production from Electronically Excited $NO_2$ and $H_2O$", Science, 324, 336 b, doi: 10.1126/science.1166669, 2009.

Cox, R. A.: The photolysis of nitrous acid in the presence of carbon monoxide and sulphur dioxide, J. Photochem., 3, 291 - 304, 1974.

Crowley, J. N., and Carl, S. A.: OH formation in the photoexcitation of $NO_2$ beyond the dissociation threshold in the presence of water vapor, J. Phys. Chem. A, 101, 4178-4184, 1997.

Daly, H. M., and Horn, A. B.: Heterogeneous chemistry of toluene, kerosene and diesel soots, Phys. Chem. Chem. Phys., 11, 1069–1076, 2009.

D'Anna, B., Monge, M. E. and George, C.: personal communication, 2010.

Diesch, J.-M., Drewnick, F., Zorn, S. R., von der Weiden-Reinmüller, S.-L., Martinez, M. and Borrmann, S.: Variability of aerosol, gaseous pollutants and meteorological characteristics associated with continental, urban and marine air masses at the SW Atlantic coast of Iberia, in preparation, 2011.

Dillon, M. B., Lamanna, M. S., Schade, G. W., Goldstein, A., and Cohen, R. C.: Chemical evolution of the Sacramento urban plume: Transport and oxidation, J. Geophys. Res., 107, 4045, 10.1029/2001JD000969, 2002.

Ensberg, J. J., Carreras-Sospedra, M., and Dabdub, D.: Impacts of electronically photo-excited $NO_2$ on air pollution in the South Coast Air Basin of California, Atmos. Chem. Phys., 10, 1171–1181, 2010.

Fang, Q., Han, J., Jiang, J., Chen, X., and Fang, W.: The conical intersection dominates the generation of tropospheric hydroxyl radicals from $NO_2$ and $H_2O$, J. Phys. Chem. A, 114, 4601–4608, 2010.

Febo, A., Perrino, C., and Allegrini, I.: Measurement of nitrous acid in Milan, Italy, by DOAS and diffusion denuders, Atmos. Environ., 30 3599-3609, 1996.

Fernandes, M. B., Skjemstad, J. O., Johnson, B. B., Wells, J. D. and Brooks, P.: Characterization of carbonaceous combustion residues. I. Morphological, elemental and spectroscopic features, Chemosphere, 51, 785–795, 2003.

Finlayson-Pitts, B. J., Wingen, L. M., Sumner, A. L., Syomin, D., and Ramazan, K. A.: The heterogeneous hydrolysis of $NO_2$ in laboratory systems and in outdoor and indoor atmospheres: An integrated mechanism, Phys. Chem. Chem. Phys., 5, 223-242, 2003.

Finlayson-Pitts, B. J.: Reactions at surfaces in the atmosphere: integration of experiments and theory as necessary (but not necessarily sufficient) for predicting the physical chemistry of aerosols, Phys. Chem. Chem. Phys., 11, 7760–7779, 2009.

George, C., Strekowski, R. S., Kleffmann, J., Stemmler, K., and Ammann, M.: Photoenhanced uptake of gaseous $NO_2$ on solid organic compounds: a photochemical source of HONO?, Faraday Discuss., 130, 195–210, 2005.

Gonçalves, M ., Dabdub, D., Chang, W. L. , F. Saiz, F., O. Jorba, O., and Baldasano, J. M.: The impact of different nitrous acid sources in the air quality levels of the Iberian Peninsula, Atmos. Chem. Phys. Discuss., 10, 28183–28230, 2010

Gustafsson, R. J., Orlov, A., Griffiths, P. T., Cox, R. A., and Lambert, R. M.: Reduction of $NO_2$ to nitrous acid on illuminated titanium dioxide aerosol surfaces: implications for photocatalysis and atmospheric chemistry, Chem. Commun., 37, 3936–3938, 2006.

Gustafsson, R. J., Kyriakou, G., and Lambert, R. M.: The molecular mechanism of tropospheric nitrous acid production on mineral dust surfaces, ChemPhysChem, 9, 1390-1393, 2008.

Gutzwiller, L., Arens, F., Baltensberger, U., Gäggler, H. W., and Ammann, M.: Significance of semivolatile diesel exhaust organics for secondary HONO formation, Environ. Sci. Technol., 36, 677-682, 2002a.

Gutzwiller, L., George, C., Rössler, E., and Ammann, M.: Reaction kinetics of $NO_2$ with resorcinol and 2,7-naphthalenediol in the aqueous phase at different pH, J. Phys. Chem. A, 106, 12045-12050, 2002b.

Hanst, P. L., Spence, J. W., and Miller, M.: Atmospheric chemistry of n-nitroso dimethylamine, Environ. Sci. Technol., 11, 403-405, 1977.

Harrison, R. M., and Kitto, A.-M. N.: Evidence for a surface source of atmospheric nitrous acid, Atmos. Environ., 28, 1089-1094, 1994.

Harrison, R. M., Peak, J. D., and Collin, G. M.: Tropospheric cycle of nitrous acid, J. Geophys. Res., 101, 14429–14439, 1996.

Heland, J., Kleffmann, J., Kurtenbach, R., and Wiesen, P.: A new instrument to measure gaseous nitrous acid (HONO) in the atmosphere, Environ. Sci. Technol., 35, 3207–3212, 2001.

Hosaynali Beygi, Z., Fischer, H., Harder H. D., Martinez, M., Sander, R., Williams, J., Brookes, D. M., Monks, P. S. and Lelieveld, J.: Oxidation photochemistry in the Southern Atlantic boundary layer: unexpected deviations of photochemical steady state, Atmos. Chem. Phys., 11, 8497-8513, 2011.

IUPAC Subcommittee on Gas Kinetic Data Evaluation: http://www.iupac-kinetic.ch.cam.ac.uk/, access 10 January 2011.

Jenkin, M. E., Cox, R. A., and Williams, D. J.: Laboratory studies of the kinetics of formation of nitrous acid from the thermal reaction of nitrogen dioxide and water vapour, Atmos. Environ., 22 487-498, 1988.

Killus, J. P., and Whitten, G. Z.: Background reactivity in smog chambers, Int. J. Chem. Kinet., 22, 547-575, 1990.

Kinugawa, T., Enami, S., Yabushita, A., Kawasaki, M., Hoffmann, M. R., and Colussi, A. J.: Conversion of gaseous nitrogen dioxide to nitrate and nitrite on aqueous surfactants, Phys. Chem. Chem. Phys., 13, 5144-5149, DOI: 10.1039/C0CP01497D, 2011.

Kirchstetter, T. W., Harley, R. A., and Littlejohn, D.: Measurement of nitrous acid in motor vehicle exhaust, Environ. Sci. Technol., 30, 2843-2849, 1996.

Kleffmann, J., Becker, K. H., and Wiesen, P.: Heterogeneous $NO_2$ conversion processes on acid surfaces: possible atmospheric implications, Atmos. Environ., 32, 2721-2729, 1998.

Kleffmann, J., Becker, K. H., Lackhoff, M., and Wiesen, P.: Heterogeneous conversion of $NO_2$ on carbonaceous surfaces, Phys. Chem. Chem. Phys., 1, 5443-5450, 1999.

Kleffmann, J., Heland, J., Kurtenbach, R., Lörzer, J., and Wiesen, P.: A new instrument (LOPAP) for the detection of nitrous acid (HONO), Environ. Sci. Pollut. R., 4, 48–54, 2002.

Kleffmann, J., Kurtenbach, R., Lörzer, J., Wiesen, P., Kalthoff, N., Vogel, B., and Vogel, H.: Measured and simulated vertical profiles of nitrous acid—Part I: Field measurements, Atmos. Environ., 37, 2949–2955, 2003.

Kleffmann, J., Benter, T., and Wiesen, P.: Heterogeneous reaction of nitric acid with nitric oxide on glass surfaces under simulated atmospheric conditions, J. Phys. Chem. A, 108, 5793-5799, 2004.

Kleffmann, J., Gavriloaiei, T., Hofzumahaus, A., Holland, F., Koppmann, R., Rupp, L., Schlosser, E., Siese, M., and Wahner, A.: Daytime formation of nitrous acid: A major source of OH radicals in a forest, Geophys. Res. Lett., 32, L05818, doi:10.1029/2005GL022524, 2005.

Kleffmann, J.: Daytime sources of nitrous acid (HONO) in the atmospheric boundary layer, ChemPhysChem, 8, 1137 – 1144, 2007.

Kraus, A., and Hofzumahaus, A.: Field measurements of atmospheric photolysis frequencies for $O_3$, $NO_2$, HCHO, $CH_3CHO$, $H_2O_2$, and HONO by UV spectroradiometry, J. Atmos. Chem., 31, 161–180, 1998.

Kubota, M., Asami, T.: Source of nitrous acid volatilized from upland soils, Soil Sci. Plant Nutr., 31, 35-42, 1985

Kurtenbach, R., Becker, K. H., Gomes, J. A. G., Kleffmann, J., Lörzer, J. C., Spittler, M., Wiesen, P., Ackermann, R., Geyer, A., and Platt, U.: Investigations of emissions and heterogeneous formation of HONO in a road traffic tunnel, Atmos. Environ., 35, 3385-3394, 2001.

Lammel, G., and Cape, J. N.: Nitrous acid and nitrite in the atmosphere, Chem. Soc. Rev., 25, 361-369, 1996.

Li, S., Matthews, J., and Sinha, A.: Atmospheric hydroxyl radical production from electronically excited $NO_2$ and $H_2O$, Science, 319, 1657-1660, doi: 10.1126/science.1151443, 2008.

Li, S., Matthews, J., and Sinha, A.: Response to comment on "Atmospheric hydroxyl radical production from electronically excited $NO_2$ and $H_2O$", Science, 324, 336 c, 2009.

Madronich, S. and Flocke, S., The role of solar radiation in atmospheric chemistry, in The Handbook of Environmental Chemistry / Reactions and Processes / Environmental Photochemistry Part I: BD 2 / Part L, Boule, P. (ed.), Springer-Verlag, Heidelberg, 373 (pp. 1-26), 1998.

Martinez, M., Harder, H., Kubistin, D., Rudolf, M., Bozem, H., Eerdekens, G., Fischer, H., Klüpfel, T., Gurk, C., Königstedt, R., Parchatka, U., Schiller, C. L., Stickler, A., Williams, J., and Lelieveld, J.: Hydroxyl radicals in the tropical troposphere over the Suriname rainforest: airborne measurements, Atmos. Chem. Phys., 10, 3759-3773, 2010.

Monge, M. E., D'Anna, B., Mazri, L., Giroir-Fendler, A., Ammann, M., Donaldson, D. J., and George, C.: Light changes the atmospheric reactivity of soot, P. Natl. Acad. Sci. USA, 107, 6605–6609, 2010.

NASA.:Ozone over your house, http://jwocky.gsfc.nasa.gov/teacher/ozone_overhead.html, access January 2011.

Ndour, M., D'Anna, B., George, C., Ka, O., Balkanski, Y., Kleffmann, J., Stemmler, K., and Ammann, M.: Photoenhanced uptake of $NO_2$ on mineral dust: Laboratory experiments and model simulations, Geophys. Res. Lett., 35, L05812, doi:10.1029/2007GL032006, 2008.

Perner, D., and Platt, U.: Detection of nitrous acid in the atmosphere by differential optical absorption, Geophys. Res. Lett., 6, 917-920, 1979.

Pitts Jr., J.N., Biermann, H. W., Winer, A. M., and Tuazon, E. C.: Spectroscopic identification and measurement of gaseous nitrous acid in dilute auto exhaust, Atmos. Environ., 18, 847-854, 1984.

Pitts Jr,, J. N., Grosjean, D., Cauwenberghe, K. V., Schmid, J. P., and Fitz, D. R.: Photooxidation of aliphatic amines under simulated atmospheric conditions: formation of nitrosamines, nitramines, amides, and photochemical oxidant, Environ. Sci. Technol., 12 946-953, 1978.

Raivonen, M., Bonn, B., Sanz, M. J., Vesala, T., Kulmala, M., and Hari, P.: UV-induced NOy emissions from Scots pine: Could they originate from photolysis of deposited $HNO_3$? , Atmos. Environ., 40, 6201- 6213, 2006.

Ren, X., Harder, H., Martinez, M., Lesher, R. L., Oliger, A., Simpas, J. B., Brune, W. H., Schwab, J. J., Demerjian, K. L., He, Y., Zhou, X., and Gao, H.: OH and $HO_2$ chemistry in the urban atmosphere of New York City, Atmos. Environ., 37, 2003.

Ren, X., Brune, W. H., Mao, J., Mitchell, M. J., Lesher, R. L., Simpas, J. B., Metcalf, A. R., Schwab, J. J., Cai, C., Li, Y., Demerjian, K. L., Felton, H. D., Boynton, G., Adams, A., Perry, J., He, Y., Zhou, X., and Hou, J.: Behavior of OH and HO$_2$ in the winter atmosphere in New York City, Atmos. Environ., 40, 3639-3651, 2006.

Rockne, K. J., Taghon, G. L. and Kosson, D. S.: Pore structure of soot deposits from several combustion sources, Chemosphere, 41, 1125-1135, 2000.

Rohrer, F., Bohn, B., Brauers, T., Bruning, D., Johnen, F.-J., Wahner, A., and Kleffmann, J.: Characterisation of the photolytic HONO-source in the atmosphere simulation chamber SAPHIR, Atmos. Chem. Phys., 5, 2189–2201, 2005.

Sakamaki, F., Hatakeyama, S., and Akimoto, H.: Formation of nitrous acid and nitric oxide in the heterogeneous dark reaction of nitrogen dioxide and water vapour, Int. J. Chem. Kinet., 15, 1013 -1029, 1983.

Saliba, N. A., Yang, H., and Finlayson-Pitts, B. J.: Reaction of gaseous nitric oxide with nitric acid on silica surfaces in the presence of water at room temperature, J. Phys. Chem. A, 105, 10339-10346, 2001.

Sander, S. P., Friedl, R. R., Golden, D. M., Kurylo, M. J., Moortgat, G. K., Keller-Rudek, H., Wine, P. H., Ravishankara, A. R., Kolb, C. E., Molina, M. J., Finlayson-Pitts, B. J., Huie, R. E., and Orkin, V. L.: Chemical kinetics and photochemical data for use in atmospheric studies evaluation number 15, Jet Propulsion Laboratory, Pasadena, 523, 2006.

Sarwar, G., Pinder, R. W., Appel, K. W., Mathur, R., and Carlton, A. G.: Examination of the impact of photoexcited NO$_2$ chemistry on regional air quality, Atmos. Environ., 43, 6383–6387, 2009.

Schmid, H. P.: Footprint modeling for vegetation atmosphere exchange studies: a review and perspective, Agr. Forest. Meteorol., 113, 159–183, 2002.

Sleiman, M., Gundel, L. A., Pankow, J. F., Jacob, P., Singer, B. C., and Destaillats, H.: Formation of carcinogens indoors by surface-mediated reactions of nicotine with nitrous acid, leading to potential thirdhand smoke hazards, P. Natl. Acad. Sci. USA, 107, 6576-6581, 2010.

Sörgel, M., Trebs, I., Serafimovich, A., Moravek, A., Held, A., and Zetzsch, C.: Simultaneous HONO measurements in and above a forest canopy: influence of turbulent exchange on mixing ratio differences, Atmos. Chem. Phys., 11, 841–855, 2011.

Stemmler, K., Ammann, M., Donders, C., Kleffmann, J., and George, C.: Photosensitized reduction of nitrogen dioxide on humic acid as a source of nitrous acid, Nature, 440, 195-198, 2006.

Stemmler, K., Ammann, M., Elshorbany, Y., Kleffmann, J., Ndour, M., D'Anna, B., George, C., and Bohn, B.: Light-induced conversion of nitrogen dioxide into nitrous acid on submicron humic acid aerosol, Atmos. Chem. Phys., 7, 4237–4248, 2007.

Stull, R. B.: An introduction to boundary layer meteorology, Atmospheric and Oceanographic Sciences Library, Kluwer Academic Publishers, Dordrecht, 670 pp., 1988.

Stutz, J., Alicke, B., and Neftel, A.: Nitrous acid formation in the urban atmosphere: Gradient measurements of NO$_2$ and HONO over grass in Milan, Italy, J. Geophys. Res., 107, 8192, doi:10.1029/2001JD000390, 2002.

Stutz, J., Alicke, B., Ackermann, R., Geyer, A., Wang, S., White, A. B., Williams, E. J., Spicer, C. W., and Fast, J. D.: Relative humidity dependence of HONO chemistry in urban areas, J. Geophys. Res., 109, D03307, doi:10.1029/2003JD004135, 2004.

Su, H., Cheng, Y. F., Cheng, P., Zhang, Y. H., Dong, S., Zeng, L. M., Wang, X., Slanina, J., Shao, M., and Wiedensohler, A.: Observation of nighttime nitrous acid (HONO) formation at a non-urban site during PRIDE-PRD2004 in China, Atmos. Environ., 42, 6219–6232, 2008a.

Su, H., Cheng, Y. F., Shao, M., Gao, D. F., Yu, Z. Y., Zeng, L. M., Slanina, J., Zhang, Y. H., and Wiedensohler, A.: Nitrous acid (HONO) and its daytime sources at a rural site during the 2004 PRIDE-PRD experiment in China, J. Geophys. Res., 113, D14312, doi:10.1029/2007JD009060, 2008b.

Su, H., Cheng,Y., Oswald, R., Behrendt, T., Trebs, I., Meixner, F.-X., Andreae, M. O., Cheng, P., Zhang,Y., and Pöschl, U.: Soil Nitrite as a Source of Atmospheric HONO and OH Radicals, Science, 333 (6049), 1616-1618, DOI: 10.1126/science.1207687, 2011.

Svensson, R., Ljungstrom, E., and Lindqvist, O: Kinetics of the reaction between nitrogen dioxide and water vapour, Atmos. Environ., 21 1529-1539, 1987.

Trebs, I., Bohn, B., Ammann, C., Rummel, U., Blumthaler, M., Königstedt, R., Meixner, F. X., Fan, S., and Andreae, M. O.: Relationship between the $NO_2$ photolysis frequency and the solar global irradiance, Atmos. Meas. Tech., 2, 725–739, 2009.

Trick, S.: Formation of nitrous acid on urban surfaces - a physical-chemical perspective-, Ph.D. thesis, University Heidelberg, Germany, 290 pp., 2004.

Veitel, H.: Vertical profiles of $NO_2$ and HONO in the boundary layer, Ph.D. thesis, University, Heidelberg, Germany, 270 pp., 2002.

Vesala, T., Kljun, N., Rannik, Ü., Rinne, J., Sogachev, A., Markkanen, T., Sabelfeld, K., Foken, T., and Leclerc, M. Y.: Flux and concentration footprint modelling: State of the art, Environ. Pollut., 152, 653-666, 2008.

Vogel, B., Vogel, H., Kleffmann, J., and Kurtenbach, R.: Measured and simulated vertical profiles of nitrous acid—Part II. Model simulations and indications for a photolytic source, Atmos. Environ., 37, 2957–2966, 2003.

Wennberg, P., O., and Dabdub, D.: Rethinking ozone production, Science, 319, 1624-1625, 2008.

Wentzell, J. J. B., Schiller, C. L., and Harris, G. W.: Measurements of HONO during BAQS-Met, Atmos. Chem. Phys., 10, 12285–12293, 2010

Wong, K. W., Oh, H.-J. , Lefer, B. L. , Rappenglück, B. , and Stutz, J.: Vertical profiles of nitrous acid in the nocturnal urban atmosphere of Houston, TX, Atmos. Chem. Phys., 11, 3595–3609, 2011.

Yabushita, A., Enami, S., Sakamoto, Y., Kawasaki, M., Hoffmann, M. R., and Colussi, A. J.: Anion-catalyzed dissolution of $NO_2$ on aqueous microdroplets, J. Phys. Chem. A, 113, 4844–4848, 2009.

Yu, Y., Galle, B., Hodson, E., Panday, A., Prinn, R., and Wang, S.: Observations of high rates of $NO_2$ – HONO conversion in the nocturnal atmospheric boundary layer in Kathmandu, Nepal, Atmos. Chem. Phys., 9, 6401–6415, 2009.

Zhang, N., Zhou, X., Shepson, P. B., Gao, H., Alaghmand, M., and Stirm, B.: Aircraft measurement of HONO vertical profiles over a forested region, Geophys. Res. Lett., 36, L15820, doi:10.1029/2009GL038999, 2009.

Zhou, X., Civerolo, K., Dai, H., Huang, G., Schwab, J., and Demerjian, K.: Summertime nitrous acid chemistry in the atmospheric boundary layer at a rural site in New York State, J. Geophys. Res., 107 (D21), 4590, doi:10.1029/2001JD001539, 2002a.

Zhou, X., He, Y., Huang, G., Thornberry, T. D., Carroll, M. A., and Bertman, S. B.: Photochemical production of nitrous acid on glass sample manifold surface, Geophys. Res. Lett., 29, 1681, 10.1029/2002GL015080, 2002b.

Zhou, X., Gao, H., He, Y., Huang, G., Bertman, S. B., Civerolo, K., and Schwab, J.: Nitric acid photolysis on surfaces in low-NOx environments: Significant atmospheric implications, Geophys. Res. Lett., 30(23), 2217, doi:10.1029/2003GL018620, , 2003.

Zhou, X., Zhang, N., TerAvest, M., Tang , D., Hou, J., Bertman, S., Alaghmand, M., Shepson, P. B., Carroll, M. A., Griffith, S., Dusanter, S., and Stevens, P. S.: Nitric acid

photolysis on forest canopy surface as a source for tropospheric nitrous acid, Nat. Geosci., 4, 440–443, doi:10.1038/ngeo1164, 2011

Zhu, C., Xiang, B., Zhu, L. and Cole, R.: Determination of absorption cross sections of surface-adsorbed $HNO_3$ in the 290–330 nm region by Brewster angle cavity ring-down spectroscopy, Chem. Phys. Lett., 458, 73–377, 2008.

Zhu, C., Xiang, B., Chu, L. T. and Zhu, L.: Photolysis of nitric acid in the gas phase, on aluminum surfaces, and on ice films, J. Phys. Chem. A, 114, 2561–2568, 2010.

# Appendix C

# Simultaneous HONO measurements in and above a forest canopy: Influence of turbulent exchange on mixing ratio differences

M. Sörgel [1], I. Trebs [2], A. Serafimovich [3], A. Moravek [2], A. Held [1], C. Zetzsch [1,4]

[1] University of Bayreuth, Atmospheric Chemistry Research Laboratory, D-95440 Bayreuth, Germany

[2] Max Planck Institute for Chemistry, Biogeochemistry Department, P. O. Box 3060, 55020 Mainz, Germany

[3] University of Bayreuth, Department of Micrometeorology, D-95440 Bayreuth, Germany

[4] Fraunhofer Institute for Toxicology and Experimental Medicine, D-30625 Hannover, Germany

## Abstract

We have combined chemical and micrometeorological measurements to investigate the formation and distribution of HONO throughout a forest canopy. HONO was measured simultaneously at two heights, close to the forest floor and just above canopy. The turbulent exchange between the forest and the atmosphere above was studied using vertical profiles of eddy covariance measurements of wind velocity, sonic temperature, water vapour and $CO_2$. HONO mixing ratios at both heights showed typical diel cycles with low daytime values (~80 ppt) and high nighttime values (up to 500 ppt), but were influenced by various sources and sinks leading to mixing ratio differences (above canopy minus below) of up to +240 ppt at nighttime. In the late afternoon and early night mixing ratios increased at higher rates near the forest floor, indicating a possible ground source. Due to the simultaneous decoupling of the

forest from the air layer above the canopy, mixing ratio differences reached about -170 ppt. From the late night until the early morning mixing ratios above the forest were typically higher than close to the forest floor. For some cases, this could be attributed to advection above the forest, which only partly penetrated the canopy. Measured photolysis frequencies above and below the forest canopy differed by a factor of 10-25 resulting in HONO lifetimes of about 10 min above and 100-250 min below the canopy at noontime. However, these differences of the main daytime HONO sink were not evident in the mixing ratio differences, which were close to zero during the morning hours. Effective turbulent exchange due to a complete coupling of the forest to the air layer above the canopy in the morning has offset the differences caused by the daytime photolytic sink and added to the interplay between different HONO production and loss processes.
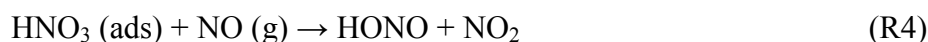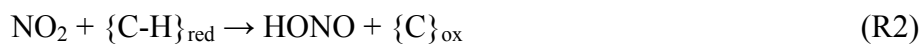
# 1  Introduction

Nitrous acid (HONO, HNO$_2$) is currently gaining substantial attention due to its contribution to the tropospheric OH radical production, which is the 'detergent' of the atmosphere. Besides its importance for the atmospheric oxidation potential, it contributes to acid and nutrient deposition to the biosphere. Moreover, growing concern exists about possible health effects due to the formation of nitrosamines (Hanst et al., 1977; Pitts et al., 1978) where HONO acts as the nitrosating agent, especially in indoor environments, e.g., so called third hand smoke after wall reactions of HONO with nicotine (Sleiman et al., 2010). Despite three decades of research since the first unequivocal detection of HONO in the atmosphere (Perner and Platt, 1979), HONO formation processes in the atmosphere are still under discussion, especially during daytime when large discrepancies were found between mixing ratios calculated from known gas-phase chemistry and measured daytime mixing ratios (Kleffmann et al., 2005). In the absence of light the most favoured formation reaction is the heterogeneous disproportionation of nitrogen dioxide (NO$_2$):

$$2NO_2 + H_2O \rightarrow HONO + HNO_3 \qquad\qquad (R1)$$

This reaction has been extensively studied on different materials like fluorinated polymers and different types of glass as reviewed by Lammel and Cape (1996), but also on building materials like concrete (Trick, 2004). It was found to be first order in NO$_2$ and water vapour (Sakamaki et al., 1983; Pitts et al., 1984; Svennson et al., 1987; Jenkin et al., 1988). A mechanism involving the formation of the NO$_2$ dimer (N$_2$O$_4$) in the gas phase was proposed (Finlayson-Pitts et al., 2003), but is not important in the real atmosphere (Kleffmann et al., 1998; Gustafsson et al., 2008). Recently, evidence for a mechanism involving reaction between adsorbed NO$_2$ and H (NO$_2$ (ads) + H(ads) $\rightarrow$ HONO (ads)) present on the surface following the dissociation of chemisorbed H$_2$O was found in a study on mineral dust particles with isotopically labelled water (Gustafsson et al., 2008), but the results are probably not transferable from laboratory to field conditions (Finlayson-Pitts, 2009). In the absence of light, HONO formation from NO$_2$ on soot decreases quite rapidly and thus was concluded to be less important for atmospheric HONO formation except for freshly emitted soot (Kleffmann et al., 1999; Arens et al., 2001; Aubin and Abbatt, 2007). The mechanism was

summarized as the reaction (R2) of reducing organic compounds {C-H}$_{red}$ with $NO_2$ (Gutzwiller et al., 2002a).

$$NO_2 + \{C\text{-}H\}_{red} \rightarrow HONO + \{C\}_{ox} \qquad (R2)$$

$$NO + NO_2 + H_2O \rightarrow 2\ HONO \qquad (R3)$$

$$HNO_3\ (ads) + NO\ (g) \rightarrow HONO + NO_2 \qquad (R4)$$

A similar reaction like R2 was postulated for the aqueous phase (Gutzwiller et al., 2002b; Ammann et al., 2005), but only proceeds at a relevant rate at high pH levels, since it is based on the well known charge transfer reaction of phenolate with $NO_2$. The Reactions R3 (via the intermediate $N_2O_3$) and R4, involving NO proposed from field measurements (Calvert et al., 1994; Andres-Hernandez et al., 1996; Saliba et al., 2001) could neither explain laboratory results under low $NO_x$ conditions (Svennson et al., 1987; Jenkin et al., 1988; Kleffmann et al., 1998; Kleffmann et al., 2004;) nor field experiments with low NO mixing ratios (Harrison and Kitto, 1994).

The daytime HONO formation recently discussed in an overview paper by Kleffmann (2007) was found to be about 60 times faster (Kleffmann et al., 2005) than the heterogeneous nighttime formation, and is even more controversial. There are a variety of proposed sources dealing with photoenhanced $NO_2$ reduction including $NO_2$ reduction on irradiated mineral surfaces like $TiO_2$ (Gustafsson et al., 2006; Ndour et al., 2008). Many studies focussed on the reduction of $NO_2$ involving organic photosensitizers (George et al., 2005) like hydrocarbons on soot (Monge et al., 2010) or humic acids (Stemmler et al., 2006; Stemmler et al., 2007). As already proposed from smog chamber experiments (Killus and Whitten, 1990), photolysis of deposited $HNO_3$/nitrate on surfaces was suggested as a daytime HONO source for rural environments by Zhou et al. (2002a; 2002b; 2003) from field studies at low $NO_x$ conditions. The mechanism is still not convincing since the photolysis of $HNO_3$ was not found to be a photolytic source of HONO in chamber experiments (Rohrer et al., 2005). Quantum yields for $HNO_3$/nitrate photolysis are too low in the gas phase and in solution (Zhou et al. 2003; Kleffmann, 2007), but this process can be enhanced at surfaces (Finlayson-Pitts, 2009) or via organic photosensitizers as speculated by Kleffmann (2007). An additional source may be the photolysis of o-nitrophenols (Bejan et al., 2006) depending on pollution levels that govern the formation of nitrophenols.

A problem that arises when comparing kinetics derived from laboratory experiments with those calculated from field data is that the heterogeneous production may be decoupled from the release to the atmosphere (Finlayson-Pitts, 2009). Desorption processes of HONO formed at the surface or deposited to the surface might be governed by co-adsorption of water molecules as, e.g., formulated in a model developed for chamber measurements (Trick, 2004). Furthermore, the condensation of water vapour might block surface active sites (Lammel and Cape, 1996). This was found to inhibit photo-enhanced reactions (Gustafsson et al., 2006; Stemmler et al., 2007). The relative humidity (RH) dependence of HONO mixing ratios was investigated in several field (Stutz et al., 2004; Su et al., 2008; Qin et al., 2009; Yu et al., 2009) and laboratory studies (Ammann et al., 1998; Wainmann et al., 2001; Arens et al., 2002; Trick 2004) as well as its relation to nitrite in dew (Rubio et al., 2002; He et al., 2006; Rubio et al., 2008). The findings of all studies do not allow a simple interpretation of the relationship between RH and HONO mixing ratios as already stated by Lammel and Cape (1996), but should be taken into account for modelling activities (Stutz et al., 2004). For the heterogeneous formation not only the chemistry at the surface and adsorption/desorption of reactants and products are important, but also the available surface area per volume air (S/V) and the dispersion or accumulation of formed HONO depending on turbulent transport and, hence, on atmospheric stability. Correlations of HONO mixing ratios or $HONO/NO_x$ ratios, which should be less sensitive to boundary layer processes, with the aerosol surface concentration ($S/V_{aerosol}$) were often found (Lammel and Perner, 1988; Notholt et al., 1992; Andres-Hernandez et al., 1996), but a complete separation from boundary layer processes was not possible (Andres-Hernandez et al., 1996; Reisinger, 2000). Recent studies (Qin et al., 2009; Yu et al., 2009) found a good correlation with PM10 ($S/V_{aerosol}$), but concluded that the aerosol surface is of minor importance compared to the ground surface. Thus, the relative importance of aerosol surface versus ground surface (vegetation, buildings) depends on the respective surface areas available, on the nature of these surfaces and on the turbulent mixing and the meteorological conditions at a specific site. There is ample evidence from other ground-based field measurements (Stutz et al., 2002; Veitel, 2002; Kleffmann et al., 2003; Zhang et al., 2009), aircraft profiles (Zhang et al., 2009) and modeling studies (Vogel et al., 2003) that the ground surface is a major source of HONO. Hence, turbulent exchange has a significant impact on near surface HONO mixing ratios as already proposed by Febo et al. (1996). These authors found a good correlation of HONO with radon, which is exclusively

emitted from the ground. Furthermore, profiles from recent aircraft measurements were closely related to atmospheric stability (Zhang et al., 2009).

The efficiency of the physicochemical and/or surface HONO production and of the uptake by forest vegetation and soils is determined by the interaction of turbulent transport and chemical reactions in and above the forest canopy. In this paper, we have investigated HONO mixing ratio differences between above and below a forest canopy using the coupling processes by coherent exchange (Thomas and Foken, 2007) between different canopy layers and the air above the canopy. The definition of so-called coupling regimes is based on the detection of coherent structures, which are organized structures in the turbulent (stochastic) flow. For the first time, we demonstrate how measurements of HONO can be combined with a micrometeorological approach in tall vegetation, providing an appropriate tool to investigate processes affecting HONO mixing ratios measured within and above the canopy.


# 2  Experimental


During the **I**ntensive **O**bservation **P**eriods (IOPs) of the EGER project (**E**xchan**GE** processes in a mountainous **R**egion) simultaneous measurements of micrometeorological and chemical parameters were made in order to investigate the exchange of energy and matter between a forest ecosystem and the atmosphere. The "Waldstein-Weidenbrunnen" research site is located in the Fichtelgebirge mountains in northeast Bavaria (50° 09 'N, 11°52' E, 775 m above sea level), Germany, in a rural forested region. There are no larger towns to the east within 70 km. The motorway (A9) is about 9 km to the west, running form north to south. The cities of Kulmbach (~ 30000 inhabitants) and Bayreuth (73000 inhabitants) are situated 30 km west and south-west, respectively. This site has been extensively studied by the University of Bayreuth (Matzner, 2004, Gerstberger et al. 2004) and is a part of the FLUXNET (Baldocchi et al., 2001). The site is covered by a Norway spruce (Picea abies (L.) Karst.) forest with a canopy height of 23 - 25 m (Staudt and Foken, 2007). An extensive description of the experiment and the meteorological conditions can be found in the experiment documentation by Serafimovich et al. (2008). Furthermore, an extensive overview with a detailed description of the aims of the EGER project and the instrumental setup during the IOPs is given in Foken et al. (2011). The measurements discussed in this paper were made at three different sites in the forest stand. A thin 36 m high tower ("turbulence tower") located about 60 m southeast of

the main tower (31 m walk-up tower) was used for (undisturbed) turbulence measurements. The *forest floor exchange site* was located about 30 m northwest of the main tower.

Simultaneous measurements of HONO were conducted at a height of 24.5 m (just above canopy) on the main tower and close to the forest floor in 0.5 m at the *forest floor exchange site* from 13 to 25 Sep. 2007. HONO was measured by two LOPAP instruments (**LO**ng **P**ath **A**bsorption **P**hotometer, QUMA Elektronik & Analytik, Wuppertal, Germany). The LOPAP is based on a wet chemical technique, with fast sampling of HONO as nitrite in a stripping coil and subsequent detection as an azo dye using long path absorption in 2.4 m long Teflon AF tubing. A detailed description of the instrument has been given by Heland et al. (2001) and Kleffmann et al. (2002). The instruments were placed outside in the forest or directly on the tower in ventilated aluminum boxes without temperature control. The temperature of the stripping coils was kept constant at 20°C by thermostats to assure constant sampling conditions.

From 27 Sep. to 3 Oct. both LOPAPs were compared side-by-side near the forest floor at a height of 1 m. The sampling inlets had a distance of about 50 cm and were directed northwards to sample perpendicularly to the westerly flow. No T-piece was used as inlet to avoid artificial HONO formation or adsorption on the inner walls of the tubing. Both instruments were supplied with the same reagents via T-pieces.

Temperature and humidity profiles were measured at the main tower using Frankenberger-type psychrometers (Frankenberger, 1951). The relative humidity (RH) was calculated from the dry and wet bulb temperature of the psychrometers using the Magnus formula after Sonntag (1990) for the saturation vapour pressure and the Sprung formula for the actual vapour pressure (Foken, 2008). Psychrometers were mounted on the main tower at 0, 2, 5, 12, 21 and 32 m. Additionally, visibility was measured with a PWD11 (Vaisala,Vantaa, Finland) present weather detector mounted on the main tower.

Aerosol number size distributions were measured on the main tower at 28 m height using a Scanning Mobility Particle Sizer (SMPS, Grimm, Ainring, Germany). Boundary layer heights were derived from SODAR (SOund Detection And Ranging, Metek Meteorologische Messtechnik, Elmshorn, Germany) measurements at a nearby clearing.

Vertical profiles of nitrogen oxides (NO and $NO_2$) were measured on the main tower and on the *forest floor exchange site* by red-filtered detection of the chemiluminescence produced by the reaction of NO with $O_3$ (CLD 780 TR, ECO Physics, Duernten, Switzerland). $NO_2$ was photolytically converted to NO by exposure of the sample air to a solid-state blue-light converter (Meteorologie Consult, Königstein, Germany) and subsequently detected by the

chemiluminescence analyzer. Sample air was drawn through 55 m of non-transparent and heated PFA tubing from each inlet height. Inlet heights of the system were located at 0.05, 0.3, 1, 2, 5, 10, 16, and 24 m. The lower heights of up to 2 m were located at the *forest floor exchange site*, while the upper heights were mounted at the main tower, for details see Moravek (2008).

To detect the coupling regimes between the subcanopy, canopy and layer above the canopy the eddy-covariance measurements were used. Six eddy-covariance systems consisting of sonic anemometers and fast response $CO_2$ and $H_2O$ gas analyzers were installed at the turbulence tower in 2.25, 5.5, 13, 18, 23 and 36 m. The wavelet transform was used to detect and extract ramp-like structures (coherent structures) from high frequency measurements of wind, sound temperature, $CO_2$ and $H_2O$ concentrations (Thomas and Foken, 2005). These structures are responsible for the turbulent coherent transport of the momentum and matter in forested ecosystems. Analysis of a sensible heat transport by coherent structures reveals the portions of the forest canopy coupled by coherent exchange with the air above the canopy (Thomas and Foken, 2007). The experimental setup and the analysis of the coupling regimes during the EGER intensive observation periods are described in more detail by Serafimovich et al. (2010).

The HONO photolysis frequency ($j$(HONO)) was calculated from the $NO_2$ photolysis frequency measured by filter radiometers (Meteorologie Consult, Königstein, Germany) according to Kraus and Hofzumahaus (1998) and Trebs et al. (2009). The radiometers were mounted on top of the main tower at a height of 28 m, and at 2 m above the forest floor at the *forest floor exchange site*.

For statistical computing the free statistics software "R" was used (http://www.R-project.org.).


# 3   Results and discussion

## *3.1   Comparison of the two LOPAP instruments*

The LOPAP instruments from the University of Bayreuth (UBAY) and the Max-Planck-Institute for Chemistry (MPIC) were compared side-by-side at 1 m above the forest floor between 27 Sep. and 3 Oct. to evaluate the precision of the instruments. For this purpose the relative differences of the measured HONO mixing ratios were calculated by normalizing the difference of [HONO]$_{UBAY}$ minus [HONO]$_{MPIC}$ by the arithmetic mean of these mixing ratios.

The temporal evolution of these relative mixing ratio differences is shown in Fig. 1 together with the visibility as an indicator of foggy events. During rainy and foggy weather conditions indicated by the reduced visibility, we observed systematic deviations between the two LOPAP instruments. Large relative differences of the HONO signals during periods with low visibilities are related to fog events. Bröske et al. (2003) reported no measurable particle losses in the sampling glass coil for SOA (secondary organic aerosol) particles with diameters from 50-800 nm but Kleffmann et al. (2006) argued that large particles like fog droplets might be sampled by the coil. Thus, the sampling of fog droplets containing nitrite is a plausible explanation for deviations under wet conditions. However, this should affect both instruments by introducing more scatter and cannot explain the systematic deviation. Another potential reason could be that the surfaces of the inlets (first centimetre of the coils before contact with the sampling reagent) exhibited different wettabilites during these periods.
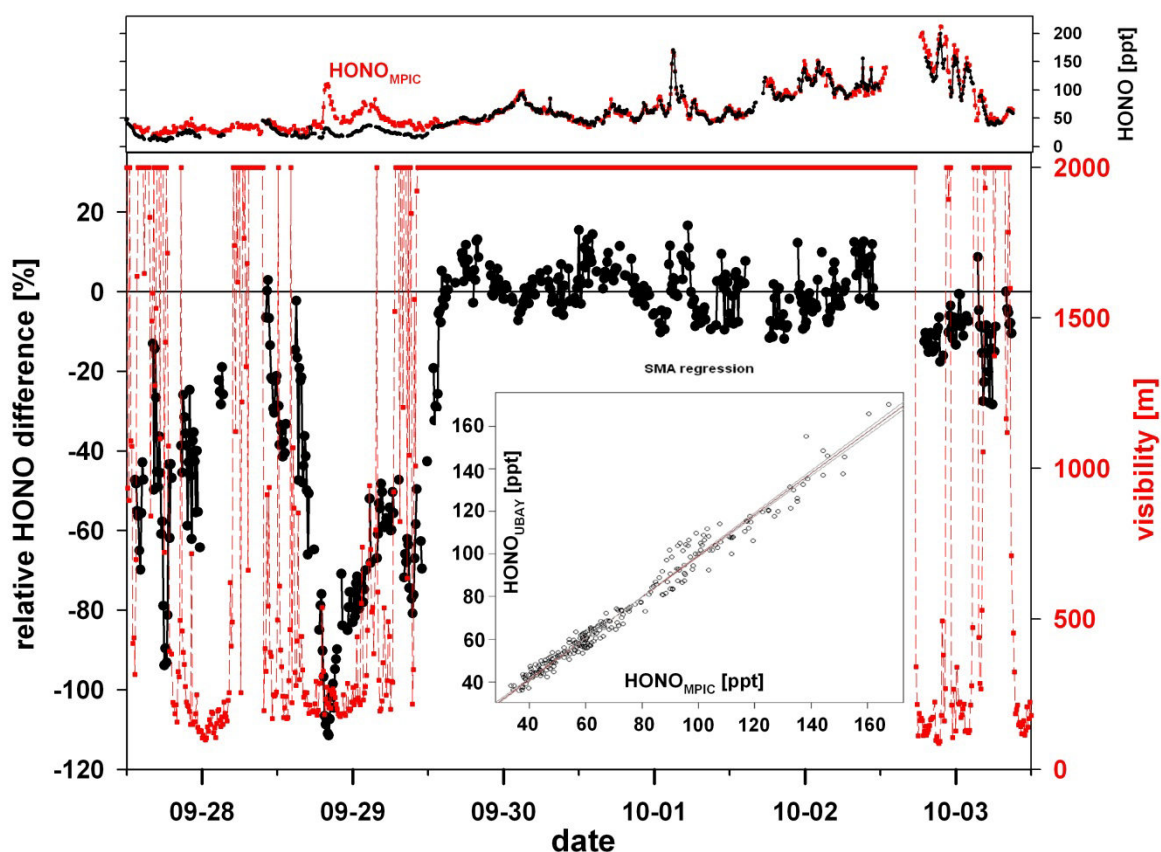


Figure 1. Side-by-side measurements of the two LOPAP instruments from 27 Sep. (noon) to 3 Oct. 2007 (noon) at the "Waldstein-Weidenbrunnen" research site. Relative differences of the HONO signals (black dots) and visibility range (red squares, dashed lines, maximum range 2000 m). The insert shows the regression obtained during dry conditions (N = 247) from 29 Sep. (14:00 CET) to 2 Oct. (10:00 CET) using standard major axis (SMA) regression. The upper panel shows the mixing ratios measured by the two LOPAP instruments. Missing values are due to zero air measurements and calibration of the LOPAP instruments.

During the dry conditions (visibilities of more than 2000 m, which is the maximum detectable by the instrument) between 29 Sep. (14:00 CET) and 2 Oct. (10:00 CET) HONO levels ranged from 35 ppt to 170 ppt and the instruments agreed within 12 % ($2\sigma$), which is within the range of the estimated instrumental error under the given conditions (e.g., detection unit not air conditioned). Omitting the wet conditions before and after the dry period the relative errors correspond to a Gaussian distribution centred at zero. Thus, no systematic deviation of the instruments was found during dry conditions. The insert on Fig. 1 shows the correlation between the two instruments. Applying standard major axis regression analysis (Sokal and Rohlf, 1995; Legendre and Legendre, 1998), which is suitable for two random variables (e.g., Ayers, 2001) by reducing deviations perpendicularly to the regression line, yields an intercept of 2.3 ppt, which is close to the detection limit of the instruments ($3\sigma$-definition). The slope is 0.97 and the coefficient of determination $r^2 = 0.98$ for the dry weather period. Kleffmann (2006) used a T-piece and PFA tubing in front of the sampling units to compare two LOPAP instruments in order to avoid any influence from inhomogeneities in the sampled air. The linear correlation of these two LOPAPs was very good over a large mixing ratio range from about 200 ppt to 1.6 ppb, with a slope of 0.993 and an intercept of 1.4 ppt. However, since it is well known that any tubing in front of the sampling unit may cause artefacts due to wall reactions of $NO_2$ we avoided this approach. Furthermore, there was no dependency of the relative error on the friction velocity (u*) or the horizontal wind speed, indicating no significant influence from inhomogeneities in the sampled air. This is expected because the sampling units were only about 50 cm apart. At wind speeds as low as 0.5 m s$^{-1}$ it took only 1 s to pass both sampling units, whereas the response time of both instruments is about 7 min. Thus, small scale inhomogeneities should contribute equally to both signals.

We conclude that the LOPAP instruments can be used to reliably measure vertical HONO mixing ratio differences under dry conditions.

## 3.2 Factors controlling HONO mixing ratio levels

### 3.2.1 General observations in the time series

HONO is effectively scavenged by precipitation due to its good water solubility with a Henry`s law constant of about 50 mol L$^{-1}$ atm$^{-1}$ (Sander, 1999). Precipitation was found to structure the time series ranging from 13 of Sep. to 3 Oct. on a time scale of about a week due

to synoptic weather conditions (low and high pressure systems). Although not precisely measurable (see section 3.1) due to large relative errors of both instruments during foggy conditions, HONO values were clearly lower at both heights during these wet periods. HONO/$NO_x$ ratios were below 2 % at both heights because (due to lower Henry's law constants of NO (about $2 \times 10^{-3}$ mol $L^{-1}$ atm$^{-1}$) and $NO_2$ (1-4 x $10^{-2}$ mol $L^{-1}$ atm$^{-1}$) (Sander, 1999)) $NO_x$ is not significantly influenced by precipitation scavenging or enhanced deposition on wet surfaces. During the entire IOP, three dry periods occurred between rain events. Dry periods were characterized by steadily increasing nighttime HONO mixing ratios up to 500 ppt, while HONO mixing ratios dropped during rain events to about 20 ppt. One of these dry periods (20 - 25 Sep.) is shown in Figs. 2 and 3. Below canopy measurements of HONO, $NO_x$ and HONO/$NO_x$ are presented together with rain fall measurements in Fig. 2. An overview graph for above canopy meteorological (wind direction, friction velocity, temperature, relative humidity and $j$(HONO)) and chemical (NO, $NO_2$, HONO and ozone) measurements is given in Fig. 3.
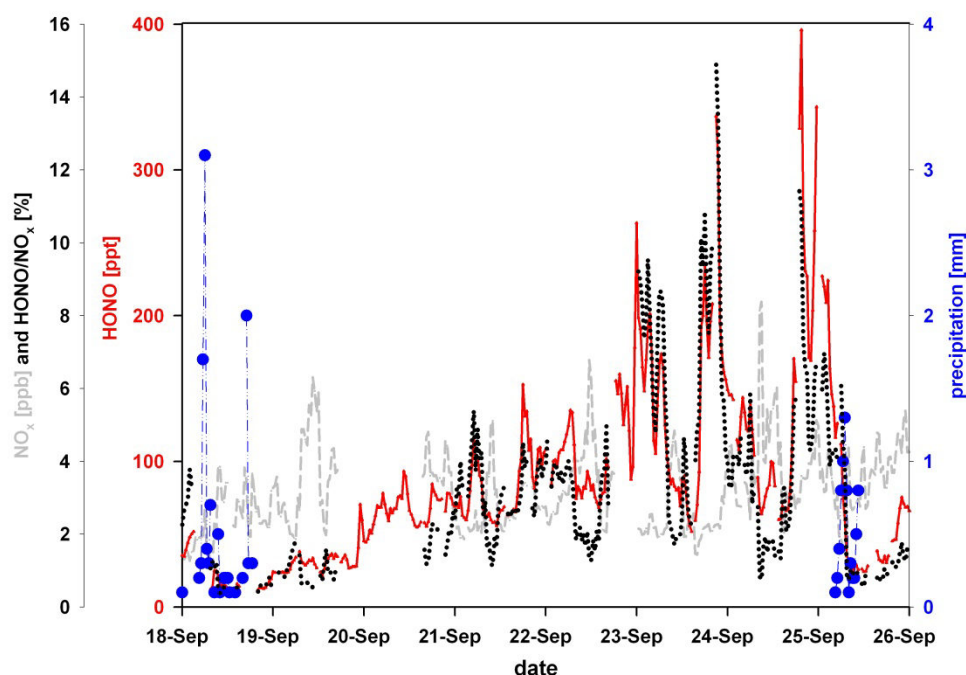


Figure 2. Time series of HONO at 0.5 m above the forest floor (red line), $NO_x$ (grey dashed line) and HONO/$NO_x$ ratio (black dotted line) from 18 (0:00 CET) to 26 (0:00 CET) Sep. 2007 at the "Waldstein-Weidenbrunnen" research site. This dry period was delimited by rain events marked with blue dots (half hourly values).
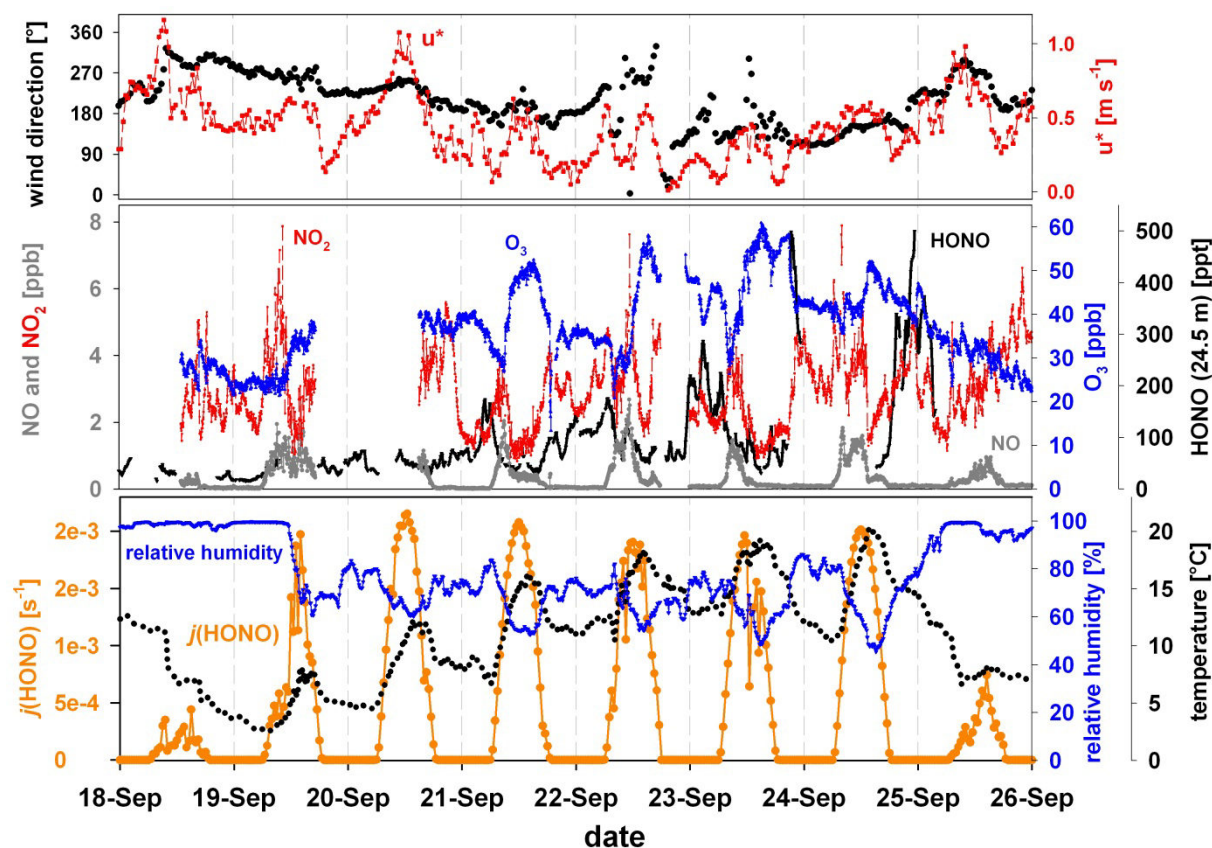
Figure 3. The upper panel shows the wind direction above canopy (32 m) and the friction velocity (u*) at the top of the canopy (21 m). In the middle panel the trace gases (NO, NO$_2$, O$_3$ and HONO) measured above the canopy (24.5 m) are presented. Time series of the HONO photolysis frequency $j$(HONO) parameterized from the measured NO$_2$ photolysis frequency at a height of 28 m (orange line and dots), relative humidity and air temperature measured at the canopy top (21 m) from 18 (0:00 CET) to 26 (0:00 CET) Sep. 2007 at the "Waldstein-Weidenbrunnen" research site are presented in the lower panel.

During the dry period winds from south-west and south-east were dominating. Temperatures were increasing and daytime RH values were decreasing. The friction velocity (u*), which is a measure for the wind shear and thus wind generated turbulence, was calculated from eddy covariance measurements of horizontal and vertical wind speed. During the dry period u* is lower (especially at night) than before and afterwards. Significant NO values (at the above canopy level) were only measured during day. At the beginning of the dry period, HONO increased continuously with a rate of about 2 ppt h$^{-1}$ without a pronounced diel cycle, although the 20 Sep. was a clear-sky day with $j$(HONO) values of about 0.002 s$^{-1}$ around noon (see Fig. 3).

An increasing trend in both the time series of the HONO mixing ratio and the HONO/NO$_x$ ratio is evident. To our knowledge this type of accumulation behaviour was not reported so far, and it was not directly linked to an increase of the precursor NO$_2$ (Fig. 3). Although clarifying the reason for this is far beyond our applied measurement setup, a mechanism that might explain these observations would be the accumulation of (photo-) chemically formed or

deposited HONO at the surface and the subsequent release by increasing RH, according to a Langmuir-type surface mechanism proposed by Trick (2004) due to enhanced adsorption of water molecules and subsequent release of HONO, as RH increases in the late afternoon. Additionally, HONO formation due to photolysis of deposited $HNO_3$/nitrate as suggested by Zhou et al. (2002a; 2002b; 2003) might be an explanation, since the precursor ("sticky" $HNO_3$) is deposited efficiently to the canopy (Wolff et al., 2010) and accumulates at the needle surface (Zhou et al., 2002a).

### 3.2.2 S/V$_{ground}$ versus S/V$_{aerosol}$

The needle surface also constitutes the largest fraction of the total ground surface. Therefore, we estimated the ground surface from measurements of the projected plant surface neglecting stem and understory contributions. The average PAI (Plant Area Index) of this forest stand is 5 $m^2$ $m^{-2}$ (Staudt et al., 2010). This projected area can be converted to a surface area by multiplying with $\pi$ for wooden parts (assuming they are round), which contribute about 20 % (5-35 % (Gower et al., 1999)) to the PAI and by a factor of 2.65 derived by Oren et al. (1986) to convert the projected LAI ($\sim$ 80% of PAI) to the geometric needle surface. From that simple scheme we derive a total geometric surface of the crown of 13.7 $m^2$ $m^{-2}$ (10.6 $m^2$ $m^{-2}$ needle surface and 3.6 $m^2$ $m^{-2}$ wooden surface). From SODAR (SOund Detection And Ranging) measurements we inferred an average NBL (Nocturnal Boundary Layer) height of 120 m by a steep change in reflectivity of the sound signal. Using this value as an upper limit for the volume (1 $m^2$ as base area), and for a lower limit ground surface the geometric needle surface of the canopy, we get a S/V$_{ground}$ of 0.1 $m^{-1}$, which is an order of magnitude higher than e.g. reported by Yu et al. (2009). However, Yu et al. (2009) took only the inverse of the mixed layer height as S/V$_{ground}$, not accounting for any roughness of the surface. Especially, during nighttime the boundary layer height represents an upper limit for the volume, because mixing is very limited within the stable thermally stratified NBL (Stull, 1988). Vogel et al. (2003) used a value of 0.1 $m^{-1}$ to model heterogeneous HONO production in the lowest box of their model but increased S/V ground to 0.3 $m^{-1}$, which matched the observations better. This is consistent with our observations that (S/V$_{ground}$) 0.1 $m^{-1}$ reflects a lower limit. In contrast, the S/V$_{ground}$ values given by Lammel and Cape (1996) were an order of magnitude higher, e.g., considering vegetation surfaces with 0.6-1.4 $m^{-1}$ (for a mixed layer height of 100 m). Additionally, we calculated the aerosol surface from the measured aerosol number size

distributions and we found that S/V$_{aerosol}$ was typically less than 1% of S/V$_{ground}$. Due to the different reactivity and gas diffusivity for ground and aerosol surfaces a direct comparison of S/V$_{ground}$ and S/V$_{aerosol}$ is complicated. Since we measured close to surfaces and these surface areas are about two orders of magnitude larger than the respective aerosol surface for the whole mixed layer, we expect the contribution of aerosol surfaces to HONO formation to be of minor importance in our study. This is in line with measurements from Kleffmann et al. (2003) who found that gradients of HONO were not related to gradients in S/V$_{aerosol}$.

A decrease of the boundary layer height increases S/V$_{ground}$. Hence, with the same surface more HONO is concentrated in a smaller volume. However, at the same time turbulence is suppressed during these stable conditions. This reduces the exchange between the atmosphere and the surface.

### 3.2.3  Nighttime HONO conversion frequencies

HONO nighttime conversion frequencies F$_{HONO,night}$ from the heterogeneous disproportionation of NO$_2$ (cf. R1+R2) can be estimated for the dry periods. Su et al. (2008) discussed the problem of different scaling methods for HONO production and suggested to use a combined scaling approach of different quantities emitted close to the ground like black carbon (HONO/BC) or carbon monoxide (HONO/CO), and the "classical" HONO/NO$_2$ or HONO/NO$_x$. The scaling was (originally) introduced to reduce influences from boundary layer processes such as dilution or vertical mixing. However, local sources of the scaling quantities will affect the ratio (Su et al., 2008). As discussed above, humid surfaces or precipitation will also alter the HONO/NO$_x$ ratio due to different solubilities as well as the advection of NO$_x$ from road traffic during the morning hours at our site. Due to the lack of carbon monoxide (CO) and black carbon (BC) measurements we use the NO$_x$ scaling approach, which was used in many other studies (e.g. Sjödin, 1988; Alicke et al., 2002; Kleffmann et al., 2003;). The approach of Alicke et al. (2002) for inferring conversion frequencies, taking a linear increase of HONO during nighttime divided by the average NO$_2$ mixing ratio in this time interval is most commonly used.

$$\overline{F_{HONO,night}} = \frac{[HONO](t_2) - [HONO](t_1)}{(t_2 - t_1)\overline{[NO_2]_{night}}}$$

$$(1)$$

There is still no reliable way of inferring HONO conversion frequencies using objective criteria. Yu et al. (2009) used a fixed time interval from 18:00 local time (LT) to midnight (LT) to determine HONO conversion frequencies. This approach leads to a very large scatter in our conversion frequencies. In addition, it yields mainly negative conversion frequencies in the lower height, because HONO increases already before sunset, thus starting at higher levels, and peak mixing ratios are reached before midnight. We also tried an approach different from the "classical" one, not using the maximum HONO mixing ratio as end point but the maximum HONO/NO$_x$ ratio that can be regarded as the maximum amount of HONO produced by NO$_x$.

1) Evaluating individual increases of HONO by the "classical" approach, excluding advection events and other disturbances

This approach could be used for evaluating data from five nights of the whole IOP (13-25 Sep.) and yielded a value of F$_{HONO, night}$ $\pm$ $\sigma$ = (1.1 $\pm$ 0.65) % h$^{-1}$ for the measurements above the canopy and a value of (0.75 $\pm$ 0.45) % h$^{-1}$ close to the ground. The lower value for the lower height may be caused by choosing the starting point after sunset, whereas the first pronounced increase in HONO mixing ratios occurs already in the hours before sunset. Thus, the starting mixing ratio level is already higher at the lower height, whereas the increase at the upper height normally occurs later and is therefore completely captured. However, the influence of photochemistry has to be excluded for a proper comparison of heterogeneous production, and therefore we cannot use the data before sunset. The values of F$_{HONO,night}$ at both heights agree within their standard deviation (variation over five nights) and are consistent with literature values between 0.4 % h$^{-1}$ and 1.8 % h$^{-1}$ recently summarized by Su et al. (2008). The value for the upper height also compares quite well with a value of 1.4 $\pm$ 0.4 % h$^{-1}$ reported by Yu et al. (2009), which was not included in the comparison by Su et al. (2008).

2) Evaluating the period from sunset to the maximum HONO/NO$_x$ ratio

Conversion frequencies inferred by this approach are identical to the "classical" ones for the conditions during our campaign. The values and the variation of HONO/NO$_x$ ratios were mainly correlated to HONO mixing ratios (see Figs. 4 a, b). Therefore, the HONO/NO$_x$ maxima occurred simultaneously with the maximum HONO mixing ratios (Fig. 2).

Additionally, HONO mixing ratios were nearly independent of its precursor $NO_2$ (see Fig. 4c). A direct correlation could not be expected since the HONO formation rate dHONO/dt should correlate with $NO_2$ instead of HONO mixing ratios, due to first order formation of HONO from $NO_2$. Nevertheless, assuming similar heterogeneous conversion rates, higher $NO_2$ values should cause higher HONO values and Fig. 4c should reflect this trend. The lack of this trend was attributed to the fact that in contrast to studies in urban areas low $NO_2$ mixing ratios were prevailing. About 90 % of the $NO_2$ values were below 5 ppb and 70 % of the values ranged between 1 and 4 ppb, indicating quite constant $NO_2$ levels. The highest HONO and $HONO/NO_x$ values typically occurred before or around midnight (see Fig. 2) at moderate (2-5 ppb) $NO_2$ mixing ratios, whereas the highest $NO_x$ values occurred in the morning hours (advection from road traffic). The weak correlation of HONO to $NO_x$ does not necessarily mean that $NO_2$ is not a precursor for HONO. We simply do not see a correlation, which is similar to results from another rural forest site (Zhou et al 2002a). This indicates that other processes like deposition or re-emission are also important.

Nevertheless, conversion frequencies, as summarized above, are within the range of values reported in literature. Referring to the different conditions and methods used in these experiments, this range is narrow and might provide some guidance for modelling studies.
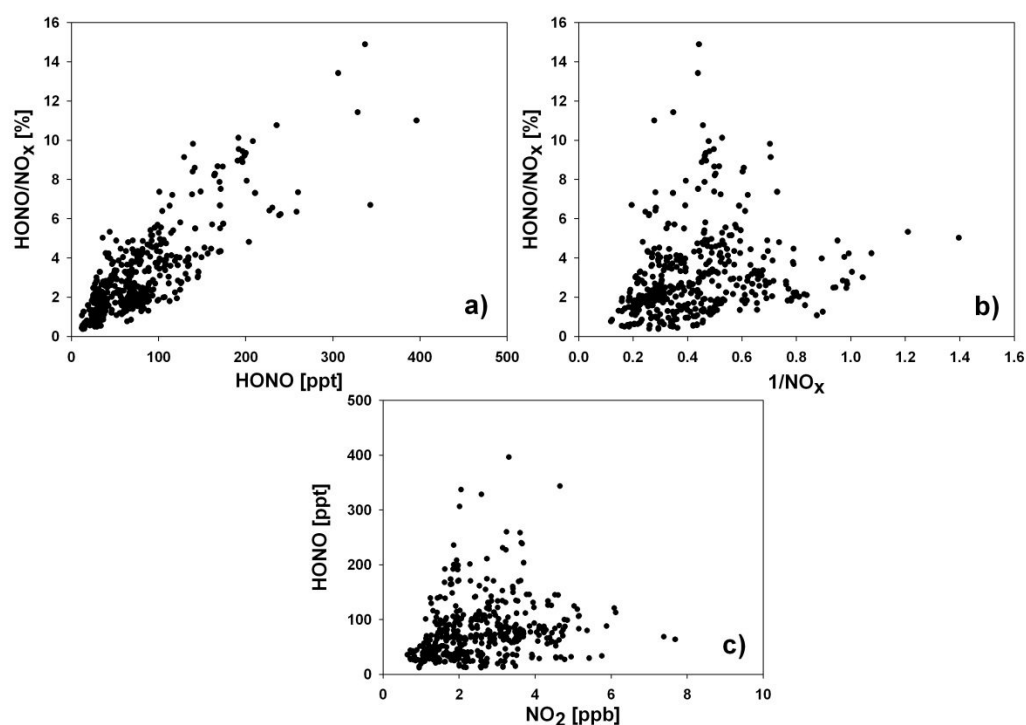


Figure 4. Relationships of HONO and $NO_x$ for the measurement height close to the forest floor (0.5m) for the period 13 - 25 September at the "Waldstein-Weidenbrunnen" research site. The upper graphs (a, b) show a better correlation of $HONO/NO_x$ to HONO than to $1/NO_x$, i.e. variations in $HONO/NO_x$ are more likely explained by variations in HONO mixing ratios than by $NO_x$ values.

## 3.3  HONO mixing ratio differences and coupling regimes

The investigation of the coupling regimes of the forest to the air layer above the canopy, as well as the coupling inside the forest is crucial to study the surface-atmosphere exchange of trace gases. The shaded and more humid subcanopy featured different environmental conditions than the atmosphere above the canopy, where the humidity was lower and photochemistry was more active. Vertical mixing processes link these two environments. As an indicator for the effectiveness of vertical mixing, the detection of coherent structures was used. Thomas and Foken (2007) state that the strong vertical motion typically associated with coherent structures enables them to penetrate deeply into the canopy forcing an exchange of air between different regions of the canopy. The residence time of air is therefore assumed to be controlled by the arrival frequency of coherent structures and limits the time available for physical, chemical and photochemical transformation of constituents within the canopy. Coherent structures are well organized in contrast to the random-like distributed turbulence (Holmes et al., 1996). They cause typical ramp like structures in time series of e.g. $CO_2$ and $H_2O$ and can thus be separated from random-like turbulence, e.g. with a wavelet tool (Thomas and Foken 2005). A more detailed analysis of sensible heat exchange provides information about the portion of the canopy controlled by coherent exchange (exchange regimes). Thomas and Foken (2007) defined five different coupling regimes:

*Wave motion (Wa).* The flow above the canopy is dominated by linear wave motion rather than by turbulence, and therefore decoupled from the subcanopy and the canopy.

*Decoupled canopy (Dc).* The air above the canopy is decoupled from the canopy, because there is no transfer of energy and matter into and out of the canopy by coherent structures.

*Decoupled subcanopy (Ds).* The layer above the canopy is coupled to the canopy, but decoupled from the subcanopy.

*Coupled sub canopy by sweeps (Cs).* The coherent exchange between the canopy air and the subcanopy is forced by strong sweep motion of coherent structures only.

*Fully coupled canopy (C).* The layer above the canopy, the canopy and the sub canopy are in a fully coupled state.

The detailed analysis of the coherent exchange and the coupling regimes for this particular experiment is given in Serafimovich et al. (2010).
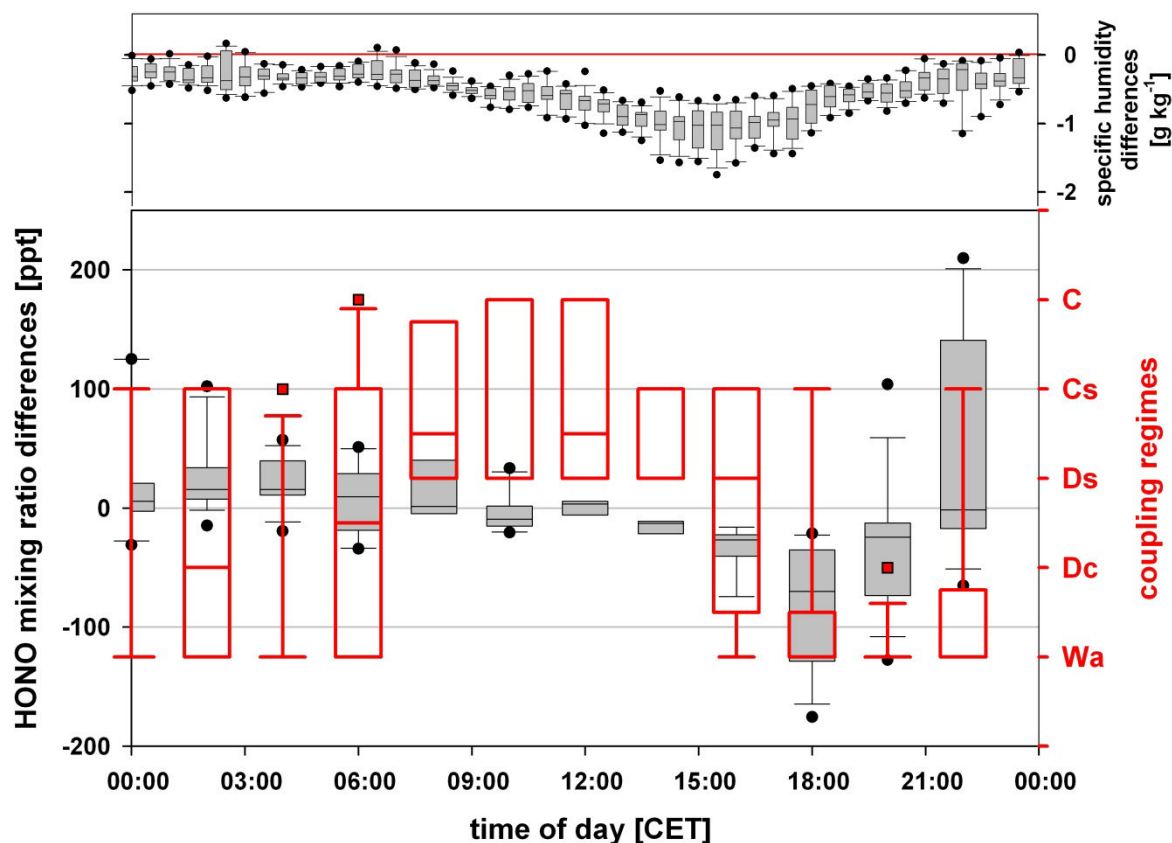
Fig. 5. Box-and-whisker plot for coupling regimes (red open bars) and HONO mixing ratio differences (grey filled bars) for the five-day dry period 20–25 September 2007 at the "Waldstein-Weidenbrunnen" research site. Coupling regimes (right hand side) are: Wa (Wave motion ~ no turbulent exchange), Dc (decoupled canopy ~ whole canopy decoupled from the air layer above), Ds (decoupled subcanopy ~ only subcanopy decoupled), Cs (coupled by sweeps ~ canopy and subcanopy coupled by sweep motion) and C (fully coupled canopy). The upper panel shows the specific humidity difference between 21 m and the forest floor for comparison. The upper end of the boxes represents the 75th percentile, the lower end the 25th percentile and the line within the boxes the median. Whiskers denote the 10th (lower whisker) and 90th (upper whisker) percentiles. Outliers are marked as points (HONO difference) or squares (coupling regimes). If only whiskers appear, there are no other values between the values marked by the whiskers. For the boxes at 10:00 and 14:00 CET the median falls in line with the lower end of the boxes (Ds).
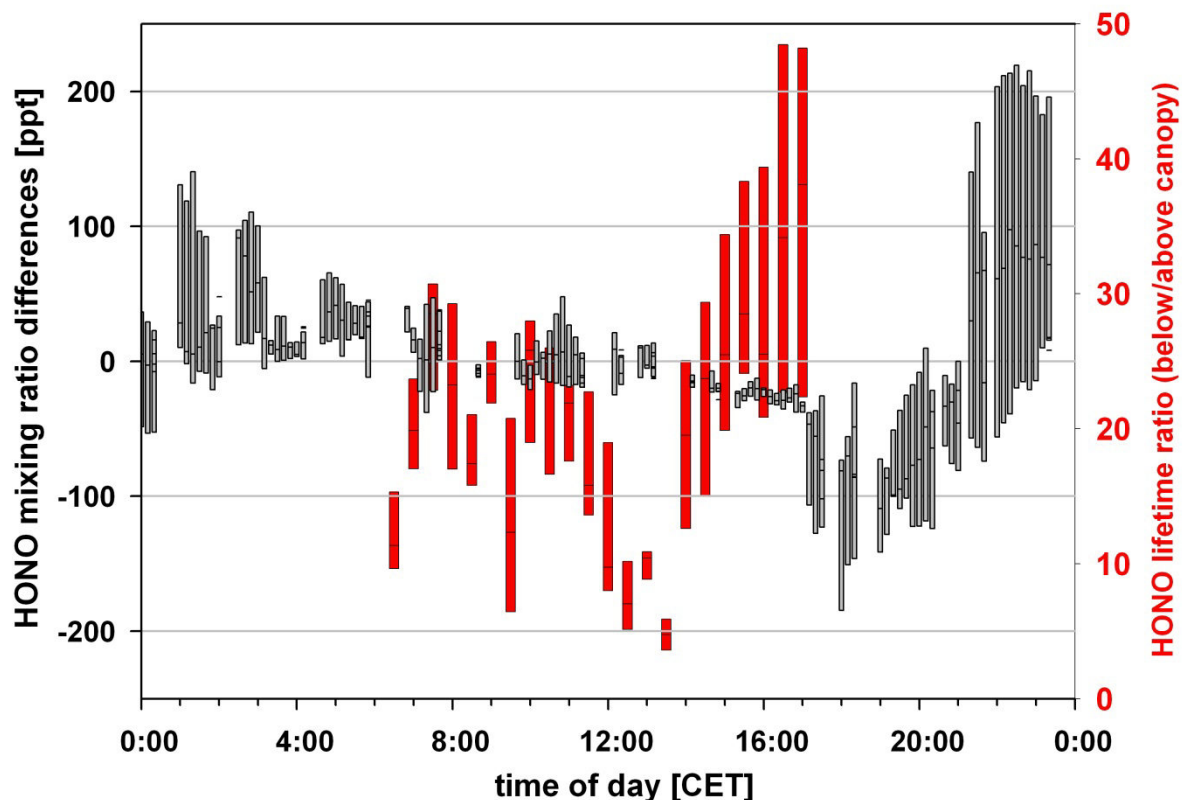
Figure 6. HONO mixing ratio differences (grey bars, 10 min averages) and lifetime ratios (below to above canopy) (red bars, 30 min averages) for the five-day dry period 20-25 Sep. 2007 at the "Waldstein-Weidenbrunnen" research site. The upper end of the boxes represents the 75th percentile, the lower end the 25th percentile and the line within the boxes the median.

The diel cycle of HONO mixing ratio differences (above canopy minus below canopy) shown in Figs. 5 and 6 can be subdivided into four typical periods:

1) Early night (17:30-21:00 CET): There was no photolytic sink (sunset at 17:30 CET), but also no turbulent exchange (Wa). These were from a micrometeorological perspective the most stable conditions during the day, with a complete decoupling of the forest from the layer above the canopy (Wa, Dc). Due to the increasing nighttime values in the dry period, absolute HONO differences increased as well and induced a higher variability at nighttime (Fig. 5). Mixing ratio differences of up to minus 170 ppt were measured. The higher HONO mixing ratios close to the forest floor in the early night can be explained by formation of HONO at the ground surface and accumulation in the trunk space, since the exchange with the layer above the canopy was very limited due to the decoupling of the forest. Above the canopy, mixing ratios increased at a lower rate or were fairly constant during this period, resulting in negative mixing ratio differences. The increasing differences could be observed similarly in the

specific humidity (Fig. 5), which was not affected by photolysis or chemical reactions. The sign of the HONO mixing ratio differences changed during the early night at about 21:00 CET, when mixing ratios above canopy rose quickly and exceeded the values measured near the ground. This effect was more pronounced at the end of the dry period, when nighttime maximum values were much higher than during the first two days after the rain event.

2) Late night to early morning (21:00-06:30 CET): Increasing mixing ratios above the canopy, exceeding the values below the canopy caused positive mixing ratio differences (max. ~ 240 ppt). The main contribution to the large positive differences originates from the last two days (of the dry period) when mixing ratios where highest. On the 23rd this increase can be attributed to an air mass change (see section 3.4). On the 24th wind direction changes but other than on the 23rd other trace gases exhibit no significant change. In addition to these two extreme values, HONO and HONO/$NO_x$ are predominantly higher above the canopy all the time from 21:00 to sunrise. We see a relation to RH but can only speculate about the reasons, which might be e.g., a mechanism similar to that proposed by Trick (2004). On the other hand, at nighttime the HONO lifetime is only limited by deposition and thus quite long. Thus, advection may also be a possible explanation. To distinguish between advection and local emission more measurements and an adequate modelling approach would be required.

3) Early morning to noon (6:30-13:00 CET): HONO mixing ratios decreased at both heights due to photolysis. The mixing ratio differences were close to zero (within the uncertainty of both instruments, see section 3.1), although photolytic lifetimes differed by a factor of 10-25 (median values) between both heights (Fig. 6). Around noon of clear-sky days, lifetimes were about 10 minutes above and 100-250 minutes below the canopy. If no exchange between both heights had occurred, a steep mixing ratio gradient should be observed. However, coupling of all forest compartments to the layer above the canopy was achieved during this period, as indicated by the dominance of C and Cs coupling regimes with Ds intermissions (Fig. 5). Hence, effective mixing has offset the differences in HONO lifetimes due to photolysis (Fig. 6).

4) Afternoon (13:00-17:30 CET): When decoupling of the subcanopy (Ds) became the predominant regime in the early afternoon (13:00 CET) and HONO lifetime ratios

increased to a factor of 25-40 (median values), we always measured negative mixing ratio differences with a surprisingly low variation over the entire dry period (Figs. 5 and 6).

The HONO/NO$_x$ vertical differences (not shown) have a similar diel cycle (see Figs. 5 and 6), as variations were mainly caused by the HONO mixing ratios (see section 3.2). Differences were in the range of -6 % (evening) to + 5 % (at night) and around zero from early morning to noon (very similar to HONO itself). Therefore, changes in the HONO mixing ratio differences can be attributed to changes in source or sink processes leading to higher (or lower) values in relation to NO$_x$ values. Under conditions with virtually no turbulent exchange of the forest with the layer above canopy (Dc and Wa regimes), which occurred in the late afternoon / early night, we found systematically higher values below canopy. This is an indication that HONO was formed and/or released at the ground.

The diel cycle of the mixing ratio differences can be explained by differences in source and sink processes throughout the canopy, whereas the magnitude of these mixing ratio differences is determined by the exchange conditions as derived from the coherent structures.

## 3.4  Case study: 23 September

In order to exemplify the interplay of different HONO source and sink processes, Fig. 7 shows a contour plot of RH and the HONO mixing ratios measured at 0.5 and 24.5 m above the ground on 23 September.

From midnight to 06:30 CET, HONO mixing ratios were typically higher above the canopy than below. The HONO/NO$_x$ ratios were between 6 and 10 % at both heights. We found a positive correlation ($r^2 = 0.78$) with RH at 24.5 m but no correlation at the lower height ($r^2 = 0.07$) during the same time period. This might be attributed to higher RHs up to 90% at the ground, representing a transition to a completely wetted vegetation surface (i.e. formation of epicuticular water films) above 90 % RH (Burkhardt and Eiden, 1994; Klemm et al., 1998; Lammel, 1999) thus leading to HONO uptake.
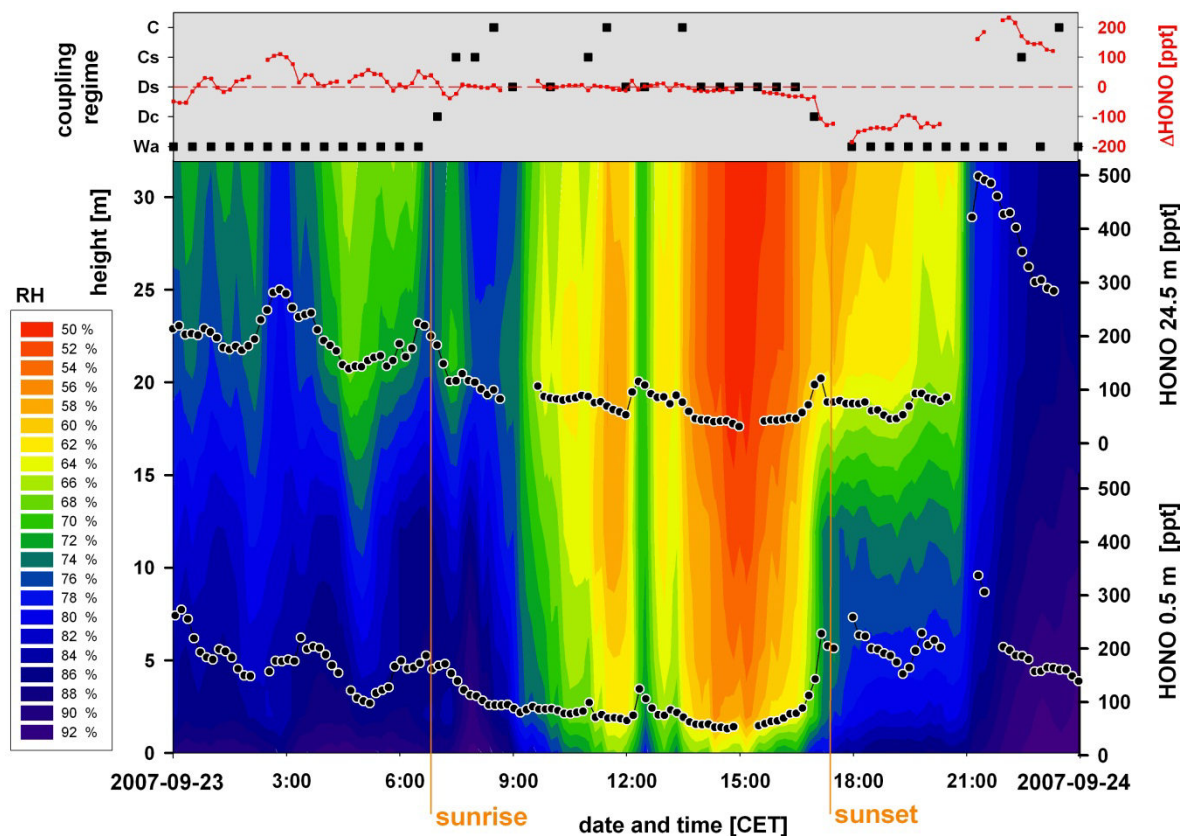
Figure 7. Simultaneous HONO time series at 0.5 m (lower graph, circles and lines) and 24.5 m (upper graph, circles and lines), overlaid with a contour plot of the vertical profile of measured RH (colour-coded 50-92 %) for 23 Sep. 2007 at the "Waldstein-Weidenbrunnen" research site. Missing values in the HONO measurements are due to zero air measurements. Sunrise and sunset (inferred from $j$(NO$_2$) as a proxy for $j$(HONO) and global radiation measurements) are marked as vertical (orange) lines. The upper panel shows the mixing ratio differences between 24.5 m and 0.5 m ($\Delta$HONO) and the coupling regimes in the forest.

During the first two hours after sunrise (6:30-8:30 CET), HONO mixing ratios decreased continuously with a rate of 60 ppt h$^{-1}$ above the canopy and with 40 ppt h$^{-1}$ close to the forest floor. If only photolysis was active, the calculated loss rate (i.e., $j$(HONO)x[HONO]) above the canopy would be faster (76 ppt h$^{-1}$) than observed. Below the canopy, the calculated loss rate would be much slower (5.5 ppt h$^{-1}$) due to shading. This discrepancy can be explained by vertical mixing. Downward mixing of HONO-depleted air from aloft resulted in a much faster loss rate below the canopy than calculated from photolysis alone. The overall HONO loss is expected to be faster than the photolytic loss alone since the mixed layer growth in the morning contributes to a decrease of near surface HONO that was trapped in the thermodynamically stable NBL.

From 8:30 CET until noontime, slightly decreasing HONO mixing ratios (10-15 ppt h$^{-1}$ most likely due to photolysis and mixing) were accompanied by a fast decrease of RH by 6 % h$^{-1}$ due to surface heating, causing rising surface temperatures. Therefore both measured variables were well correlated, but the correlation was mainly driven by radiation. Even

though HONO lifetimes above and below canopy differ by a factor of 10 to 25 (median values) in the morning (Fig. 6), the difference in HONO mixing ratios is less than 5 ppt (Fig. 7 upper panel) from 10:00 to 12:00 CET, which is within the uncertainty of both instruments. This can be explained by vertical exchange, taking place within the HONO lifetime above canopy.

Just after noontime, we observed a pronounced increase of HONO mixing ratios and of HONO/$NO_x$ ratios at both heights, with a simultaneous increase of RH by 10%. These patterns were most likely caused by passing clouds, increasing the HONO lifetime by a factor of three (from 9 min to 26 min above canopy, see Fig. 3), but were also related to a change in wind direction.

After the noontime peak, HONO mixing ratios decreased again at both heights but with a lower rate below canopy due to the 10 times lower photolysis frequencies. Further increases of lifetime ratios in the afternoon from 25 to 40 may have contributed to the increasing differences. While these differences were counter-balanced by effective vertical mixing, as indicated by a predominantly full coupling of the forest to the air layer above the canopy (C, Cs) in the morning hours, in the afternoon the HONO mixing ratio differences were maintained due to a lack of effective vertical mixing in the decoupled subcanopy (Ds) regime. Thus, only during periods when the subcanopy or even the whole forest are decoupled from the layer above the canopy, the different loss and production processes acting close to the forest floor and in the upper canopy become obvious. We propose a combination of lifetime differences due to shading of the canopy and the intensity of vertical mixing to explain the observed mixing ratio differences during daytime.

About two hours before sunset, HONO mixing ratios started to increase at both measurement heights. Above canopy, an increase rate of 40 ppt $h^{-1}$ led to a slightly higher level of HONO mixing ratios of $70 \pm 16$ ppt, whereas close to the forest floor, an increase rate of about 90 ppt $h^{-1}$ resulted in a higher and nearly constant level of about $200 \pm 20$ ppt. The steep increase in HONO mixing ratios at the ground coincided with an obvious RH increase below canopy, which is not as pronounced as above canopy.

After sunset, photolysis no longer affects the atmospheric lifetime of HONO. Thus, the occurrence of different HONO mixing ratios and at the same time different HONO/$NO_x$ ratios (about 5 % higher below canopy) at the two measuring heights provide evidence for different HONO-source processes throughout the canopy. The slight increase above the canopy and the strong increase below canopy in the absence of solar radiation and turbulent exchange with the air layer above canopy (Wa) give a strong indication that HONO was formed and released

at the ground. We found a good correlation ($r^2 = 0.74$) of HONO and RH for the whole period from 16:00 to 20:30 CET close to the forest floor due to accumulation of HONO and humidity below the canopy after decoupling of the forest. Above the canopy the correlation coefficient is very weak ($r^2 = 0.3$).

Between 20:30 and 21:00 CET a steep increase of HONO mixing ratios was observed. This event is considered to be dominated by an air mass change and not by local HONO production or release, although there are no clear signals in wind speed or direction. But almost all quantities (except NO) changed substantially (see Fig. 3). For example, ozone mixing ratios dropped by about 20 ppb (at 24.5 m), RH increased by 16 % from 20:30 to 22:00 CET and $NO_x$ increased from about 2 ppb to 4.5 ppb, which could not be explained by local chemistry alone. Maximum HONO mixing ratios were reached at 21:30 CET with 480 ppt above and 340 ppt below the canopy. This resulted in HONO/$NO_x$ ratios of up to 18 % above the canopy.

After 21:00 CET, the HONO mixing ratios decreased again at both heights while RH continued to increase. Thus, a negative RH dependence was observed with coefficients of determination of 0.9 at 24.5 m height (RH = 78-85 %) and 0.94 at 0.5 m height (RH = 88-93 %). The slopes are nearly identical but the humidity range is very different. Therefore, it is speculative at best to draw any conclusions about the underlying physical or chemical processes. Although we often found a good correlation of HONO and RH, we could not infer a simple relationship between RH and HONO mixing ratios. One reason for this is that both quantities exhibited a diel cycle that was affected by different (independent) environmental factors, e.g. radiation. HONO was formed near the ground and accumulated during nighttime, whereas RH increased due to cooling of the surface and evaporation still occurring in the afternoon and subsequent accumulation. During daytime HONO was photolyzed, whereas RH decreased due to surface heating although evaporation is enhanced. HONO and RH both decreased during daytime due to dilution by mixing with dryer and HONO depleted air from aloft. The only obvious relation are declining HONO mixing ratios at RHs above 95 % as already observed by Yu et al (2009).

## 4  Conclusions

For the first time, we have measured HONO mixing ratios simultaneously at two heights within and above a forest canopy using interference-corrected wet chemical analyzers (two

LOPAP instruments). The instruments agreed within 12 % (2σ) during side-by-side measurements under fair and relatively dry weather periods, allowing for a detailed interpretation of the measured mixing ratio differences. The measured HONO mixing ratios were influenced by a combination of several processes, such as (a) available surface area for heterogeneous formation, (b) co-deposition of species related to HONO formation, (c) HONO desorption from the surface and interaction with RH and (d) turbulent exchange of air masses between the forest and the atmosphere above (coupling).

The combination of micrometeorological and chemical measurements allowed us to explain the diel variations of the HONO mixing ratio differences measured below and above a spruce forest canopy. Differences of source or sink processes between above and below canopy became obvious only during periods when they were not overcome by turbulent mixing. For example, rising mixing ratios close to the forest floor in the late afternoon and early night, when the forest canopy was decoupled from the air layer above, provided a clear indication of HONO formation at the ground surface. Higher mixing ratios above the forest canopy in the late night until the morning were in some cases due to advection above the forest, which did only partly penetrate the canopy. In the morning, vertical exchange was most efficient and thus differences in HONO mixing ratios varied around zero despite large differences of photolysis frequencies (factor of 10-25) below and above the canopy.

Moreover, we observed a build-up of HONO during dry periods that was not related to a build-up of its precursor $NO_2$. We could not infer a simple relationship between RH and HONO mixing ratios. This study particularly demonstrated the strong effect of turbulent vertical transport and the influence of humidity conditions on HONO mixing ratios within and above the forest canopy. Nevertheless, in order to further untangle and quantify all different HONO sources and sinks, additional measurements both in the laboratory and in the field are required.

# References

Alicke, B., Platt, U., and Stutz, J.: Impact of nitrous acid photolysis on the total hydroxyl radical budget during the Limitation of Oxidant Production Pianura/Padana Produzione di Ozono study in Milan, J. Geophys. Res., 107, 8196, doi:10.1029/2000JD000075, 2002.

Ammann, M., Kalberer, M., Arens, F., Lavanchy, V., Gäggler, H. W., and Baltensperger, U.: Nitrous acid formation on soot particles: Surface chemistry and the effect of humidity, J. Aerosol. Sci., 29, 1031-1032, 1998.

Ammann, M., Rössler, E., Strekowski, R., and George, C.: Nitrogen dioxide multiphase chemistry: Uptake kinetics on aqueous solutions containing phenolic compounds, Phys. Chem. Chem. Phys., 7, 2513 – 2518, 2005.

Andrés-Hernández, M. D., Notholt, J., Hjorth, J., and Schrems, O.: A DOAS study on the origin of nitrous acid at urban and non-urban sites, Atmos. Environ., 30, 175-180, 1996.

Arens, F., Gutzwiller, L., Baltensperger, U., Gäggler, H. W., and Ammann, M.: Heterogeneous reaction of $NO_2$ on diesel soot particles, Environ. Sci. Technol., 35, 2191-2199, 2001.

Arens, F., Gutzwiller, L., Gäggeler, H. W., and Ammann, M.: The reaction of $NO_2$ with solid anthrarobin (1,2,10-trihydroxy-anthracene), Phys. Chem. Chem. Phys., 4, 3684–3690, 2002.

Aubin, D. G., and Abbatt, J. P. D.: Interaction of $NO_2$ with hydrocarbon soot: focus on HONO yield, surface modification, and mechanism, J. Phys. Chem. A, 111, 6263-6273, 2007.

Ayers, G. P.: Comment on regression analysis of air quality data, Atmos. Environ., 35, 2423-2425, 2001.

Baldocchi, D., Falge, E., Gu, L., Olson, R., Hollinger, D., Running, S., Anthoni, P., Bernhofer, C., Davis, K., Evans, R., Fuentes, J., Goldstein, A., Katul, G., Law, B., Lee, X., Malhi, Y., Meyers, T., Munger, W., Oechel, W., Paw U, K. T., Pilegaard, K., Schmid, H. P., Valentini, R., Verma, S., Vesala, T., Wilson, K., and Wofsy, S.: FLUXNET: A new tool to study the temporal and spatial variability of ecosystem-scale carbon dioxide, water vapor, and energy flux densities, B. Am. Meteorol. Soc., 82, 2415-2434, 2001.

Bejan, I., Aal, Y. A. E., Barnes, I., Benter, T., Bohn, B., Wiesen, P., and Kleffmann, J.: The photolysis of ortho-nitrophenols: a new gas phase source of HONO, Phys. Chem. Chem. Phys., 8, 2028–2035, DOI: 10.1039/b516590c, 2006.

Bröske, R., Kleffmann, J., and Wiesen, P.: Heterogeneous conversion of $NO_2$ on secondary organic aerosol surfaces: A possible source of nitrous acid (HONO) in the atmosphere?, Atmos. Chem. Phys., 3, 469–474, 2003.

Burkhardt, J., and Eiden, R.: Thin water films on coniferous needles, Atmos. Environ., 28, 2001-2017, 1994.

Calvert, J. G., Yarwood, G., and Dunker, A. M.: An evaluation of the mechanism of nitrous acid formation in the urban atmosphere, Res. Chem. Intermediat., 20, 463-502, 1994.

Febo, A., Perrino, C., and Allegrini, I.: Measurement of nitrous acid in Milan, Italy, by DOAS and diffusion denuders, Atmos. Environ., 30 3599-3609, 1996.

Finlayson-Pitts, B. J., Wingen, L. M., Sumner, A. L., Syomin, D., and Ramazan, K. A.: The heterogeneous hydrolysis of $NO_2$ in laboratory systems and in outdoor and indoor atmospheres: An integrated mechanism, Phys. Chem. Chem. Phys., 5, 223-242, 2003.

Finlayson-Pitts, B. J.: Reactions at surfaces in the atmosphere: integration of experiments and theory as necessary (but not necessarily sufficient) for predicting the physical chemistry of aerosols, Phys. Chem. Chem. Phys., 11, 7760–7779, 2009.

Foken, T.: Micrometeorology, Springer, Berlin-Heidelberg, 308 pp., 2008.

Foken, T., Meixner, F. X. ,Falge, E. Zetzsch, C., Serafimovich, A., Bargsten, A., Behrendt, T., Biermann, T., Breuninger, C., Gerken, T., Hunner, M., Lehmann-Pape, L., Hens, K., Jocher, G., Kesselmeier, J., Lüers, J., Mayer, J.-C., Moravek, A., Plake, D., Riederer, M., Rütz, F., Scheibe, M., Schier, S., Siebicke, L., Sörgel, M., Staudt, K., Trebs, I., Tsokankunku, A., Welling, M., Wolf, V. and Zhu, Z.: Atmospheric transport and chemistry in forest ecosystems-overview of the EGER-project, manuscript in preparation, 2011.

Frankenberger, E.: Untersuchungen über den Vertikalaustausch in den unteren Dekametern der Atmosphäre, Annalen der Meteorologie, 4, 358–374, 1951.

George, C., Strekowski, R. S., Kleffmann, J., Stemmler, K., and Ammann, M.: Photoenhanced uptake of gaseous $NO_2$ on solid organic compounds: a photochemical source of HONO?, Faraday Discuss., 130, 195–210, 2005.

Gerstberger, P., Foken, T., and Kalbitz, K.: The Lehstenbach and Steinkreuz catchments in NE Bavaria, in: Biogeochemistry of forested catchments in a changing environment: a German case study, edited by: Matzner, E., Ecological Studies, Springer Verlag, Heidelberg, 15-44, 2004.

Gower, S. T., Kucharik, C. J., and Norman, J. M.: Direct and indirect estimation of leaf area index, $f_{APAR}$, and net primary production of terrestrial ecosystems., Remote. Sens. Environ., 70, 29-51, 1999.

Gustafsson, R. J., Orlov, A., Griffiths, P. T., Cox, R. A., and Lambert, R. M.: Reduction of $NO_2$ to nitrous acid on illuminated titanium dioxide aerosol surfaces: implications for photocatalysis and atmospheric chemistry, Chem. Commun., 37, 3936–3938, 2006.

Gustafsson, R. J., Kyriakou, G., and Lambert, R. M.: The molecular mechanism of tropospheric nitrous acid production on mineral dust surfaces, ChemPhysChem, 9, 1390-1393, 2008.

Gutzwiller, L., Arens, F., Baltensberger, U., Gäggler, H. W., and Ammann, M.: Significance of semivolatile diesel exhaust organics for secondary HONO formation, Environ. Sci. Technol., 36, 677-682, 2002a.

Gutzwiller, L., George, C., Rössler, E., and Ammann, M.: Reaction kinetics of $NO_2$ with resorcinol and 2,7-naphthalenediol in the aqueous phase at different pH, J. Phys. Chem. A, 106, 12045-12050, 2002b.

Hanst, P. L., Spence, J. W., and Miller, M.: Atmospheric chemistry of n-nitroso dimethylamine, Environ. Sci. Technol., 11 403-405, 1977.

Harrison, R. M., and Kitto, A.-M. N.: Evidence for a surface source of atmospheric nitrous acid, Atmos. Environ., 28, 1089-1094, 1994.

He, Y., Zhou, X., Hou, J., Gao, H., and Bertman, S. B.: Importance of dew in controlling the air-surface exchange of HONO in rural forested environments, Geophys. Res. Lett., 33, L02813, doi:10.1029/2005GL024348, 2006.

Heland, J., Kleffmann, J., Kurtenbach, R., and Wiesen, P.: A new instrument to measure gaseous nitrous acid (HONO) in the atmosphere, Environ. Sci. Technol., 35, 3207-3212, 2001.

Holmes, P., Lumley, J. L., and Berkooz, G.: Turbulence, coherent structures, dynamical systems and symmetry, Cambridge University Press, Cambridge, 420 pp., 1996.

Jenkin, M. E., Cox, R. A., and Williams, D. J.: Laboratory studies of the kinetics of formation of nitrous acid from the thermal reaction of nitrogen dioxide and water vapour, Atmos. Environ., 22, 487-498, 1988.

Killus, J. P., and Whitten, G. Z.: Background reactivity in smog chambers, Int. J. Chem. Kinet., 22, 547-575, 1990.

Kleffmann, J., Becker, K. H., and Wiesen, P.: Heterogeneous $NO_2$ conversion processes on acid surfaces: possible atmospheric implications, Atmos. Environ., 32, 2721-2729, 1998.

Kleffmann, J., Becker, K. H., Lackhoff, M., and Wiesen, P.: Heterogeneous conversion of $NO_2$ on carbonaceous surfaces, Phys. Chem. Chem. Phys., 1, 5443-5450, 1999.

Kleffmann, J., Heland, J., Kurtenbach, R., Lörzer, J., and Wiesen, P.: A new instrument (LOPAP) for the detection of nitrous acid (HONO), Environ. Sci. Pollut. R., 4, 48 – 54, 2002.

Kleffmann, J., Kurtenbach, R., Lörzer, J., Wiesen, P., Kalthoff, N., Vogel, B., and Vogel, H.: Measured and simulated vertical profiles of nitrous acid—Part I: Field measurements, Atmos. Environ., 37, 2949–2955, 2003.

Kleffmann, J., Benter, T., and Wiesen, P.: Heterogeneous reaction of nitric acid with nitric oxide on glass surfaces under simulated atmospheric conditions, J. Phys. Chem. A, 108, 5793-5799, 2004.

Kleffmann, J., Gavriloaiei, T., Hofzumahaus, A., Holland, F., Koppmann, R., Rupp, L., Schlosser, E., Siese, M., and Wahner, A.: Daytime formation of nitrous acid: A major source of OH radicals in a forest, Geophys. Res. Lett., 32, L05818, doi:10.1029/2005GL022524, 2005.

Kleffmann, J.: Manual LOPAP-3, version 1.3.0, Bergische Universität Wuppertal, QUMA Elektronik & Analytik GmbH, Wuppertal, 2006.

Kleffmann, J., Lörzer, J. C., Wiesen, P., Kern, C., Trick, S., Volkamer, R., Rodenas, M., and Wirtz, K.: Intercomparison of the DOAS and LOPAP techniques for the detection of nitrous acid (HONO), Atmos. Environ., 40, 3640–3652, 2006.

Kleffmann, J.: Daytime sources of nitrous acid (HONO) in the atmospheric boundary layer, ChemPhysChem, 8, 1137 – 1144, 2007.

Klemm, O., Burkhardt, J., and Gerchau, J.: Leaf wetness: A quantifiable parameter in deposition studies, in: Proceedings of the EUROTRAC-2 Symposium 98: Transport and chemical transformation in the troposphere, edited by: Borell, P. M. and Borell, P., WIT press, Southampton, 238-242, 1999.

Kraus, A., and Hofzumahaus, A.: Field measurements of atmospheric photolysis frequencies for $O_3$, $NO_2$, HCHO, $CH_3CHO$, $H_2O_2$, and HONO by UV spectroradiometry, J. Atmos. Chem., 31, 161–180, 1998.

Lammel, G., and Perner, D.: The atmospheric aerosol as a source of nitrous acid in the polluted atmosphere, J. Aerosol. Sci., 19, 1199-1202, 1988.

Lammel, G., and Cape, J. N.: Nitrous acid and nitrite in the atmosphere, Chem. Soc. Rev., 25, 361-369, 1996.

Lammel, G.: Formation of nitrous acid: Parameterisation and comparison with observations, Max Planck Institute for Meteorology, Hamburg, report No. 286, 36, 1999.

Legendre, P., and Legendre, L.: Numerical ecology, 2nd English ed., Developments in environmental modelling, Elsevier Science BV, Amsterdam, 1998.

Monge, M. E., D'Anna, B., Mazri, L., Giroir-Fendler, A., Ammann, M., Donaldson, D. J., and George, C.: Light changes the atmospheric reactivity of soot, P. Natl. Acad. Sci. USA, 107, 6605–6609, 2010.

Moravek, A.: Vertical distribution of reactive and non-reactive trace gases in and above a spruce canopy, master thesis, University Karlsruhe, Germany, 124 pp., 2008.

Ndour, M., D'Anna, B., George, C., Ka, O., Balkanski, Y., Kleffmann, J., Stemmler, K., and Ammann, M.: Photoenhanced uptake of $NO_2$ on mineral dust: Laboratory experiments and model simulations, Geophys. Res. Lett., 35, L05812, doi:10.1029/2007GL032006, 2008.

Notholt, J., Hjorth, J., and Raes, F.: Formation of HNO$_2$ on aerosol surfaces during foggy periods in the presence of NO and NO$_2$, Atmos. Environ., 26, 211-217, 1992.

Oren, R., Schulze, E.-D., Matyssek, R., and Zimmermann, R.: Estimating photosynthetic rate and annual carbon gain in conifers from specific leaf weight and leaf biomass, Oecologia, 70, 187-193, 1986.

Perner, D., and Platt, U.: Detection of nitrous acid in the atmosphere by differential optical absorption, Geophys. Res. Lett., 6, 917-920, 1979.

Pitts, J. N. Jr., Biermann, H. W., Winer, A. M., and Tuazon, E. C.: Spectroscopic identification and measurement of gaseous nitrous acid in dilute auto exhaust, Atmos. Environ., 18, 847-854, 1984.

Pitts, J. N. Jr., Grosjean, D., Cauwenberghe, K. V., Schmid, J. P., and Fitz, D. R.: Photooxidation of aliphatic amines under simulated atmospheric conditions: formation of nitrosamines, nitramines, amides, and photochemical oxidant, Environ. Sci. Technol., 12 946-953, 1978.

Qin, M., Xie, P., Su, H., Gu, J., Peng, F., Li, S., Zeng, L., Liu, J., Liu, W., and Zhang, Y.: An observational study of the HONO–NO$_2$ coupling at an urban site in Guangzhou City, South China, Atmos. Environ., 43, 5731–5742, 2009.

Reisinger, A. R.: Observations of HNO$_2$ in the polluted winter atmosphere: possible heterogeneous production on aerosols, Atmos. Environ., 34, 3865-3874, 2000.

Rohrer, F., Bohn, B., Brauers, T., Bruning, D., Johnen, F.-J., Wahner, A., and Kleffmann, J.: Characterisation of the photolytic HONO-source in the atmosphere simulation chamber SAPHIR, Atmos. Chem. Phys., 5, 2189–2201, 2005.

Rubio, M. A., Lissi, E., and Villena, G.: Nitrite in rain and dew in Santiago city, Chile. Its possible impact on the early morning start of the photochemical smog, Atmos. Environ., 36, 293–297, 2002.

Rubio, M. A., Lissi, E., and Villena, G.: Factors determining the concentration of nitrite in dew from Santiago, Chile, Atmos. Environ., 42, 7651–7656, 2008.

Sakamaki, F., Hatakeyama, S., and Akimoto, H.: Formation of nitrous acid and nitric oxide in the heterogeneous dark reaction of nitrogen dioxide and water vapour, Int. J. Chem. Kinet., 15, 1013 -1029, 1983.

Saliba, N. A., Yang, H., and Finlayson-Pitts, B. J.: Reaction of gaseous nitric oxide with nitric acid on silica surfaces in the presence of water at room temperature, J. Phys. Chem. A, 105, 10339-10346, 2001.

Sander, R.: Compilation of Henry's law constants for inorganic and organic species of potential importance in environmental chemistry, available at: http://www.mpch-mainz.mpg.de/~sander/res/henry.html, last access 4 January 2011, 1999.

Serafimovich, A., Siebicke, L., Staudt, K., Lüers, J., Biermann, T., Schier, S., Mayer, J.-C., Foken, T.: ExchanGE processes in mountainous Regions (EGER) Documentation of the Intensive Observation Period (IOP1) September, 6th to October, 7th 2007, Arbeitsergebnisse Nr. 36, Bayreuth, Germany, print ISSN 1614-8916; internet ISSN 1614-8924, 2008.

Serafimovich, A., Thomas, C. and Foken, T.: Vertical and horizontal transport of energy and matter by coherent motions in a tall spruce canopy, revised manuscript, Bound.-Lay. Meteorol., 2010.

Sjödin, Å: Studies of the diurnal variation of nitrous acid in urban air, Environ. Sci. Technol., 22, 1086-1089, 1988.

Sleiman, M., Gundel, L. A., Pankow, J. F., Jacob, P., Singer, B. C., and Destaillats, H.: Formation of carcinogens indoors by surface-mediated reactions of nicotine with nitrous acid, leading to potential thirdhand smoke hazards, P. Natl. Acad. Sci. USA, 107, 6576-6581, 2010.

Sokal, R. R., and Rohlf, F. J.: Biometry - The principles and practice of statistics in biological research, 3rd ed., W. H. Freeman, New York, 1995.

Sonntag, D.: Important new values of the physical constants of 1986, vapor pressure formulations based on the ITS-90 and psychrometer formulae, Z. Meteorol., 70, 340–344, 1990.

Staudt, K., and Foken, T.: Documentation of reference data for the experimental areas of the Bayreuth Centre for Ecology and Environmental Research (BayCEER) at the Waldstein site, University of Bayreuth, Dept. of Micrometeorology Bayreuth, report No.37, print ISSN 1614-8916; internet ISSN 1614-8924., 2007.

Staudt, K., Falge, E., Pyles, R. D., Paw U, K. T., and Foken, T.: Sensitivity and predictive uncertainty of the ACASA model at a spruce forest site, Biogeosciences Discuss., 7, 4223–4271, doi:10.5194/bgd-7-4223-2010, 2010.

Stemmler, K., Ammann, M., Donders, C., Kleffmann, J., and George, C.: Photosensitized reduction of nitrogen dioxide on humic acid as a source of nitrous acid, Nature, 440, 195-198, 2006.

Stemmler, K., Ammann, M., Elshorbany, Y., Kleffmann, J., Ndour, M., D'Anna, B., George, C., and Bohn, B.: Light-induced conversion of nitrogen dioxide into nitrous acid on submicron humic acid aerosol, Atmos. Chem. Phys., 7, 4237–4248, 2007.

Stull, R. B.: An Introduction to Boundary Layer Meteorology, Atmospheric and Oceanographic Sciences Library, Kluwer Academic Publishers, Dordrecht, 670 pp., 1988.

Stutz, J., Alicke, B., and Neftel, A.: Nitrous acid formation in the urban atmosphere: Gradient measurements of $NO_2$ and HONO over grass in Milan, Italy, J. Geophys. Res., 107 (D22), 8192, doi:10.1029/2001JD000390, 2002.

Stutz, J., Alicke, B., Ackermann, R., Geyer, A., Wang, S., White, A. B., Williams, E. J., Spicer, C. W., and Fast, J. D.: Relative humidity dependence of HONO chemistry in urban areas, J. Geophys. Res., 109, D03307, doi:10.1029/2003JD004135, 2004.

Su, H., Cheng, Y. F., Cheng, P., Zhang, Y. H., Dong, S., Zeng, L. M., Wang, X., Slanina, J., Shao, M., and Wiedensohler, A.: Observation of nighttime nitrous acid (HONO) formation at a non-urban site during PRIDE-PRD2004 in China, Atmos. Environ., 42, 6219–6232, 2008.

Svensson, R., Ljungström, E., and Lindqvist, O.: Kinetics of the reaction between nitrogen dioxide and water vapour, Atmospheric Environment, 21 1529-1539, 1987.

Thomas, C., and Foken, T.: Detection of long-term coherent exchange over spruce forest using wavelet analysis, Theor. Appl. Climatol., 80, 91-104, 2005.

Thomas, C., and Foken, T.: Flux contribution of coherent structures and its implications for the exchange of energy and matter in a tall spruce canopy Bound.-Lay. Meteorol., 123, 317-337, doi:10.1007/s10546-006-9144-7, 2007.

Trebs, I., Bohn, B., Ammann, C., Rummel, U., Blumthaler, M., Königstedt, R., Meixner, F. X., Fan, S., and Andreae, M. O.: Relationship between the NO2 photolysis frequency and the solar global irradiance, Atmos. Meas. Tech., 2, 725–739, 2009.

Trick, S.: Formation of nitrous acid on urban surfaces - a physical-chemical perspective-, Ph.D. thesis, University Heidelberg, Germany, 290 pp., 2004.

Veitel, H.: Vertical profiles of $NO_2$ and HONO in the boundary layer, Ph.D. thesis, University, Heidelberg, Germany, 270 pp., 2002.

Vogel, B., Vogel, H., Kleffmann, J., and Kurtenbach, R.: Measured and simulated vertical profiles of nitrous acid—Part II. Model simulations and indications for a photolytic source, Atmos. Environ., 37, 2957–2966, 2003.

Wainmann, T., Weschler, C. J., Lioy, P. J., and Zhang, J.: Effects of surface type and relative humidity on the production and concentration of nitrous acid in a model indoor environment, Environ. Sci. Technol., 35, 2200-2206, 2001.

Wolff, V., Trebs, I., Foken, T., and Meixner, F. X.: Exchange of reactive nitrogen compounds: concentrations and fluxes of total ammonium and total nitrate above a spruce canopy, Biogeosciences, 7, 1729–1744, doi:10.5194/bg-7-1729-2010, 2010.

Yu, Y., Galle, B., Hodson, E., Panday, A., Prinn, R., and Wang, S.: Observations of high rates of $NO_2$ – HONO conversion in the nocturnal atmospheric boundary layer in Kathmandu, Nepal, Atmos. Chem. Phys., 9, 6401–6415, 2009.

Zhang, N., Zhou, X., Shepson, P. B., Gao, H., Alaghmand, M., and Stirm, B.: Aircraft measurement of HONO vertical profiles over a forested region, Geophys. Res. Lett., 36, L15820, doi:10.1029/2009GL038999, 2009.

Zhou, X., Civerolo, K., Dai, H., Huang, G., Schwab, J., and Demerjian, K.: Summertime nitrous acid chemistry in the atmospheric boundary layer at a rural site in New York State, J. Geophys. Res., 107 (D21), 4590, doi:10.1029/2001JD001539 , 2002a.

Zhou, X., He, Y., Huang, G., Thornberry, T. D., Carroll, M. A., and Bertman, S. B.: Photochemical production of nitrous acid on glass sample manifold surface, Geophys. Res. Lett., 29 (14), 1681, doi:10.1029/2002GL015080, 2002b.

Zhou, X., Gao, H., He, Y., Huang, G., Bertman, S. B., Civerolo, K., and Schwab, J.: Nitric acid photolysis on surfaces in low-$NO_x$ environments: Significant atmospheric implications, Geophys. Res. Lett., 30 (23), 2217, doi:10.1029/2003GL018620, 2003.

# Appendix D

# Singular System Analysis of Forest Observations of HONO and Humidity

M. Sörgel[1], A. Held[1], C. Zetzsch[2,3]

1 University of Bayreuth, Junior Professorship of Atmospheric Chemistry, Bayreuth, Germany

2 University of Bayreuth, Atmospheric Chemistry Research Laboratory, Bayreuth, Germany

3 Fraunhofer Institute for Toxicology and Experimental Medicine, Hannover, Germany

## Abstract

This study investigates the relation of atmospheric nitrous acid (HONO) and relative humidity (RH) from three different field campaigns. As mixing ratios of HONO and RH co-vary on different timescales, especially considering a pronounced diurnal cycle, we used Singular System Analysis (SSA) to extract signal contributions from these different timescales. By using the advantage of SSA to reconstruct the signal and by choosing only long term trends and variations associated with the diurnal cycle for reconstruction, we were able to extract the residual signal containing the higher frequency contributions. As this residual signal is only about 2 % of the original RH signal and about 20 % of the original HONO signal, identification of processes which couple RH and HONO by correlation studies was not fully convincing. However, other than measured time series, all residual time series (N = 4 pairs) showed a slight positive correlation (r~0.2) of HONO with RH pointing to a potential

influence of RH on HONO formation on shorter timescales. The basic analysis of the data set revealed, that HONO values were log-normal distributed and RH values were normal or bimodal distributed. Thus the logarithmic HONO values were better correlated to RH. Furthermore, the data set was found to be structured similar to a previously published scheme for surface wetness.

# 1  Introduction

Mixing ratios of many compounds of interest in atmospheric chemistry exhibit a diurnal cycle that is forced by solar radiation (i.e. through photolysis, photochemical reactions, heating or turbulence).  These parallel diurnal cycles cause a correlation of all species exhibiting the diurnal cycle. Thus it is often difficult to identify correlations other than the diurnal cycle. Singular System Analysis or Singular Spectrum Analysis (SSA) has become a widely used tool in geosciences (but not yet in atmospheric chemistry) to extract periodic and anharmonic oscillations as well as trends from a time series (e.g. Elsner and Tsonis, 1996). Employing SSA opens the possiblity to reconstruct the time series by selecting certain oscillations, which allow us to reconstruct the signal by removing the oscillations associated with the diurnal cycle. Oscillations other than the diurnal cycle can thus be identified in the remaining part of the signal. In addition, the reconstructed signal can be analysed for correlations on longer or shorter timescales than the diurnal cycle.

Many field and laboratory studies (e.g. Arens et al., 2002; He et al., 2006; Trick, 2004; Stutz et al., 2004; Wainmann et al., 2001; Yu et al, 2009; Sörgel et al., 2011a; Rubio et al., 2008) report a relation between gas phase HONO and relative humidity (RH) or dew. Dew is a sink for HONO in addition to scavenging by precipitation (Rubio et al.,2002; Rubio et al. 2008; He et al., 2006) but HONO might be re-released during evaporation of dew (Rubio et al., 2002; He et al., 2006). In accordance with the formation of liquid films or droplets above 95 % RH (Lammel, 1999), lower HONO mixing ratios and HONO/NO$_x$ ratios were reported above 95 % RH (Stutz et al., 2004; Yu et al., 2009; Sörgel et al., 2011a). Furthermore, HONO can be salted out from concentrated ammonium sulphate and sulphuric acid solutions (Becker et al., 1996; Becker et al., 1999), and its uptake in solutions is pH dependant (Hirokawa et al., 2008). The influence of surface water on HONO formation at humidities lower than 95 % is less clear. From chamber measurements, Trick (2004) and Stutz (2005) proposed HONO adsorption and desorption by a Langmuir-type mechanism, were HONO desorption from the

surface is accelerated by co-adsorption of water molecules. Additional effects could be the blocking of surface active sites for heterogeneous HONO formation due to water adsorption (Lammel and Cape, 1996), or reduced chemisorption of $H_2O$ at high humidities, (Gustavsson et al., 2008) if the chemisorption mechanism holds (Finlayson-Pitts, 2009). Although many possible processes and mechanisms were reported neither the formation mechanism nor the adsorption and desorption processes for HONO are clear. Lammel and Cape (1996) have already stated that both quantities (HONO and RH) exhibit a very pronounced diurnal cycle forced by solar radiation. However, RH is forced by the heating and cooling of surface air whereas HONO by photolysis and turbulent mixing.

Therefore, we use SSA in the present study for separating the signals from the diurnal cycles of HONO and RH in order to identify the possible influence of the above mentioned processes in the remaining signal.

# 2  Methodology

## 2.1  Mathematical background

One of the basic ideas of SSA is to use tools developed for multivariate time series for single time records (Elsner and Tsonis, 1996). In practice this is achieved by forming lag-shifted copies of the time series. A detailed description and the mathematical background of SSA are given in textbooks (e.g. Elsner and Tsonis, 1996; Golyandina et al., 2001) and more recent methodological articles (e.g. Ghil et al., 2002; Golyandina and Osipov, 2007).

Here, we briefly summarize the fundamental concepts:

From the time series $\{x_t: t=1,2,...,N_t\}$, a matrix of lagged vectors $V_i = (x_i, x_{i+1}, ...,x_{i+L-1})^T$ with $1 \leq i \leq N$ is formed and $N = N_t - L + 1$, where L is the embedding dimension or window length. The window length is one free parameter to choose for the analysis. In principal, the choice of L is a compromise between information content and statistical confidence (Elsner and Tsonis, 1996), as the window length determines the longest oscillations possible to identify. Thus, a large L improves the detection of long term trends, but provides less statistical confidence. The suggested range for L ranges from about $N_t/11$ (Ghil et al., 2002) to close to $N_t/2$ (Golyandina and Osipov, 2007).

A trajectory or augmented matrix $\mathbf{X}$ is formed from these lagged vectors, which has the dimension N by L.

$$\mathbf{X} = [V_1:...:V_N] \tag{1}$$

The lagged-covariance matrix **S** can be computed from the product of the trajectory matrix and its transposed normalized by N: $\mathbf{S} = (1/N)\ \mathbf{XX}^T$.

This matrix is then decomposed into its eigenvalues $\lambda_k$ and eigenvectors $U_k$ by means of singular value decomposition (SVD). The L eigenvectors $U_k$ of the lag-covariance matrix **S** are called temporal empirical orthogonal functions (EOFs). The eigenvalues $\lambda_k$ of **S** account for the partial variance in the direction $U_k$. In general, the eigenvectors exhibit a distinct Fourier spectrum such that the dominant frequency of the eigenvectors can be identified by applying Fourier transform and taking the largest Fourier component (Gudmundson, 2007).

The sum of all $\lambda_k$ gives the total variance of the original time series $x_t$. Therefore, a subset of $\lambda_k$ represents a portion of the variance of the original signal.

The principal components $a^k$ can be calculated by projecting the original time series on the eigenvectors:

$$a_i^k = \sum_{j=1}^{L} x_{i+j-1} e_j^k \tag{2}$$

where $e_j^k$ is the $j^{th}$ component of the $k^{th}$ eigenvector for i=1,2,…,N.

The principal components are then used to reconstruct the time series by

$$x_{i+j-1} = \sum_{k=1}^{L} a_i^k e_j^k \tag{3}$$

with i = 1, 2, …, N and j = 1, 2, …, L.

By choosing only a selection of principal components the time series can be filtered. As a complete reconstruction is computationally intensive, we chose to reconstruct only the leading (first) EOFs and subtract them from the originally time series. The residual was analysed for correlations on shorter timescales than the diurnal cycle and long term trends, which were contained in the first EOFs.

## *2.2 Experimental*

In this paper we compare measured data of HONO and RH from three field campaigns. The two Intensive Operating Periods (IOP I and IOP II) of the project "ExchanGE processes in a mountainous Region" (EGER) took place at a spruce forest site in the Fichtelgebirge Mountains in south-east Germany.  For IOP I, which was conducted in September 2007, we measured RH and HONO at two heights in parallel below and above the canopy as described by Sörgel et al. (2011a). IOP II took place in June/July 2008 with HONO and RH

measurements 1 m above the forest floor. A detailed description of the experiment and the meteorological conditions during both IOPs has been given by Foken et al. (2011).

Measurements of HONO were conducted by commercial LOPAP instruments (LOng Path Absorption Photometer, QUMA Elektronik & Analytik, Wuppertal, Germany). The LOPAP is based on a wet chemical technique, with fast sampling of HONO as nitrite in a stripping coil and subsequent detection as an azo dye using long path absorption in 2.4 m long Teflon AF tubing. Detailed descriptions of the instrument have been given by Heland et al. (2001) and Kleffmann et al. (2002). The instruments were placed outside directly on the scaffolds in ventilated aluminium boxes without temperature control. The temperature of the stripping coils was kept constant at 20 °C by thermostats to assure constant sampling conditions. The overall relative error of the LOPAP instruments was found to be 12 % in a recent side by side intercomparison in the field (Sörgel et al., 2011a). During IOP I and IOP II detection limits of the LOPAPs ranged from 1 to about 4 ppt.

Humidity profiles during IOP I and II were measured at the main tower using Frankenberger-type psychrometers (Frankenberger, 1951). The relative humidity (RH) was calculated from the dry and wet bulb temperature of the psychrometers using the Magnus formula after Sonntag (1990) for the saturation vapour pressure and the Sprung formula for the actual vapour pressure (Foken, 2008).

The campaign "Diel Oxidant Mechanism In relation to Nitrogen Oxides" (DOMINO) took place from mid-November to mid-December 2008 at a pine forest site in south west Spain. A description of the experimental setup has been given by Sörgel et al. (2011b). Detection limits for the LOPAPs during DOMINO, calculated as 3 σ of the noise during zero air measurements, were between 1 and 2.5 ppt. Relative humidity (RH) and wind direction were measured with a WXT510 (Vaisala, Helsinki, Finland) meteorological station on top of the MoLa (Mobile Laboratory) inlet system, which was at 10 m height 10 m southeast of the scaffold, were the LOPAP was placed (also at 10 m height).

For the calculations of SSA we used the free statistics software "r" (version 2.13.0, http://www.r-project.org/). The package for calculating SSA (package 'simsalabim' version 0.1-3) was provided by Gudmundson (2008). The extension of SSA to time series with missing values according to Schoellhamer (2001) and Golyandina and Osipov (2007) was used.

# 3   Results and discussion

## *3.1  "Classical statistics" of HONO and RH*

If we follow the hypothesis of a relation of HONO and RH we can start by discussing a simple scatter plot (Fig.1a). Obvious features are low HONO values at low relative humidity as well as low values above 95 % RH. Maximum values occur between 70 and 90 % RH. In different campaigns, the increase of HONO values starts at different RHs, which at this stage might point to a simple coincidence (night-time increase of both quantities) instead of physical or chemical reasons. The same coincidence can be observed for the IOP I values measured at two different heights but at the same time (Fig. 1: IOP I 0.5 m and IOP I 24 m). RH values are higher close to the ground and thus maximum HONO values occur at higher RH. In order to determine the coefficient of determination for the overall HONO and RH relation, we investigated the distributions of HONO and RH values. Relative humidity values were either normal or bimodal distributed, whereas HONO values were log-normal distributed. Therefore, the logarithm of the HONO values has to be correlated with the RH values (Fig 1b).
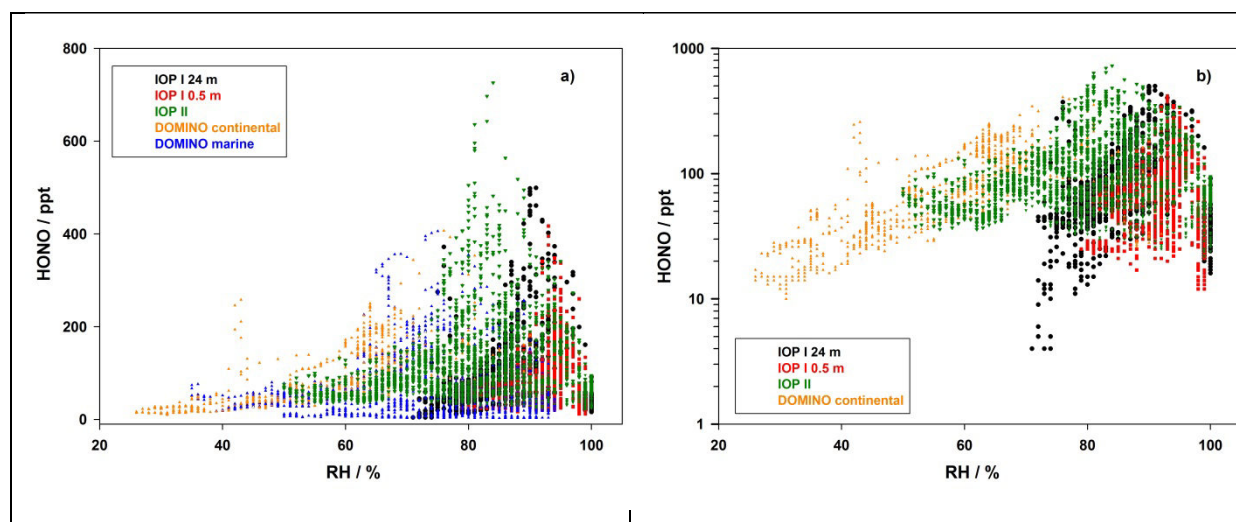


Figure 1: a) HONO values from three different campaigns versus relative humidity. DOMINO (winter, Spain), IOP I (autumn, Germany), IOP II (summer, Germany). b) The same data (without DOMINO marine) with HONO data on a logarithmic scale.

There seems to be an overall RH dependence of the HONO maximum values with an increase up to 85 % RH and then continuously lower values with a steep decrease above 95 %. Based on the studies of Burkhardt and Eigen (1994) and Klemm et al. (1999), Lammel (1999) proposed a scheme of surface wetness. In this scheme below 55 % RH surfaces are regarded

as "dry", between 55 % and 90 % RH they are classified as "partially wet" and as "wet" above 90 % RH.  This classification corresponds quite well with the features in Fig. 1 (a and b). From Fig. 1 it seems that log HONO values are well correlated to RH values up to about 65 % RH. As most of the values in this RH interval are daytime values this might be simply caused by the co-variation of HONO and RH due to the diurnal cycle. For example for DOMINO daytime RH and HONO values are well correlated ($r^2 = 0.71$) but HONO is declining due to photolysis and RH due to surface heating. But also for the night-time values (fig. 2 a) this relation persists, although there are only few data points available and the correlation can still be caused by the diurnal cycle (simultaneous increase of HONO and RH in the early night).  On these "dry" surfaces three proposed mechanisms might play a role:

- The availability of surface water for the reaction with $NO_2$ (HONO formation first order with respect to water and $NO_2$ (e.g. Sakamaki et al., 1983; and summarized by Finlayson-Pitts, 2009))
- Amount of chemisorbed water for reaction with $NO_2$ and reduced chemisorption with increasing amounts of water at the surface (Gustafsson et al., 2008)
- A Langmuir-type mechanism, where co-adsorbing water replaces HONO at the surface which is released to the gas phase (Trick, 2004, Stutz, 2005)

The term "partially wet" denotes that only part of the surface (e.g. of a leaf) is "wet" due to deliquescence of deposited compounds which are (partly) water soluble (Burkard and Eiden, 1994). This means, that in the transition region both, dry and wet surfaces exist. In the deliquescing particles themselves several processes can change HONO uptake, respectively release, in dependence of the liquid water content. As HONO uptake in liquid films or droplets is governed by pH (Hirokawa et al., 2008) a lowering in pH values due to evaporation of water (Klemm, 1988) might enhance release and hinder uptake of HONO. Furthermore, HONO is salted out in concentrated sulphuric acid and ammonium sulphate solutions (Becker et al., 1996; Becker et al., 1999), which might be transferrable to other concentrated solutions. One might speculate if the growing liquid film due to deliquescing salt particles displaces HONO adsorbed to the surface. The HONO might then be released to the atmosphere either due to low pH or high ionic strength in the liquid film as described above.

These processes would explain the occurrence of a maximum in gas phase HONO mixing ratios before the rising liquid water content enhances solubility of HONO. That both, uptake and release of HONO, can take place on these "partially wet" surfaces might explain the high variability of HONO values in this RH region.

The only obvious feature is the sharp decline of HONO values above 95 % RH as already observed by other groups (e.g. Stutz et al., 2004; Yu et al., 2009). This could be attributed to the formation of liquid films which take up HONO (i.e. "wet" surface) or to rain events (where droplets and liquid films take up HONO). Another result regarding "wet" surfaces was that the removal of HONO values associated with wind directions (140 - 330°) originating from the sea during DOMINO (based on the analysis of Diesch et al., 2011), substantially improved the correlation (see also sect. 3.3). These values were presumably influenced by the equilibrium with the sea surface as proposed by Wojtal et al. (2010).
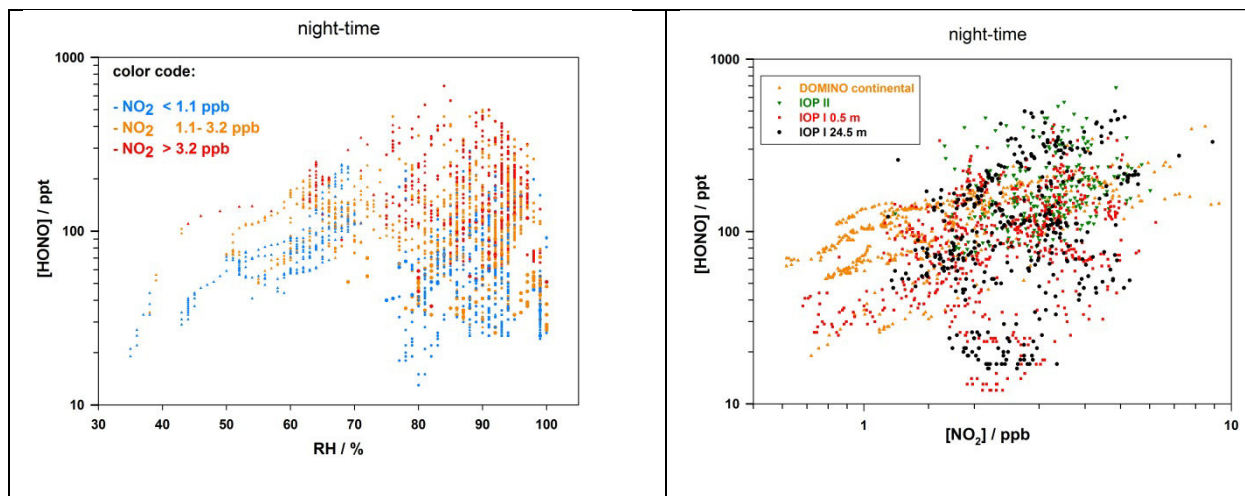


Figure 2: Night-time data of HONO versus RH are shown on the left hand side. The colour code denotes the level of the $NO_2$ precursor. The $NO_2$ levels are categorized by low (< 1.1 ppb = 25 percentile), middle (1.1 - 3.2 / 25 - 75 percentile) and high (> 3.2 = 75 percentile) values. On the right hand side, HONO values versus $NO_2$ values are shown for the same data.

Another influence on the relation of HONO and RH might arise from variations of the HONO precursor $NO_2$, but correlations of HONO and $NO_2$ were weak as well, especially for IOP I ($r^2$ = 0.14 at 24 m and $r^2$ = 0.05 at 0.5 m). The low or non-existent correlation of HONO with its precursor $NO_2$ was the starting point to think about the influence of RH. Although correlations of HONO with $NO_2$ were higher for IOP II and especially good for DOMINO ($r^2$ = 0.44), the $NO_2$ levels reflect more a tendency (higher $NO_2$ <=> higher HONO) than a strong correlation (Fig. 2). This might be attributed to the rather slow formation of HONO from $NO_2$ (max. 2 % $h^{-1}$). This means that HONO mixing ratios build up slowly and are thus more evenly distributed, whereas $NO_2$ values might be quite variable as indicated by the results of Pöhler (2010) and Harrison et al. (1996). Therefore, HONO values were not normalized to $NO_2$ to avoid disturbances of the HONO to RH correlation due to variations in $NO_2$. Usually, normalization to $NO_2$ is done to account for changes in boundary layer height and precursor concentration. Some shortcomings of this scaling approach have already been

discussed by Su et al. (2008 a). Furthermore, correlations on different timescales can be found by applying the SSA, and may possibly allow for a separation of HONO and $NO_2$ and HONO and RH correlations. The SSA (e.g. Elsner and Tsonis, 1996) was chosen for this analysis as it provides the opportunity to reconstruct the time series by using signal contributions associated with certain timescales (oscillations). This is necessary to remove the signal contributions of the diurnal cycle of HONO and RH and the long term trends in order to identify correlations on shorter timescales which might be a hint at the interaction with fast physical processes (adsorption/desorption).

## *3.2 Dominant frequencies in HONO and RH time series and their contribution to the signals*

As described in detail in sect. 2.1, the embedded time series of HONO and RH are decomposed into eigenvectors and eigenvalues by means of single value decomposition (SDV). The eigenvalues are ordered by their decreasing rank (i.e. signal contribution). A Fourier-transform of the eigenvectors yields their dominant frequency respectively dominant periodic time τ.
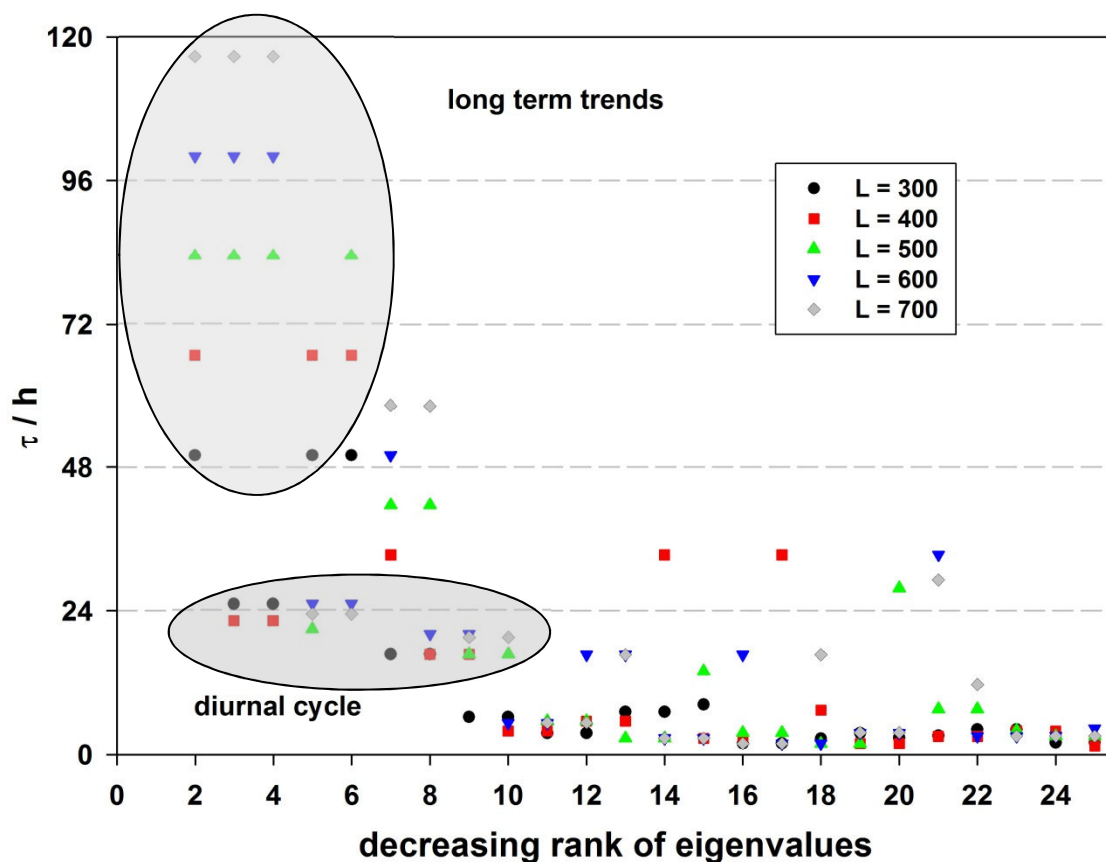


Figure 3: Dominant periodic times (τ) in hours of the eigenvectors for different window lengths (L) ordered by decreasing rank of the eigenvalues for the HONO time series measured at 0.5 m during IOP I.

As the window length is the only free parameter to choose for the SSA, Fig. 3 shows the dependency of the frequency of the 25 leading EOFs (ordered by decreasing rank, i.e. contribution to the signal) for different window lengths. The time series "IOPI 0.5 m" included $N_t = 1585$ points (10 min average values). Thus, window lengths from 300 to 700 equal $N_t/5$ to nearly $N_t/2$, which corresponds to 50 to 116 hours (Fig. 2, "long term trends").

For all chosen window lengths, the first leading EOF has the window length as dominant periodic time ($\tau$) which consists of the mean value respectively mean trend. For L close to 24 hours (50-67 hours; L=300 and L=400) the next important periodic time is the diurnal cycle. In contrast, for longer window lengths, the first three EOFs represent long term signals. The whole time-series under study is limited to 11 days. Therefore, oscillations due to high and low pressure regimes (~ 7 days) identified visually by Sörgel et al. (2011a) in this time series are not captured by SSA. Due to its good water solubility, HONO is washed out by rain and increases during the dry periods (Sörgel et al., 2011a). These strong forcing mechanisms, which are not resolved by the maximum possible L, may be the reason for the dominance of eigenvectors with the main frequency being the window length. The diurnal cycle is identified as an important signal contribution independent of the choice of L, thus providing confidence for further analysis after subtraction of the diurnal cycle. We chose the maximum L=700 for further analysis of all time series.
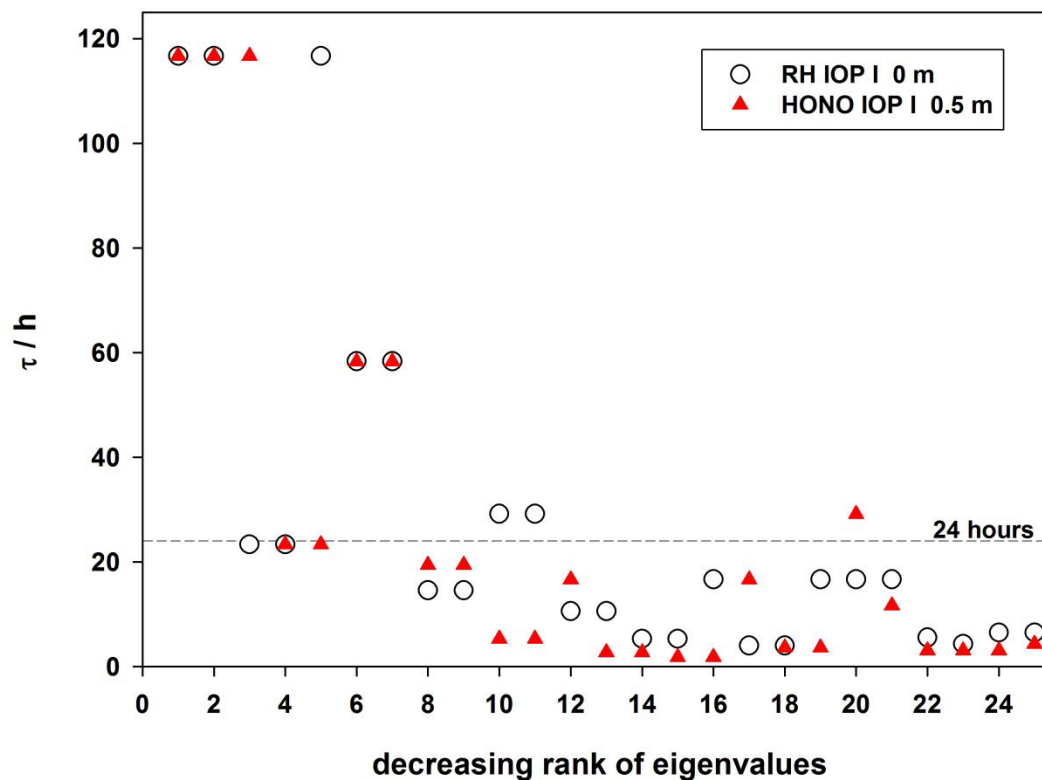


Figure 4: Dominant periodic times ($\tau$) in hours of the eigenvectors (ordered by decreasing rank) of RH (open circles) and HONO (red triangles) from IOP I close to the forest floor.

Figure 4 shows the $\tau$ values of the first 25 EOFs of HONO and RH (which contribute about 80-90 % to the HONO signal and 98 % to the RH signal, cf. Fig. 5). The first 10 EOFs are almost identical and represent the long term trends and the diurnal cycle. The pairs of

eigenvectors with the same frequency denote oscillations (Vautard and Ghil, 1989; Elsner and Tsonis, 1996; Ghil et al., 2002) which can be harmonic or anharmonic. These co-variations can be attributed to a real cause (wash out by rain) on the longer timescales, but the diurnal cycles of both might be simply co-variations due to solar radiation. The diurnal cycle of RH is mainly driven by the temperature, with lower values at higher temperatures during the day and increasing values during cooling at night. For HONO the photolysis (UV part of solar radiation) is the most important sink during the day, whereas HONO accumulates at night. As humidity mainly originates from evaporation (soil) or evapotranspiration (plants) and previous studies suggest HONO formation at the ground (e.g. Febo and Perrino, 1996; Harrison et al., 1996; Zhang et al., 2009; Sörgel et al., 2011a,b; Wong et al., 2011), both RH and HONO mixing ratios are sensitive to the mixing height (dilution by vertical mixing). The mixing height and thus vertical turbulent diffusion respectively exhibit a diurnal cycle as well. Therefore, HONO and RH are expected to be correlated at the timescale of the diurnal cycle but not necessarily due to interaction of chemical or physical processes.
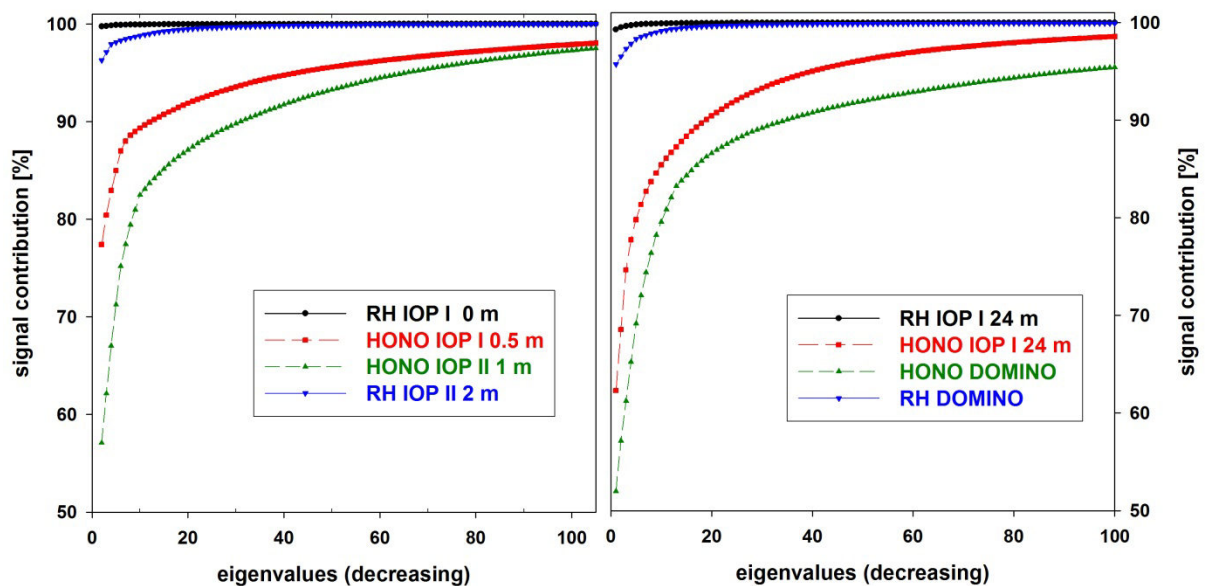


Figure 5: Cumulative signal contribution in % of the first 100 EOFs of HONO and RH for all campaigns.

As the sum of all eigenvalues represents the total variance of the original time series one can express the signal contribution of the EOFs by the contribution of their associated eigenvalues to the total variance (Vautard and Ghil, 1989). A first obvious difference between HONO and RH time series is the amount of variance explained by the leading EOFs (Fig.5). The first EOF, which consists of the mean and long term trends, comprises more than 98 % of the RH signal but only about 50 to 80 % of the HONO signal. This might be attributed to the

statistical distributions of the underlying data sets. HONO values are log-normal distributed whereas RH values are more or less normal or bimodal distributed. Figure 5 shows the eigenvalues contribution in % of the total sum of eigenvalues (= 100 %) plotted by decreasing rank. This can be interpreted similar to a so called "scree-diagram", where the eigenvalues themselves are plotted by decreasing rank (i.e. decreasing value). The "scree-diagram" can be used for a first simple separation into the EOFs comprising the signal and those for the noise. Typically, the signal part is assigned to the first EOFs before the break in the slope (looks like a hockey stick) of the "scree-diagram", but especially for larger L (as used in this study) there might be no "noise floor" and the break is smoothed (Vautard and Ghil, 1989). The break for RH values already occurs after three EOFs whereas for HONO the break occurs after eight EOFs.  However, apparently the first 20 to 30 eigenvalues still contain signal information.

## 3.3  Correlations in the signals after subtraction of diurnal and long term contributions

In order to extract possible correlations of HONO and RH apart from the diurnal cycle and the long term trends, which are the dominant signal contributions (Fig. 4 and 5 sect. 3.2), we subtract these contributions from the original time series. Figure 6 (upper panel) shows the measured time series and the reconstructed time series of HONO and RH for IOP I 0.5m using the first 11 EOFs.  Using all 700 EOFs, the reconstruction would be identical to the original time series, but this complete reconstruction would be very computational intensive.
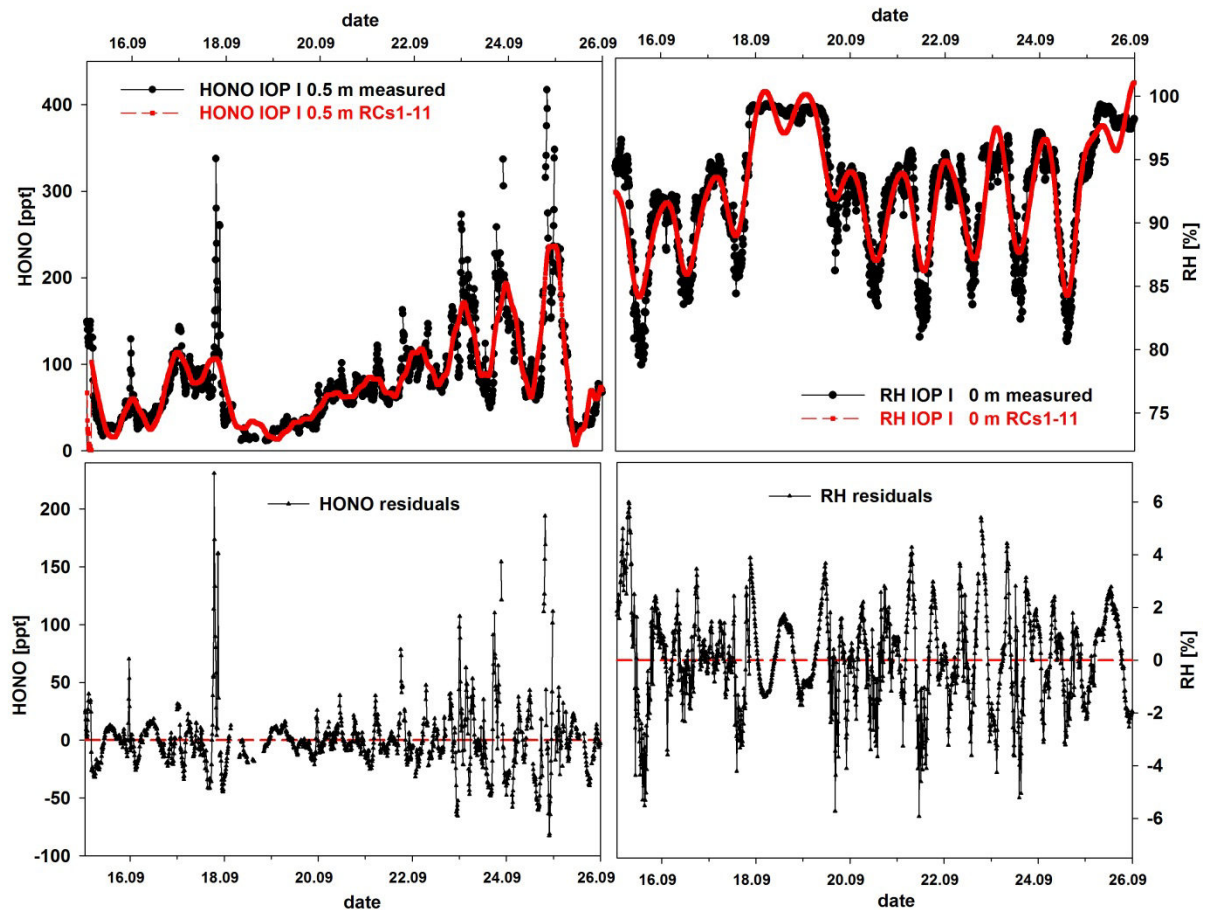
Fig. 6: Upper left panel: HONO measured (black dots) and reconstructed time series (red line) using the first 11 EOFs; upper right panel: measured RH (black dots) and reconstructed time series (red line) using the first 11 EOFs; lower panels: residuals after subtracting the reconstructed time series from the measured ones for HONO (left) and RH (right).

The lower panel of Fig. 6 shows the residuals after subtracting the reconstructed time series containing long term trends and the diurnal cycle. For both HONO and RH, trends are efficiently removed. Also, oscillations in the residuals have higher frequencies than the diurnal cycle, thus also proving that the diurnal cycle has been removed and higher frequency contributions remain. Only during the rainy periods (18th to 20th September) with almost constant RH and HONO values this method induced a diurnal cycle by restricting the reconstruction to the first EOFs (Fig. 6). Table 1 contains the correlation coefficients of the measured time series ("original"), the residuals after subtracting long term and diurnal contributions ("orig-RC"), and the residuals from subtracting the RCs not from the original time series, but also from a reconstructed one with higher frequency contributions (first 20 to 30 EOFs) which is equivalent to reconstruct RC11 to RC30 ("RC-RC").

Table 1: Correlation coefficients (according to Pearson and Spearman) of the measured time series of HONO and RH ("original"), the residuals after subtracting the reconstructed time series ("orig-RC") and the residuals using not the original time series but a reconstructed time series with higher frequency contributions ("RC-RC").

| Correlation coefficient | IOP I 0.5m | IOP I 24m | IOP II | DOMINO |
|---|---|---|---|---|
| **original** (Spearman) | 0.009 | 0.234 | 0.467 | -0.042 <br> 0.74* |
| **orig-RC** (Pearson) | 0.163 | 0.225 | 0.309 | 0.189 |
| **orig-RC** (Spearman) | 0.163 | 0.270 | 0.311 | 0.206 |
| **RC-RC** (Pearson) | 0.021 | 0.131 | 0.192 | 0.224 |
| **RC-RC** (Spearman) | -0.003 | 0.148 | 0.243 | 0.268 |

* Correlation coefficient derived excluding values with marine influence.

As described in sect. 3.1, HONO values were log-normal distributed and RH values were normal or bimodal distributed. Therefore, for the original time series only the rank correlation (Spearman) coefficients are given. The values are quite variable ($\sim$ -0.04 to 0.47). The poor correlations obtained for the DOMINO data were presumably caused by the equilibrium of HONO with the sea surface as proposed by Wojtal et al. (2010), as the correlation improved substantially to 0.74 by removing values associated with marine air masses.

Correlations of the residuals after subtraction ("orig-RC") of long term and diurnal contributions are less variable (0.16 - 0.31) and thus all slightly positive correlated.

An attempt to improve the correlation by reducing the contribution of noise ("RC-RC") did not result in higher correlation coefficients. All correlations for "RC-RC" except for "DOMINO" are lower than the correlations of the original time series and that of the residuals "orig-RC". This attempt was based on the visual inspection of the "scree diagram" (see section 3.2), and it was first concluded from the visual inspection that the first 20 to 30 EOFs still contain signal. This is possibly not the case, and relatively large signal contributions (between EOF 11 and EOF 30) are noise components. Thus, it remains to be solved by using more sophisticated tools like Monte-Carlo-SSA (e.g. Allen and Smith, 1996) whether the correlations are weak due to the influence of noise, or if the noise causes the correlation. With this method the significance of oscillations or signal contributions can be tested against a noise model (white noise and coloured noise, e.g. Allen and Smith., 1996). This would help to create a set of RCs which contain signal information alone and use them for reconstruction.

Furthermore, the interaction of HONO and RH on timescales shorter than the diurnal variation is not necessarily a linear (Pearson) or a monotonic function (Spearman). On the other hand, the heterogeneous formation reaction of HONO from the disproportionation of $NO_2$ has a first order dependence on water vapour (e.g. Sakamaki et al., 1983). But this reaction should be also sensitive to $NO_2$. Possibly, the better correlations of HONO and RH as well as HONO and $NO_2$ during DOMINO and IOP II were caused by the prevailing dry weather and thus more values under "dry surface" conditions. Under the dry surface conditions HONO and RH are expected to be positively correlated due to a) first order dependence of heterogeneous HONO formation on water vapour (e.g. Sakamaki et al. 1983), b) possibly due to HONO replacement by co-adsorption of water (Trick, 2004; Stutz, 2005). Furthermore, if we only take the dry period of IOP I 0.5m (i.e. from 20th to 25th of Sept.; cf. Fig. 5) the correlation coefficients improve from 0.16 to 0.34 (Spearman), which is close to the values of the summer campaign "IOP II".

# 4  Conclusions

In contrast to other studies, which can be interpreted as an attempt to estimate the influence of RH on the modulation of the amplitude of the diurnal cycle of HONO (e.g. Stutz et al., 2004; Yu et al., 2009), we tried to identify the interactions of HONO and RH on shorter timescales. To achieve this goal, the diurnal cycle and the long term trends have to be removed from the signal. SSA has been shown to successfully detect long term trends and the signal contributions of the diurnal cycle in HONO and RH time series. Therefore, it was possible to reconstruct the time series from the signal contributions of the diurnal cycle and the long term trends by subtracting it from the measured one (original). Trends and the diurnal cycle were efficiently removed by this method, and the residuals where slightly positive correlated for all-time series. Unfortunately, identification of correlations which are an indicator (but not a proof) for underlying processes in the remaining signal (2-20 %) was quite a challenge. There might be several reasons:

- the remaining signal also contains noise contributions, which might be resolved by a better separation of signal and noise by more sophisticated tools like Monte Carlo SSA
- the amplitude of the HONO signal is modulated by RH instead of the signal directly depending on RH

- other parameters like the HONO precursor $NO_2$ are more important for the variations than RH alone

- time resolution of the instruments (about 10 min for HONO) is still too low to resolve these processes

- precision of the HONO measurements (about 12 %) is still too low

The overall picture of the relation of HONO and RH was found to fit quite well to the scheme of surface wetness proposed by Lammel (1999) as "dry" (< 55 % RH), "partially wet" (55 – 90 % RH) and "wet" (> 90 % RH). Below 60/65 % RH correlations of HONO and RH were high, but consist of a few (< 100) data points only. For DOMINO a good correlation was obtained only after removing values from marine air masses. The mostly lower HONO values were presumably caused by the equilibrium with the sea surface as proposed by Wojtal et al. (2010). In the RH range of the "dry" surface the first order dependence of HONO formation on water vapour (e.g. Sakamaki et al., 1983) and the displacement of HONO from the surface by co-adsorbing water (proposed by Trick, 2004; Stutz, 2005) are proposed to cause the correlation. The "partially wet" surfaces denote a mixture of processes, as "dry" and wet surfaces coexist. The "partially wet" surfaces are caused by deliquescing salts. They can either release or take up HONO depending on ionic strength and pH (Becker et al., 1996; Becker et al. 1998; Hirokawa et al., 2008). This might be responsible for the high variability of HONO in the corresponding RH range (~70 to 95 %), which is accompanied with low correlations to both RH and $NO_2$. A rather clear result denotes the "wet" surfaces as HONO values drop above 95 % RH. This has already been observed by other groups (e.g. Stutz et al., 2004; Yu et al., 2009).

Another point, which should be considered in future studies, was that HONO values were log-normal distributed, whereas RH values were normal or bimodal distributed. Thus, for a standard (Pearson) correlation the log (HONO) values have to be taken or the rank correlation coefficient (Spearman) has to be used instead.

Thus, SSA has proven to be a useful tool to extract signal contributions aside the diurnal cycle, which is important for atmospheric chemistry. Nevertheless, further investigation of the noisy residuals needs more sophisticated statistical tools or higher frequency and less noisy time series.

# References

Allen, M. R., Smith, L. A.: Monte Carlo SSA: Detecting irregular oscillations in the presence of colored noise, J. Climate, 9, 3373 – 3404, 1996.

Arens, F., Gutzwiller, L., Gäggeler, H. W., and Ammann, M.: The reaction of $NO_2$ with solid anthrarobin (1,2,10-trihydroxyanthracene), Phys. Chem. Chem. Phys., 4, 3684–3690, 2002.

Becker, K. H., Kleffmann, J., Kurtenbach, R. and Wiesen, P.: Solubility of nitrous acid (HONO) in sulfuric acid solutions, J. Phys. Chem., 100, 14984-14990, 1996.

Becker, K. H., Kleffmann, J., Negri, R. M. and Wiesen, P.: Solubility of nitrous acid (HONO) in ammonium sulfate solutions, J. Chem. Soc., Faraday Trans., 94, 1583-1586, 1998.

Burkhardt, J. and Eiden, R.: Thin water films on coniferous needles, Atmos. Environ., 28, 2001–2017, 1994.

Diesch, J.-M., Drewnick, F., Zorn, S. R., von der Weiden-Reinmüller, S.-L., Martinez, M., and Borrmann, S.: Variability of aerosol, gaseous pollutants and meteorological characteristics associated with continental, urban and marine air masses at the SW Atlantic coast of Iberia, Atmos. Chem. Phys. Discuss., 11, 31585-31642, doi:10.5194/acpd-11-31585-2011, 2011.

Elsner, J.B. and Tsonis, A.A.: Singular Spectral Analysis. A New Tool in Time Series Analysis, Plenum Press, New York, USA, 1996.

Febo, A., Perrino, C., and Allegrini, I.: Measurement of nitrous acid in Milan, Italy, by DOAS and diffusion denuders, Atmos. Environ., 30 3599-3609, 1996.

Finlayson-Pitts, B. J.: Reactions at surfaces in the atmosphere: integration of experiments and theory as necessary (but not necessarily sufficient) for predicting the physical chemistry of aerosols, Phys. Chem. Chem. Phys., 11, 7760–7779, 2009.

Foken, T.: Micrometeorology, Springer, Berlin-Heidelberg, Germany, 308 pp., 2008.

Foken, T., Meixner, F. X., Falge, E., Zetzsch, C., Serafimovich, A., Bargsten, A., Behrendt, T., Biermann, T., Breuninger, C., Dix, S., Gerken, T., Hunner, M., Lehmann-Pape, L., Hens, K., Jocher, G., Kesselmeier, J., Lüers, J., Mayer, J.-C., Moravek, A., Plake, D., Riederer, M., Rütz, F., Scheibe, M., Siebicke, L., Sörgel, M., Staudt, K., Trebs, I., Tsokankunku, A., Welling, M., Wolff, V., and Zhu, Z.: ExchanGE processes in mountainous Regions (EGER) – overview of design, methods, and first results, Atmos. Chem. Phys. Discuss., 11, 26245-26345, doi:10.5194/acpd-11-26245-2011, 2011.

Frankenberger, E.: Untersuchungen über den Vertikalaustausch in den unteren Dekametern der Atmosphäre, Annalen der Meteorologie, 4, 358–374, 1951.

Gudmundsson, L.: Singular system analysis and synchronisation of distributed stream flow data, diploma thesis, Bayreuth, Germany, 2007.

Gudmundsson, L.: R – forge pages for simsalabim - the SSA implementation in R, https://r-forge.r-project.org/projects/simsalabim/, last access December 2011.

Gustafsson, R. J., Kyriakou, G., and Lambert, R. M.: The molecular mechanism of tropospheric nitrous acid production on mineral dust surfaces, ChemPhysChem, 9, 1390-1393, 2008.

Ghil, M., Allen, M. R., Dettinger, M. D., Ide, K., Kondrashov, D., Mann, M. E., Robertson, A. W., Saunders, A., Tian, Y., Varadi, F. and Yiou, P.: Advanced spectral methods for climatic time series, Rev. Geophys., 40, 1003, doi:10.1029/2000RG000092., 2002.

Golyandina, N., Nekrutkin, V. and Zhigljavsky, A.: Analysis of Time Series Structure: SSA and related techniques, Chapman and Hall/CRC, Boca Raton, USA, 305 pp, 2001.

Golyandina, N. and Osipov, E.: The "Caterpillar"-SSA method for analysis of time series with missing values, J. Stat. Plan. Infer., 137, 2642-2653, 2007.

Harrison, R. M., Peak, J. D., and Collin, G. M.: Tropospheric cycle of nitrous acid, J. Geophys. Res., 101, 14429–14439, 1996.

He, Y., Zhou, X., Hou, J., Gao, H., and Bertman, S. B.: Importance of dew in controlling the air-surface exchange of HONO in rural forested environments, Geophys. Res. Lett., 33, L02813, doi:10.1029/2005GL024348, 2006.

Hirokawa, J., Kato, T. and Mafune, F.: Uptake of gas-phase nitrous acid by pH-controlled aqueous solution studied by a wetted wall flow tube, J. Phys. Chem. , 112, 12143-12150, 2008.

Klemm, O.: Säure/Base- und redoxchemische Simulation des Verdampfens von Niederschlagswasser von Fichtennadeln, PhD thesis, Bayreuth, Germany, 214 pp, 1988.

Klemm, O., Burkhardt, J., and Gerchau, J.: Leaf wetness: A quantifiable parameter in deposition studies, in: Proceedings of the EUROTRAC-2 Symposium 98: Transport and chemical transformation in the troposphere, edited by: Borell, P. M. and Borell,P., WIT press, Southampton, UK, 238–242, 1999.

Lammel, G., and Cape, J. N.: Nitrous acid and nitrite in the atmosphere, Chem. Soc. Rev., 361-369, 1996.

Lammel, G.: Formation of nitrous acid: Parameterization and comparison with observations, Max Planck Institute for Meteorology, Hamburg, Germany, report No. 286, 36 pp., 1999.

Pöhler, D.: Determination of two dimensional trace gas distributions using tomographic LP-DOAS measurements in the city of Heidelberg, Germany, Ph.D. thesis, University Heidelberg, Germany, 334 pp., 2010.

Rubio, M. A., Lissi, E., and Villena, G.: Nitrite in rain and dew in Santiago city, Chile. Its possible impact on the early morning start of the photochemical smog, Atmos. Environ., 36, 293–297, 2002.

Rubio, M. A., Lissi, E., and Villena, G.: Factors determining the concentration of nitrite in dew from Santiago, Chile, Atmos. Environ., 42, 7651–7656, 2008.

Sakamaki, F., Hatakeyama, S., and Akimoto, H.: Formation of nitrous acid and nitric oxide in the heterogeneous dark reaction of nitrogen dioxide and water vapour, Int. J. Chem. Kinet., 15, 1013 -1029, 1983.

Schoellhamer, D. H.: Singular spectrum analysis for time series with missing data, Geophys. Res. Lett., 28 (16), 3187–3190, doi:10.1029/2000GL012698, 2001.

Sörgel, M., Trebs, I., Serafimovich, A., Moravek, A., Held, A., and Zetzsch, C.: Simultaneous HONO measurements in and above a forest canopy: influence of turbulent exchange on mixing ratio differences, Atmos. Chem. Phys., 11, 841–855, 2011a.

Sörgel, M., Regelin, E., Bozem, H., Diesch, J.-M., Drewnick, F., Fischer, H., Harder, H., Held, A., Hosaynali-Beygi, Z., Martinez, M., and Zetzsch, C.: Quantification of the unknown HONO daytime source and its relation to $NO_2$, Atmos. Chem. Phys., 11, 10433-10447, doi:10.5194/acp-11-10433-2011, 2011b.

Sonntag, D.: Important new values of the physical constants of 1986, vapour pressure formulations based on the ITS-90 and psyhrometer formulae, Z. Meteorol., 70, 340–344, 1990.

Stemmler, K., Ammann, M., Donders, C., Kleffmann, J., and George, C.: Photosensitized reduction of nitrogen dioxide on humic acid as a source of nitrous acid, Nature, 440, 195-198, 2006.

Stutz, J., Alicke, B., Ackermann, R., Geyer, A., Wang, S., White, A. B., Williams, E. J., Spicer, C. W., and Fast, J. D.: Relative humidity dependence of HONO chemistry in urban areas, J. Geophys. Res., 109, D03307, doi:10.1029/2003JD004135, 2004.

Stutz, J.: Final report "Nitrogen oxides in the nocturnal boundary layer: Chemistry of nitrous acid and the nitrate radical", U.S. Department of Energy Project Number: DE-FG02-01ER63094, University California Los Angeles, Los Angeles, California, USA, 159 pp., 2005.

Svennson, R., Ljungstrom, E., and Lindqvist: Kinetics of the reaction between nitrogen dioxide and water vapour, Atmos. Environ., 21 1529-1539, 1987.

Trick, S.: Formation of nitrous acid on urban surfaces - a physical-chemical perspective-, Ph.D. thesis, University Heidelberg, Germany, 290 pp., 2004.

Vautard, R. and Ghil, M.: Singular spectrum analysis in nonlinear dynamics, with applications to paleoclimatic time series. Physica D 35, 395-424, 1989.

Wainmann, T., Weschler, C. J., Lioy, P. J., and Zhang, J.: Effects of surface type and relative humidity on the production and concentration of nitrous acid in a model indoor environment, Environ. Sci. Technol., 35, 2200–2206, 2001.

Wojtal, P., Halla, J.D. and McLaren, R.: Pseudo steady states of HONO measured in the nocturnal marine boundary layer: a conceptual model for HONO formation on aqueous surfaces, Atmos. Chem. Phys., 11, 3243–3261, 2011.

Wong, K. W., Oh, H.-J. , Lefer, B. L., Rappenglück, B., and Stutz, J.: Vertical profiles of nitrous acid in the nocturnal urban atmosphere of Houston, TX, Atmos. Chem. Phys., 11, 3595–3609, 2011.

Yu, Y., Galle, B., Hodson, E., Panday, A., Prinn, R., and Wang, S.: Observations of high rates of $NO_2$ – HONO conversion in the nocturnal atmospheric boundary layer in Kathmandu, Nepal, Atmos. Chem. Phys., 9, 6401–6415, 2009.

Zhang, N., Zhou, X., Shepson, P. B., Gao, H., Alaghmand, M., and Stirm, B.: Aircraft measurement of HONO vertical profiles over a forested region, Geophys. Res. Lett., 36, L15820, doi:10.1029/ 2009GL038999, 2009.

## Erklärung

Hiermit erkläre ich, dass ich die Arbeit selbständig verfasst und keine anderen als die angegebenen Quellen und Hilfsmittel verwendet habe.

Ferner erkläre ich, dass ich nicht anderweitig mit oder ohne Erfolg versucht habe, eine Dissertation einzureichen oder mich einer Doktorprüfung zu unterziehen.

Bayreuth, den 19.02.2013

Matthias Sörgel